Stillwater Complex, Montana—Structure, Mineralogy, and Petrology of the Basal Zone with emphasis on the Occurrence of Sulfides

By NORMAN J PAGE

GEOLOGICAL SURVEY PROFESSIONAL PAPER 1038

UNITED STATES GOVERNMENT PRINTING OFFICE, WASHINGTON : 1979

UNITED STATES DEPARTMENT OF THE INTERIOR

CECIL D. ANDRUS, *Secretary*

GEOLOGICAL SURVEY

H. William Menard, *Director*

Library of Congress Cataloging in Publication Data
Page, Norman J
Stillwater Complex, Montana–Structure, Mineralogy, and Petrology of the Basal Zone with emphasis on the Occurrence of Sulfides
(Geological Survey Professional Paper 1038)
Bibliography: p. 61
Supt. of Docs. No.: I 19.16:1038
1. Rocks, Igneous. 2. Intrusions (Geology)–Montana. 3. Sulphides. 4. Ore-deposits–Montana.
I. Title. II. Series: United States Geological Survey Professional Paper 1038
QE461.P289 552'.1'09786 77-608351

For sale by the Superintendent of Documents, U.S. Government Printing Office
Washington, D.C. 20402
Stock Number 024-001-03179-5

CONTENTS

ILLUSTRATIONS

TABLES

STILLWATER COMPLEX, MONTANA—STRUCTURE, MINERALOGY, AND PETROLOGY OF THE BASAL ZONE WITH EMPHASIS ON THE OCCURRENCE OF SULFIDES

By NORMAN J PAGE

ABSTRACT

The Basal zone of the Stillwater Complex is divided into two members, a Basal norite and an overlying Basal bronzite cumulate. The Basal norite is composed of alternating lensoid masses or layers of rock and is extremely variable both laterally and vertically in mineralogy, texture, grain size, and crystallization sequences, and the Basal bronzite cumulate is composed of layers of fine- to coarse-grained granular orthopyroxene cumulates and exhibits relatively regular properties laterally.

The contact between the Basal zone and the metasedimentary rocks it intrudes does not follow a single stratigraphic horizon but cuts across lithologic and structural units in the country rocks. The overall shape of the Basal zone is sheetlike with an extremely large length-to-thickness ratio, but in detail it consists of a series of basinlike shapes linked by thinner units of rock. The Basal zone is composed of a variety of rocks, including: Cumulates, principally orthopyroxene cumulates but with minor amounts of one- and two-phase cumulates dominated by olivine, orthopyroxene, clinopyroxene, inverted pigeonite, plagioclase, or chromite; noncumulate igneous rocks with ophitic, subophitic, and ragged textures; contaminated and mixed rocks; rocks derived by local partial melting; sulfide-bearing and sulfide rocks; and complex breccias of the above types. The rocks and their constituents are characterized by fluctuating and repeating patterns of chemical and physical properties that, from bottom to top, include: (a) Lithologic sequences of ophitic, subophitic, ragged, and cumulus-textured rocks; (b) cumulate sequences of orthopyroxene-orthopyroxene+plagioclase, olivine+orthopyroxene-orthopyroxene, and plagioclase-plagioclase+ orthopyroxene; (c) sequences of fine- to medium- to coarse-grained cumulate rocks; (d) variation in the volume of cumulus phases present; (e) variation of orthopyroxene compositions; (f) variation of plagioclase compositions; and (g) variation of the distribution of sulfide minerals.

The model for the formation of the Basal zone proposes that immediately after or during initial emplacement of magma, several characteristics of the basal contact zone developed. Silicate magma and a sulfide-oxide liquid were injected into the metasedimentary rocks as tongues, dikes, and lenses, accounting for locally complicated geologic relations. Some early silicate magma was emplaced in rocks that were cool enough to allow it to crystallize as ophitic, subophitic, and ragged-textured noncumulates. Subsequent injections of magma cooled more slowly and developed textures characteristic of cumulate rocks. The massive sulfide lenses crystallized as temperatures decreased.

Noncumulate igneous rocks crystallized by relatively rapid cooling or quenching of magma within the main chamber near the contact with metasedimentary rocks. Large blocks and inclusions of metasedimentary rocks locally having rinds of noncumulate rocks were rafted upward in the magma chamber. Locally, cumulate crystalization began, was interrupted either by new influxes of magma or by overturning in convection cells, and was reestablished. This process was probably the major mechanism operating during the development of the Basal norite member. The approach of the magma to thermal and chemical equilibrium was also perturbed by influxes of new magma or convection.

The same cycle of crystallization and perturbation affected the remaining magma, probably producing the chemical and mineralogical repetitions and inhomogeneities exhibited by the norite member of the Basal zone. Perhaps, by the time the upper part of the Basal norite member was crystallizing or at least by the time the Basal bronzite cumulate member was accumulating, there were no new influxes of magma, and the crystallization pattern was established.

INTRODUCTION

The large tabular mass of Precambrian mafic and ultramafic rocks that forms the Stillwater Complex crops out along a northwest strike on the northern margin of the Beartooth Mountains in southwestern Montana (fig. 1). The lower part of this mass, called the Basal zone, is discontinuously exposed for about 42 km along strike in the Mt. Wood and Mt. Douglas 15-minute quadrangles (Page and others, 1973a, b). A considerable mineral potential is known for the Basal zone and adjacent rocks (Howland, 1933; Roby, 1949; Dayton, 1971; Page and Dohrenwend, 1973). Because keys to understanding the early processes involved in formation of the stratiform mafic and ultramafic complexes are hidden in the detailed geology of the Basal zone, this report concentrates on this zone exclusively.

An informal stratigraphic nomenclature to describe the internally conformable layers of the Stillwater Complex has developed from the early work of Peoples (1936, p. 358), through that of Jones, Peoples, and Howland (1960), Hess (1960), Jackson (1961a), and Page (1977), to that presented here. In addition, an extensive terminology developed by Jackson (1967) to describe rocks formed by crystal accumulation in response to gravity is used.

The Stillwater Complex is divided into four main zones: Basal, Ultramafic, Banded, and Upper. The Basal zone is split into two members; the Basal norite and the overlying Basal bronzite cumulate (Page and Nokleberg, 1975; Page, 1977). Jackson (1961a) divided the Ultramafic zone into two parts, a Peridotite member and a Bronzitite member. Only the Peridotite member, which conformably overlies the

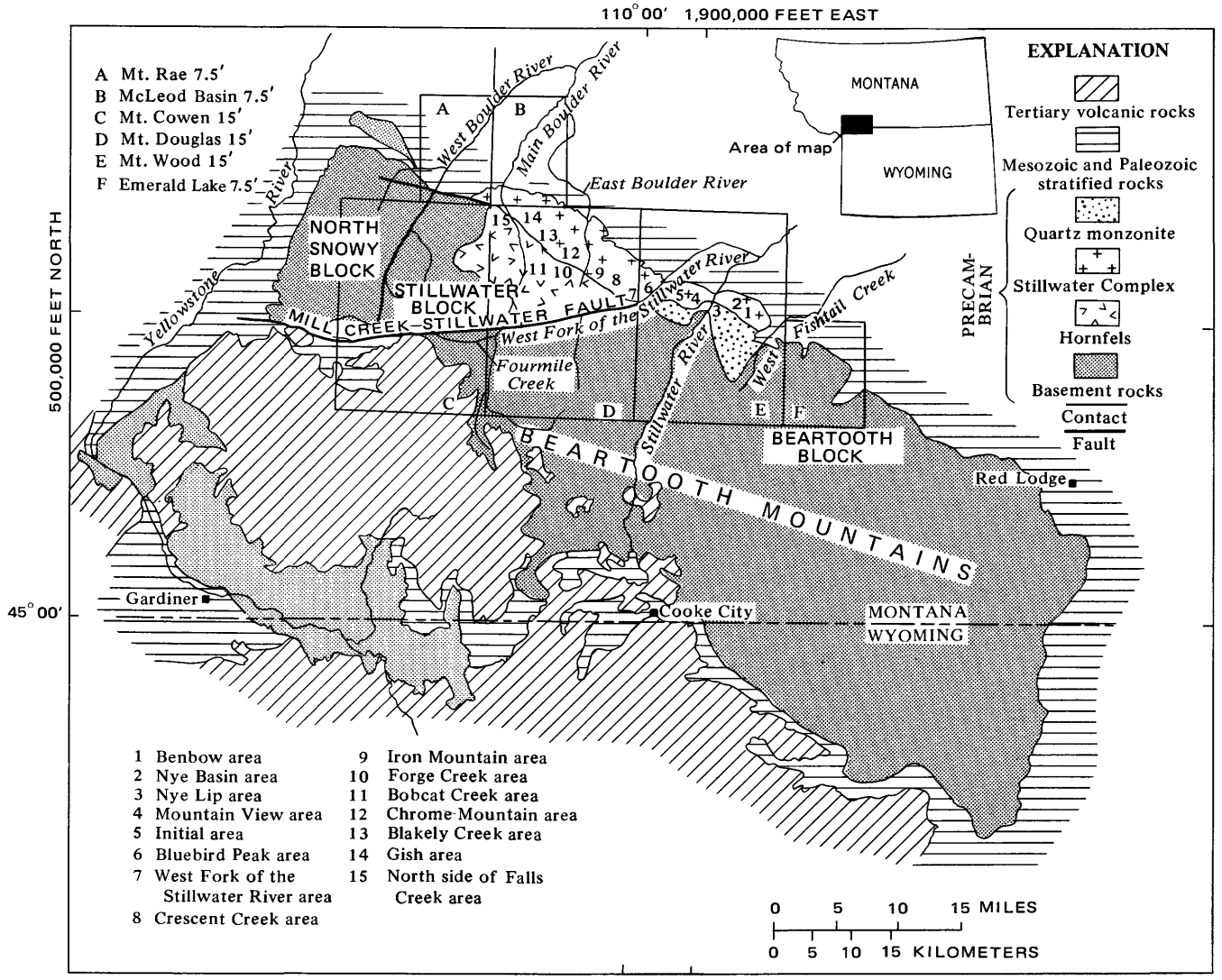

FIGURE 1. Index map of the Stillwater Complex.

Basal zone, is pertinent to this report. It consists of cyclic units (Jackson, 1961a, 1963, 1967, 1968a, 1969, 1970, 1971) that are repetitions of the cumulate sequence olivine, chromite, olivine+chromite, olivine+bronzite, and bronzite; at least 15 cycles are recognized in the Peridotite member, and 13 contain chromite and chromite+olivine cumulates near the base. The chromite cumulates have been designated by letters from A to K sequentially from the lowest to highest zone.

GEOLOGIC HISTORY OF THE STILLWATER COMPLEX AND ASSOCIATED ROCKS

The geologic history of the Stillwater Complex and associated rocks extends back over 3140 m.y. (million years) and contains at least two mountain-building events. Page (1977) summarized the Precambrian events, and Jones, Peoples, and Howland (1960) described the post-Middle Cambrian events for the Stillwater area. Foose, Wise, and Garbarini (1961) and Casella (1969) gave summaries of the geology of the encircling Beartooth Mountain region. Figure 2 is a simplified map of the geology within the Stillwater Complex compiled from Page and Nokleberg (1975) and Page, Simons, and Dohrenwend (1973a, b) that shows the geologic relations of the five major groups of rocks in the area: (1) Regionally metamorphased rocks consisting of granitic gneisses and associated metasedimentary rocks of Precambrian age; (2) hornfelsed metasedimentary rocks associated with the Stillwater Complex; (3) stratiform mafic and ultramafic rocks of the Stillwater Complex; (4) an intrusive sequence of quartz monzonitic rocks of Precambrian age; and (5) sedimentary rocks of Paleozoic and Mesozoic age. Table 1 summarizes the geologic history of the area.

PREVIOUS WORK AND ACKNOWLEDGMENTS

The Stillwater Complex and adjacent rocks have been studied since 1920 as part of several overlapping comprehensive investigations of structure, stratigraphy, geochemistry, and petrology of the complex. Mapping and studies of the chromite deposits include Westgate (1921), Peoples (1932, 1933, 1936), Howland (1933, 1955), Vhay (1934), Peoples and Howland (1940), Wimmler (1948), Howland, Garrels, and Jones (1949), Richards (1952, 1958), Peoples, Howland, Jones, and Flint (1954), Jackson, Howland, Peoples, and Jones (1954), Vail (1955), Jones, Peoples, and Howland (1960), Jackson (1960, 1961a, 1963, 1967, 1968a, 1969, 1970, 1971), and Page, Shimek, and Huffman (1972). Hess (1938a, b; 1939, 1940, 1941, 1949, 1960), and Hess and Phillips (1938, 1940) concentrated on the Banded and Upper zones. Other generalized mapping studies include Page and Nokleberg

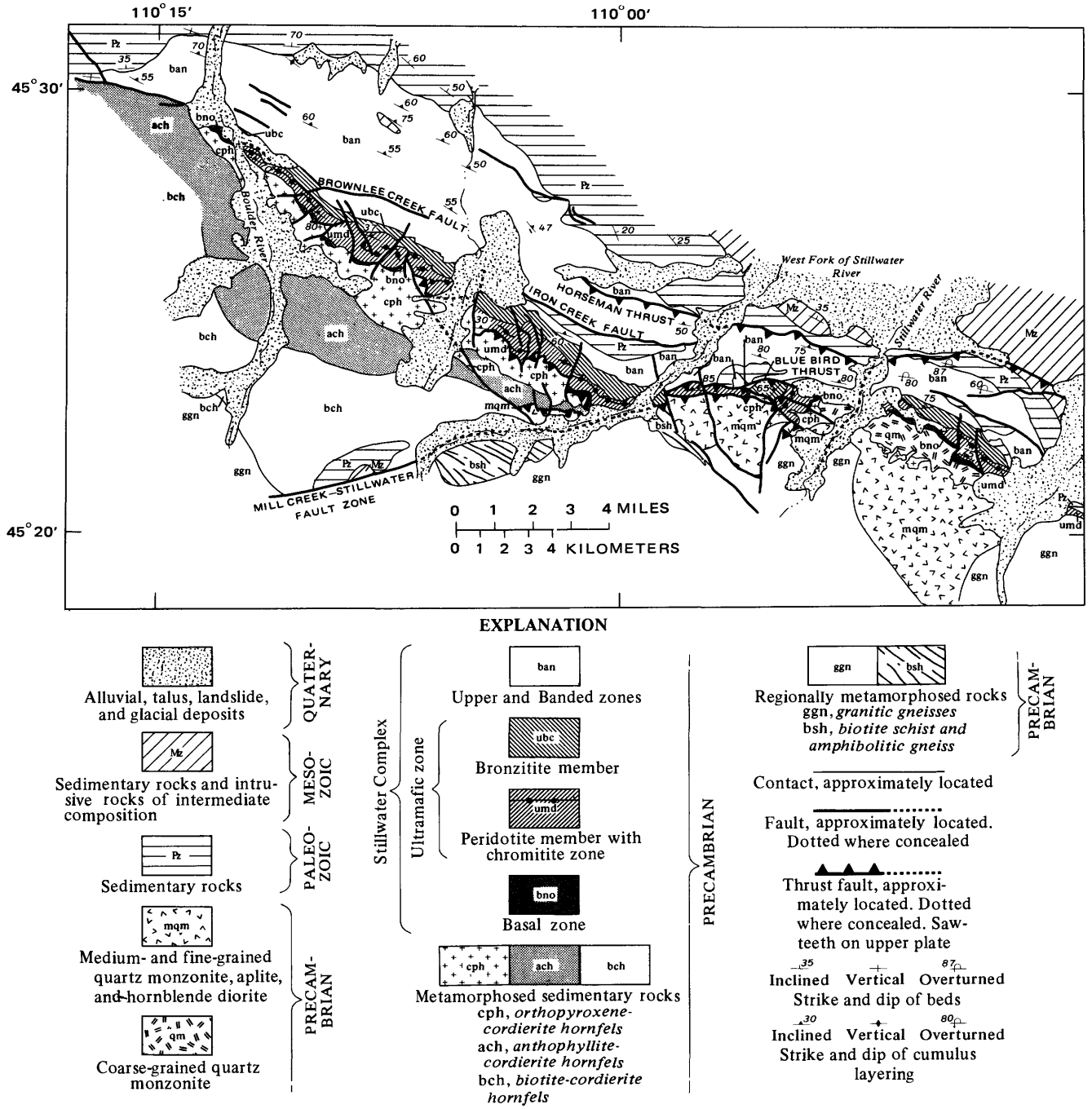

FIGURE 2.—Geologic map of the Stillwater Complex after Page and Nokleberg (1974) and Page, Simons, and Dohrenwend (1973a, b).

(1970b, 1972, 1974), and Page, Simons, and Dohrenwend (1973a, b). Studies on sulfide minerals and platinum metals include Howland (1933), Howland, Peoples, and Sampson (1936), Roby (1949), Page (1971a, b; 1972), Page and Jackson (1967), and Page, Riley, and Haffty (1969, 1971, 1972). Studies of the Basal zone by Howland (1933), Roby (1949), and E. D. Jackson (unpub. data) provide the foundation for this paper.

E. D. Jackson and A. L. Howland introduced and encouraged this study in 1967 and since then have contributed samples, unpublished maps, and recommendations. The author is grateful to W. J. Nokleberg and R. A. Koski for fieldwork and to John Stuckless, Richard Shimek, and John Dohrenwend for laboratory work. AMAX Exploration Inc., Anaconda Co., Cyprus Mines Corp., and Johns-Manville and their personnel have cooperated and facilitated this project. Richard N. Miller (Anaconda Co.) and Giles E. Walker (AMAX Exploration, Inc.) provided access to their diamond drill core for the purposes of logging and sampling.

TABLE 1.—*Generalized geologic history of the Stillwater Complex, Montana*

[After Page (1977), Jones, Peoples, and Howland (1960), and Foose, Wise, and Garbarini (1961)]

Time	Event
Precambrian W (prior to 3140 m.y.)	(1) Presence of a terrane containing mafic, ultramafic, and intermediate composition rocks which were being actively eroded. (2) Deposition of clastic and chemically precipitated magnesium- and iron-enriched sediments including iron formation; deposition of a diamictite –possible local glaciation. (3) Complex folding of magnesium- and iron-enriched sediments, possible regional metamorphism.
Precambrian W (2750-3140 m.y., probably nearer 3140 m.y.).	Strike-slip faulting, fractionation, and accumulation of magmatic sediments from Stillwater magma; intrusion of the Stillwater magma and contact metamorphism of older rocks.
Precambrian W (2750±60 m.y.).	Intrusion of quartz monzonitic rocks; contact metamorphism of older rocks.
Precambrian X (1600-1800 m.y.).	Intrusion of mafic dikes, penetrative deformation, low-grade regional metamorphism, possible thrust and normal faulting.
Pre-Middle Cambrian	Faulting, rotation, tilting, and erosion.
Middle Cambrian	Subsidence of Stillwater Complex.
Middle Cambrian through Early Cretaceous.	Deposition of 2400-3000 m of marine and continental sedimentary rocks with breaks in the Silurian and Permian.
Late Cretaceous	Extrusion of volcanic rocks; initiation of Laramide deformation.
Early Paleocene through early Eocene.	Thrust, normal, and strike-slip faulting; major uplift and deformation; folding; intrusion of siliceous and intermediate sills, dikes, and stocks; extrusion of volcanic rocks (Laramide orogeny).
Middle Eocene through early Miocene.	Erosion.
Miocene through Pliocene.	Erosion and uplift.
Pleistocene through Holocene.	Erosion and glaciation, minor faulting.

DEFINITION OF THE BASAL ZONE

The Basal zone, as previously defined (Page and Nokleberg, 1974; Page, 1977; Page, Simons, and Dohrenwend, 1973a, b; Hess, 1960; Jones, Peoples, and Howland, 1960; Jackson, 1961a, p. 2; Page, 1971b, p. 1) includes all rocks stratigraphically below the lowest cyclic unit of the Peridotite member of the Ultramafic zone. It is composed of magmatic sediments of orthopyroxene, clinopyroxene, plagioclase, olivine, or combinations thereof and of noritic and gabbroic rocks that exhibit ophitic or subophitic noncumulate igneous textures. Because the boundary between the Basal zone and the Ultramafic zone is not necessarily marked by the appearance of the first cumulus olivine, the definition is referenced to the lowest cyclic unit of the Ultramafic zone, which usually begins with an olivine cumulate but locally begins with an olivine-bronzite or bronzite cumulate owing to onlapping relations.

The Basal zone is divided into two members. The upper or Basal bronzite cumulate member is mainly composed of layers of fine- to coarse-grained hypidiomorphic granular orthopyroxene cumulates. The lower or Basal norite is composed of alternating lensoid masses or layers of rock in which are found a variety of crystallization sequences composed of olivine, orthopyroxene, clinopyroxene, plagioclase, hornblende, biotite, quartz, iron-titanium-chromium oxides, and sulfide minerals. The sequences in the Basal norite appear to be irregularly distributed and most rocks seem to be more enriched in feldspar than is the Basal bronzite cumulate. In addition, grain size varies from coarse to fine in an irregular manner. Within a small area one finds rocks with all gradations of texture from magmatic sediment with apposition fabrics to current-formed fabrics to ophitic, diabasic, and gabbroic textures. Usually the most distinctive texture is one in which the pyroxenes show ragged subhedral margins against plagioclase. Making the distinction between the two members is relatively simple in the field, where exposures are large enough to apply the above criteria, but the distinction is very difficult to make when logging drill core because of the limited surface area and because the contact between the two members is in part gradational.

DISTRIBUTION AND THICKNESS OF THE BASAL ZONE

The entire Basal zone is found on the southern margin of the complex where there are about 3.6 km^2 of exposures. This is about 9 percent of the area covered by exposures of the Stillwater Complex. Although exposed discontinuously along strike, the Basal zone is the lowermost, continuous, semitabular layer of the complex. Deep glacial valleys

cutting the complex, valley fill, and complex faulting are responsible for the observed discontinuities in exposures. For example, exposures are either sparse or nonexistent along the trend of the Basal zone in the West Fishtail Creek, Stillwater River, West Fork of the Stillwater River, East Boulder River, and Boulder River valleys because of covering valley fill. The Basal zone is covered by younger rocks thrust northward (figs. 1 and 2) from the Initial-Cathedral creek to the Upper Forge Creek areas. Between Blakely Creek and the Gish area, the surface is covered with glacial moraine and talus, but outcrops of olivine cumulate and cordierite - orthopyroxene - biotite hornfels (Page and Nokleberg, 1975) suggest that the Basal zone may in part be absent or very thin in this area. Plate 1 contains an interpretative geologic map which shows the distribution of well-known, inferred and approximate, and projected and hypothetical occurrences of the Basal zone of the Stillwater Complex. Well-known occurrences include those areas marked by abundant surface outcrops, surficial float, or detailed drilling where the boundaries of the Basal zone are well established, approximate and inferred areas include those marked by sparse outcrops, float, and drill data, and projected and hypothetical areas are enclosed by contacts established by geologic reasoning and are usually covered by extensive surficial debris.

Maximum known thicknesses of the Basal zone are on the order of 400 m, but most of the zone averages between 60 and 240 m in thickness. Stratigraphic columns along the strike of the complex (pl. 1) show estimated thicknesses of the Basal zone at 48 localities. Figure 3 summarizes the estimated thickness as a histogram; an arithmetic average of 163.16 m was calculated for the set of estimates and agrees well with visual estimates from examination of the maps and cross sections.

In most of the sections of the Basal zone, 20 to 70 percent is composed of the Basal bronzite cumulate. The maximum known thickness of the Basal bronzite cumulate exceeds 260 m and the minimum thickness is less than 18 m. The member probably averages about 80 m in thickness; however, the Basal bronzite cumulate is twice as thick in the west as in the east. On the average, the Basal bronzite cumulate accounts for about 50 percent of the Basal zone. The Basal norite has a maximum known thickness of about 260 m and averages between 60 and 90 m thick.

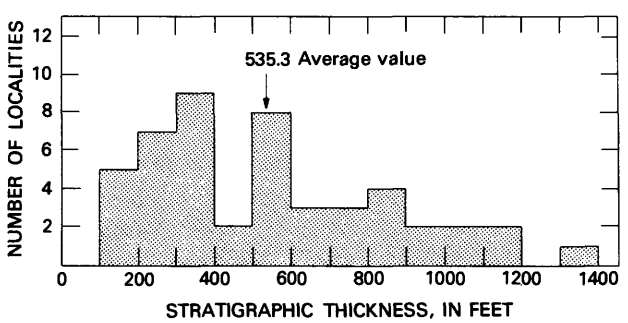

FIGURE 3.—Estimated stratigraphic thickness of Basal zone at 48 localities.

Maximum topographic relief is between 1300 and 1400 m, which affords a comparable depth of exposures down dip because of the steep tilt of the complex. The largest amounts of downdip exposure of the Basal zone are from Chrome Mountain to the Boulder River (1372 m) and from Benbow to Nye Lip (914 m).

SHAPE OF THE BASAL ZONE

The exposed part of the Basal zone has roughly the shape of a tilted, extremely thin, tabular prism about 42 km long, about 163 m thick, and with about 1370 m of downdip exposure. The eastern part of the Basal zone can be inferred to extend down dip below the surficial exposures for a lesser distance than the western part, on the basis of the distribution of the aeromagnetic high associated with the Basal and Ultramafic zones (U.S. Geol. Survey, 1971) and the aeromagnetic low associated with the Upper and Banded zones. A preliminary interpretation of the aeromagnetic data is that the eastern part of the Basal zone is cut out by faulting, intrusive quartz monzonite, or both at depth.

In detail the Basal zone does not, of course, have a prismatic shape (pl. 1) but varies in shape along its strike length because of changes in thickness. Thickest sections of the Basal zone are in the areas of Benbow, Mountain View, Crescent Creek, Iron Mountain, Chrome Mountain, and Blakely Creek, and west of the Boulder River. If the base of the Peridotite member is used as a reference horizon of constant elevation, these areas appear as depressions or basins in the country rock. If the base of the Bronzitite member is used as the reference horizon, the Peridotite member also forms several basinlike structures (Jackson, 1963, p. 48); similarly, basinlike structures can be inferred from the columnar sections of Jones, Peoples, and Howland (1960, p. 290). In the basinlike sections both the cyclic units and chromitite zones are thicker than on the adjoining shelf sections (Jackson, 1963), which suggests that more rapid crystal accumulation took place in the basin areas. Figure 4 compares basins in the Peridotite member with basinlike structures in the Basal zone. Slope angles on the sides of the basins range from less than 2° to about 20°; most estimated slopes are less than 10°. In general, basinlike structures occur in the same areas for both rock units, suggesting that the structures were present during crystallization of the Basal zone and did not begin development at a later time, although they may have continued forming during the crystallization of the Peridotite member.

Where the most data are available, the basinlike structures in the Basal zone are found to be irregular in shape (pl. 1, fig. 4). In the Benbow-Nye Lip area, the irregularities probably are caused in part by the intrusive quartz monzonites and in part by faulting. In the Chrome Mountain area and to the west, seeming irregularities may result from the wide spacing

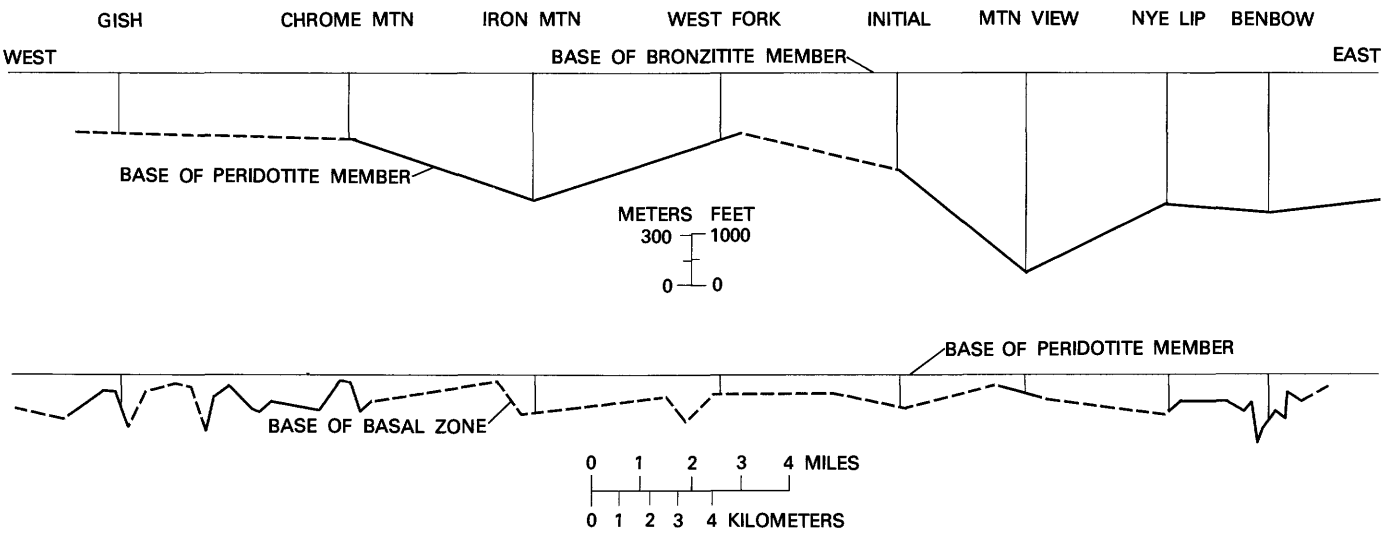

FIGURE 4.—Basin structures in Basal zone compared with those in Peridotite member. Peridotite member thicknesses after Jackson (1963, p. 48). Dashed lines hypothetical or speculative; vertical scale exaggerated.

of the geologic information used to reconstruct the sections. Between the Mountain View and the Chrome Mountain areas, the shape of the Basal zone beneath the thrusts has been estimated from the few outcrops, drilling data, and the shapes of basins in the Peridotite member. Probably the thickest parts of this basin structure lie between the Crescent Creek and the Iron Mountain areas.

DESCRIPTION OF CONTACTS

Contacts between rock units discussed here are of two kinds; those between the Basal zone and younger or older rock units which are not part of the complex, and those that are internal to the Stillwater Complex, between its various units. External contacts include the intrusive contact of the Basal zone within the metasedimentary rocks (now pyroxene hornfels facies rocks) and those with later intrusive rocks. Both the hornfels and Basal zone have been intruded by a younger sequence of coarse-grained quartz monzonite and aplites (Page and Nokleberg, 1970a, 1972; Page, 1977) and all three rock units are intruded by younger mafic dikes. Internal contacts include the upper contact of the Basal zone with the Peridotite member of the Ultramafic zone and the lower contact of the Basal bronzite cumulate member with the Basal norite member.

CONTACT OF THE BASAL ZONE WITH METASEDIMENTARY ROCKS

The contact between the Basal zone and the metasedimentary rocks has been modified on the east by later intrusive quartz monzonites and in the central part of the Stillwater Complex its position is concealed by thrust faulting. Surface exposures of the contact occur in the Mountain View area, the Initial area, discontinuously from Chrome Mountain to Blakely Creek, and in Falls Creek.

The appearance and characteristics of the rocks and the contact between them show variations. Locally, the contact may consist of (1) ophitic to subophitic noritic or gabbroic rocks in sharp, regular contact with the metasedimentary rocks, (2) the same rocks as above in contact but with dikes and tongues of gabbroic rock extending into the metasedimentary rocks, (3) orthopyroxene cumulates that collected on a floor of metasedimentary rocks, or (4) a zone of intrusive breccia composed of hornfelsed metasedimentary rock fragments, cumulates, ophitic to subophitic rocks and rocks rich in sulfides. Locally, there may be zones of hornfels inclusions above the contact or there may be zones of noritic dikes and sulfide pods well below the contact—for example, in the Mountain View area.

Iron formation and blue metaquartzite are exposed near the contact from the Boulder River to a point west of Chrome Mountain, but from there to the upper part of Forge Creek these rock units diverge toward the south from the contact. Outcrops of iron formation and metaquartzite close to the Basal zone between the upper part of Forge Creek and Bluebird Peak owe their position to a thrust fault. From Bluebird Peak to the east end of the Basal zone iron formation and blue metaquartzite are sparse. Minor amounts of these rocks occur as inclusions in the quartz monzonite on the ridge between Nye and Flume Creeks. The overall relations of rock units below the complex to the Basal zone suggests that the Basal zone contact is not parallel to a stratigraphic horizon but cuts across stratigraphic units. The contact may mark either a fault that was nearly horizontal at the time of emplacement of the complex or an unconformity.

CONTACT OF THE BASAL ZONE WITH THE ULTRAMAFIC ZONE

The contact of the Basal zone with the Ultramafic zone is located between the top of the Basal bronzite cumulate and the first cyclic unit of the Peridotite member of the Ultramafic zone. It is marked for 80 percent of the strike length by the disappearance of orthopyroxene and the appearance of olivine as cumulus minerals in the Peridotite member but may also be marked by orthopyroxene being joined by olivine as a cumulus crystal. The horizon is sharp and distinct and where observed is about one crystal thick. Over large areas the layering in the Peridotite member appears to be conformable with the layering in the Basal bronzite cumulate member, for example in the Benbow area (pl. 1).

However, the layering in the Peridotite member is not always conformable with the Basal bronzite cumulate member. In the Chrome Mountain area the lower olivine cumulate, bronzite cumulate, and olivine cumulate of the next cycle abut against the Basal bronzite cumulate. This relation can be explained as onlap on the margin of a basin, similar to onlap in sedimentary rocks. The only other example of this type of relation occurs within the Peridotite member on the west side of Iron Mountain where bronzite and olivine+bronzite cumulates abut against an olivine cumulate. Smaller scale examples of onlap have been observed by Jones, Peoples, and Howland (1960) in the chromitite zones and by W. J. Nokleberg (oral commun., 1970) in the Banded zone. Other evidence for a basin margin is the dramatic thinning of the Basal zone from northeast to southwest in the Chrome Mountain area. On the basis of this evidence onlap should be expected in the basin structures, and its possibility should not be neglected in subsurface interpretations.

CONTACT OF THE BASAL ZONE WITH YOUNGER INTRUSIVE QUARTZ MONZONITIC ROCKS

Precambrian quartz monzonite, aplite, and hornblende quartz diorite intrude the Basal zone of the Stillwater Complex from West Fishtail Creek to slightly west of the West Fork of the Stillwater River. Page (1977) and Page and Nokleberg (1972) discuss the intrusive, petrologic, and structural nature of this sequence of rocks, which is 2750 m.y. old (Nunes and Tilton, 1971). Dikes of these rocks are found in the Basal zone, and inclusions of the Basal zone were found in the quartz monzonites. These relations demonstrate that the contacts between the Basal zone and these rock units are intrusive. From the Benbow area to the Stillwater River, the quartz monzonite apparently stoped away part of the Basal zone and modified its lower contact. Evidence for this suggestion is the discrepancy in thickness of the Basal zone across the Big 7 fault. To the east of the Big 7 fault the Basal zone thickens toward the fault; immediately across the fault to the west the Basal zone is only half as thick.

CONTACT OF THE BASAL ZONE WITH MAFIC DIKES

Mafic dikes of younger Precambrian age also intrude the Stillwater Complex; most of these dikes have basaltic compositions and ophitic to subophitic textures (Page, 1977). The mafic dikes are fairly easily distinguished from the Stillwater Complex by their textures and gross form except where they intrude the Basal norite member. Within the Basal norite, intrusive mafic dikes have chilled margins of very fine grained, diabasic-textured rocks or crosscutting relations with definable units of the Basal norite. Isotopic studies also aid recognition of the dike rocks. Because faults tend to follow the mafic dikes, the dike rocks can be highly sheared, broken, and altered, a secondary criterion for their recognition. Sills or dikes subparallel to the Basal norite unit would be extremely difficult to recognize. Mafic dikes have been observed in surficial exposures in the Benbow, Initial, Chrome Mountain, and Boulder River areas. Where there has been extensive drilling, such as the Iron Mountain area, dikes have been recognized in the Basal zone in the subsurface.

CONTACT OF THE BASAL NORITE WITH THE BASAL BRONZITE CUMULATE

The contact between the Basal norite and the Basal bronzite cumulate is locally gradational and generally marked by a transition from noncumulate, subophitic-, ophitic-, diabasic-, and gabbroic-textured rocks of the Basal norite to cumulate rocks of the Basal bronzite cumulate. The Basal norite generally contains more plagioclase than the Basal bronzite cumulate. Locally this contact has been placed between apposition fabric cumulates of the Basal bronzite member and cumulates with current structures in the Basal norite member. Other contacts between lenses and layers in the Basal zone are phase contacts, ratio contacts, and form contacts. (See Jackson, 1967, for terminology.)

AGE RESTRICTIONS ON THE BASAL ZONE

The Basal zone of the Stillwater Complex is at least 2750 m.y. old and may be more than 3140 m.y. old (Page and Nokleberg, 1972; Page 1977). This conclusion is based on uranium-lead study of zircons from the intrusive quartz monzonites and from the metasedimentary rocks (Nunes and Tilton, 1971).

PETROLOGY AND MINERALOGY OF THE BASAL ZONE

ROCK TYPES IN THE BASAL ZONE

In the field, various igneous rocks, concentrations of sulfide minerals, hornfelsed metasedimentary rocks, and complex breccias were mapped as part of the Basal zone (fig. 5). The last two rock types are not strictly part of the Stillwater Complex but were included in the Basal zone where their dimensions are too small to separate at the

mapping scale and because they are closely related to the processes that formed the Basal zone. Table 2 shows schematically the interrelations of the six major rock types included in the Basal zone. The table shows that contributions from metasedimentary rocks and silicate-sulfide magma that formed the Basal zone are clearly interrelated and generated two groups of rock with mixed origins—the partial melts and contaminated rocks.

The Basal zone has been divided into four major textural types of igneous rocks: Cumulate rocks, noncumulate igneous-textured rocks, contaminated rocks, and rocks possibly derived by partial melting. In addition to the four major types of igneous rocks there are small areas of authornfelsed noncumulate rocks. This division of the Basal zone emphasizes the different processes involved in the formation of the igneous rocks of the Basal zone. Cumulate rocks owe their formation to various sedimentary processes in the magma chamber whereas the noncumulate igneous-textured rocks were derived by more typical crystallization processes. Contaminated rocks formed as a result of reaction between the magma and the metasedimentary basement rocks and appear to be distinct from those igneous rocks derived by partial melting of the metasedimentary rocks. Autohornfelsed noncumulate rocks are igneous rocks that were apparently metamorphosed after solidification by the magma from which they crystallized. The Basal norite contains all five rock types, whereas the Basal bronzite cumulate consists only of cumulates.

Sulfides are comagmatic with the silicate minerals in the Basal zone, and sulfide-bearing rocks are of three types. Massive sulfide rocks contain more than 60 percent pyrrhotite, pentlandite, and chalcopyrite; the balance of the rock is plagioclase or pyroxene phenocrysts and hornfels inclusions. Sulfides that occur as isolated blebs, aggregates, or grains throughout rocks are classed as disseminated sulfide. Between these two extremes is matrix sulfide rock in which the sulfide material forms a connected and continuous network between silicate grains; sulfide content ranges from about 10 to 60 percent.

Hornfelsed metasedimentary rocks compose part of the Basal zone as inclusions and rafts too small to map. The various assemblages in the hornfels have been discussed in detail by Page (1977) and Page and Koski (1973). The most common assemblage in the metasedimentary rocks is cordierite - orthopyroxene - quartz - plagioclase - biotite. A commonly occurring material which locally marks the contact between the Basal zone and country rocks is a breccia consisting of angular hornfels fragments in a matrix of igneous rocks and sulfides.

The number of rocks in any one locality or stratigraphic section is large and their relations complex. A general idea of the abundance, variety, and distribution of the rocks may be seen in the individual sections shown in figure 5. Thinner cumulate layers have been exaggerated slightly in apparent thickness to illustrate the variety of rocks. In general, there is a repetitive sequence of noncumulate and cumulate igneous rocks associated with metasedimentary inclusions or rafts. The sequence is increasingly dominated by cumulates upward in the sections. No intrusive relations between the repetitions of noncumulates and cumulates have been

TABLE 2.—*Rocks in the Basal zone of the Stillwater Complex, Montana*

Silicate-sulfide magma	Cumulates	Orthopyroxene cumulates	Planar, Linear	With or without inverted pigeonite, phenocrysts or olivine or plagioclase or quartz
		Inverted pigeonite cumulates		
		Plagioclase cumulates		
		Clinopyroxene cumulates		
		Chromite cumulates		
		Orthopyroxene+olivine cumulates		
		Orthopyroxene+inverted pigeonite cumulates		
		Orthopyroxene+plagioclase cumulates		
		Plagioclase+olivine cumulates		
		Plagioclase+inverted pigeonite cumulates		
		Clinopyroxene+olivine cumulates		
	Noncumulates		Ophitic textured, Subophitic textured, Ragged textured	
	Sulfide rocks	Massive sulfide		
		Matrix sulfide		
		Disseminated sulfide		
Metasedimentary rocks.	Contaminants	Cordierite replaced by plagioclase		
		Rocks crystallized from contaminated magma		
	Partial melts	Orthopyroxene (unexsolved)+plagioclase+quartz+biotite+opaque minerals		
	Contact metamorphic rocks.	Orthopyroxene-cordierite-biotite-quartz-plagioclase hornfels		
		Anthophyllite-cordierite-biotite-quartz-plagioclase hornfels		
		Biotite-cordierite-quartz-plagioclase hornfels		

observed, and none of the repetitions can be readily correlated from area to area. This suggests that repeating units have tabular lens shapes with strike dimensions of less than 1 km.

CUMULATE ROCKS OF THE BASAL ZONE

Cumulate rocks consist of (1) crystals and other elements such as sulfide-oxide liquids that accumulated by settling either under the influence of gravity alone or of currents and

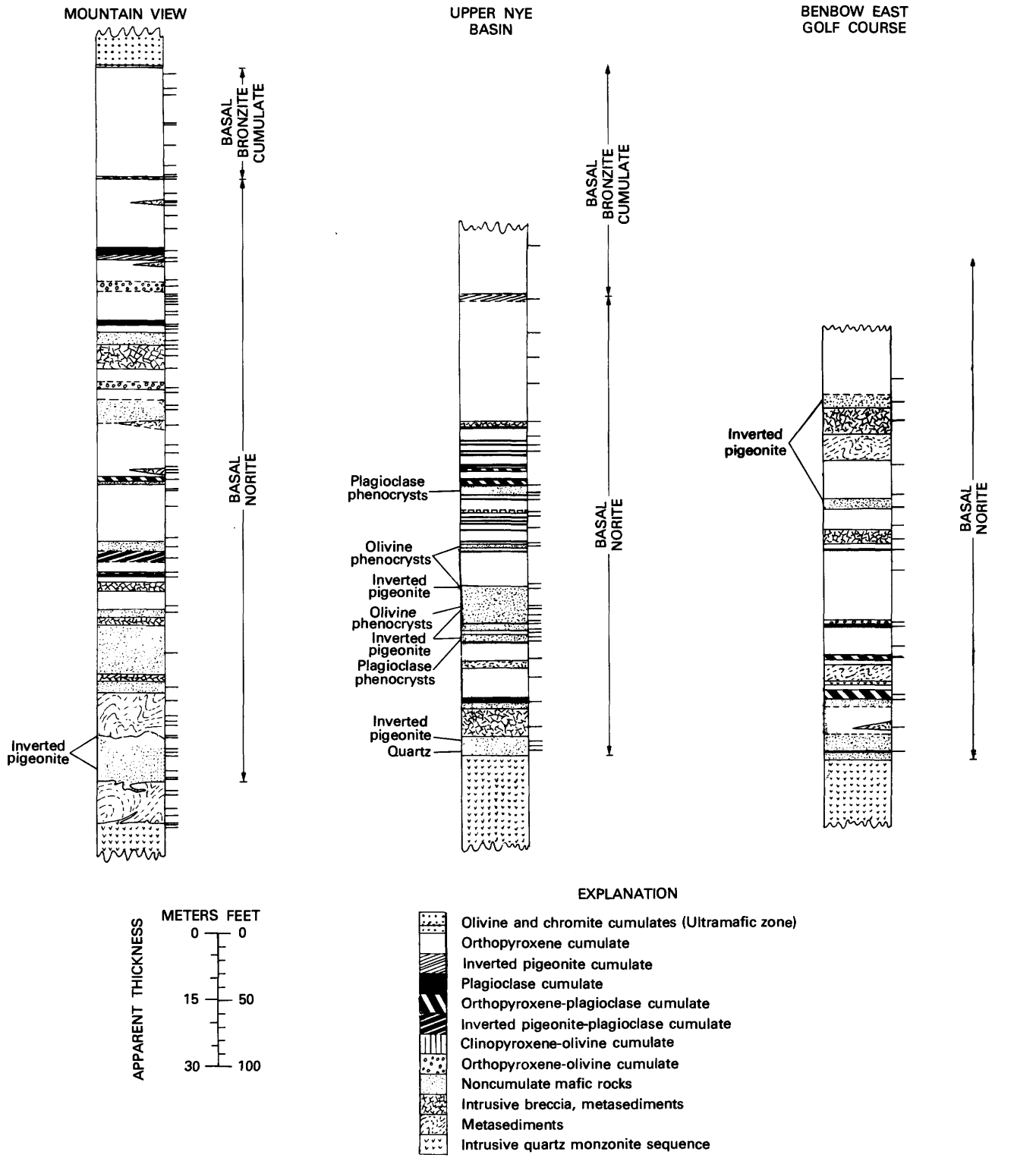

FIGURE 5. Sections showing rocks and mineralogy in Basal zone, based on detailed logging and extensive thin section examination of core. Horizontal bars on the right of each section indicate locations of thin sections.

TABLE 3.—*Generalized petrographic descriptions of cumulate rock types in the Basal zone*

[From thin sections, polished sections, and etched rock slabs. CPX, clinopyroxene; OPX, orthopyroxene; PX, pyroxene; PIG, pigeonite; OL, olivine; PL, plagioclase; QZ, quartz; KSPAR, potassium feldspar; HBN, hornblende; BIO, biotite; OPAQ, spinels and sulfides; EN, Mgx100/(Mg+Fe+Ca) by X-ray; AN, Cax100/(Ca+Na+K) by X-ray; FO, Mgx100/(Mg+Fe+Ca) by X-ray; Tr, trace]

Rock name: Orthopyroxene cumulate | **Number of sections examined: 271** | **Number of modes: 57**

Constituent minerals	Volume percent		Size range (mm)	Sorting	Crystallinity	Shape and texture	Internal features of crystals		Composition range	Alteration
	Range	Average					Exsolution, twinning	Zoning		
Orthopyroxene...	44.9-81.8	61.9	<1-35	Well to moderate	Euhedral-subhedral.	Cumulus, equidimensional, broad, narrow prismatic.	CPX blebs and lamellae || (100).	None to slight.	EN=30-97, average of 463=69.6.	Serpentine, talc, chlorite.
Clinopyroxene....	0-25.9	10.4	<1-30	.....	Anhedral-subhedral.	Postcumulus, poikilitic, interstitial, local granulation.	OPX lamellae || (100); twinned.	Present....	.....	Blue-green amphibole.
Plagioclase.....	7.4-40.7	23.9	<1-20	.....	do	Postcumulus; pokilitic, tabular mosaics; interstitial.	Twinned.....	Common.	.....	Epidote, sericite.
Brown hornblende.	0-3.6	.29	<1-4	.....	do	Postcumulus, interstitial, locally rims PX, intergrown with PX.				Green and clear amphibole.
Biotite.....	0-1.2	.35	<1-2	.....	do	Postcumulus, interstitial, locally poikilitic.				Chlorite.
Quartz.....	0-6.0	.32	<1-2	.....	Anhedral.....	Postcumulus, interstitial.				
Spinels	0-21.6	3.1	<1-2	.....	Subhedral-euhedral.	Inclusions locally in OPX.....			Spinel (locally chromite), magnetite; magnetite-ilmenite intergrowths.	
Sulfide minerals.			.....	.....	.....	Fill pores, inclusions in OPX.			Pyrrhotite, pentlandite, chalcopyrite.	
Apatite	0-0.2	Tr	<1	.....	Euhedral.....	Inclusions in BIO.				
Olivine	0-0.7	.01	<1	.....	Subhedral.					

Reactions inferred and observation:

1. Orthopyroxene→clinopyroxene; rounded OPX in CPX.
2. Orthopyroxene→quartz; irregular OPX locally against QZ.
3. Orthopyroxene+magma → orthopyroxene with overgrowth.
4. Orthopyroxene→brown hornblende, irregular OPX against HBN.
5. Clinopyroxene→brown hornblende, irregular CPX against HBN.

Special features or variants:

1. 0.7 percent olivine, armored by CPX, in clots, like xenocrysts in one sample.
2. Locally shows bimodal distribution of OPX grain sizes.
3. Spinel (dark opaque) euhedral inclusions, locally oin OPX.
4. Local green-brown isotropic (spinel?) platelets exsolving parallel to (100) plane of CPX + OPX.

Crystallization sequence: OPX, CPX and PL, HBN, BIO, QZ, OPAQ.

Rock name: Plagioclase cumulate — **Number of sections examined: 29** — **Number of modes: 8**

Constituent minerals	Volume percent: Range	Volume percent: Average	Size range (mm)	Sorting	Crystallinity	Shape and texture	Internal features of crystals: Exsolution, twinning	Internal features of crystals: Zoning	Composition range	Alteration
Orthopyroxene	15.5-35.8	18.6	<1-8	.....	Anhedral	Postcumulus, interstitial, poikilitic.	CPX lamellae || (100).	.....	EN=57.5-69.2	Talc, chlorite.
Inverted pigeonite (orthopyroxene).	0-1.5	...	<1-5	.....	do	Postcumulus, interstitial	Coarse discontinuous lamellae and blebs.			
Clinopyroxene.... pyroxene.	0-35.0	6.9	<1-5	.....	do	do	OPX lamellae || (100).			
Plagioclase	53.3-73.4	63.0	<1-10	.....	Euhedral-subhedral.	Cumulus, tabular, stubby prisms.		Common..	AN=65.3-77.2	Epidote, sericite.
Brown hornblende	0-1.7	.59	<1-2	.....	Anhedral	Postcumulus	.....	.....	.....	Chlorite.
Biotite	0-1.2	.54	<.25-1	.....	do	do.				
Quartz	0-3.7	.66	<.25-1	.....	do	Postcumulus, blebs in PL, interstitial.				
Spinels	1.7-6.3	3.3	<1-2							
Sulfide minerals			.....							
Apatite	0-Tr	Tr	<.5							

Reactions inferred:
1. Pigeonite exsolved clinopyroxene→orthopyroxene exsolved clinopyroxene.
2. Orthopyroxene→clinopyroxene.

Crystallization sequence: PL, PIG, OPX, CPX, HBN, BIO, OPAQ.

Rock name: Orthopyroxene-plagioclase cumulate — **Number of sections examined: 16** — **Number of modes: 7**

Constituent minerals	Volume percent: Range	Volume percent: Average	Size range (mm)	Sorting	Crystallinity	Shape and texture	Internal features of crystals: Exsolution, twinning	Internal features of crystals: Zoning	Composition range	Alteration
Orthopyroxene...	17.7-50.8	34.4	>2-15	.....	Euhedral-subhedral.	Cumulus, elongate prisms.	CPX lamellae and blebs || (100).		EN=67.1-73.8	
Clinopyroxene....	Tr-22.0	7.4	>.15-10	.....	Anhedral	Postcumulus, poikilitic, interstitial.	OPX lamellae || (100).			
Plagioclase	36.4-74.0	52.0	>1-3	.....	Subhedral-euhedral.	Cumulus, tabular, granular.		Common..	AN=75-78	Epidote.
Brown hornblende.	.3-3	1.1	>1	.....	Anhedral-subhedral.	Postcumulus, interstitial.				Clear amphibole.
Biotite	0-1.0	.43	>.5	.....	Anhedral	Postcumulus.				
Quartz	0-4.2	.60	>.5	.....	do	do.				
Spinels	>0.1-11.9	2.7	.....	.....	.....	.....	.....	.....	Magnetite-ilmenite.	
Sulfide minerals.			.....	.....	.....	.....	.....	.....	Pyrrhotite, chalcopyrite, pentlandite.	
Apatite	0-Tr	Tr	.....	.....	Euhedral.					

Reactions inferred:
1. Orthopyroxene brown hornblende.

Crystallization sequence: OPX and PL, CPX, HBN, BIO, QZ.

TABLE 3.—*Generalized petrographic descriptions of cumulate rock types in the Basal zone—Continued*

Rock name: Orthopyroxene-olivine cumulate — **Number of sections examined: 7** — **Number of modes: 7**

Constituent minerals	Volume percent Range	Volume percent Average	Size range (mm)	Sorting	Crystallinity	Shape and texture	Internal features of crystals: Exsolution, twinning	Internal features of crystals: Zoning	Composition range	Alteration
Orthopyroxene	29.9-50.0	38.2	2-4	Well-moderate.	Euhedral-subhedral.	Cumulus, broad, stubby prisms.	CPX lamellae and blebs || (100).		EN=74.35-74.90	Serpentine.
Clinopyroxene	5.0-20.3	14.0	1-1.5		Anhedral	Postcumulus, poikilitic rims OL, interstitial.	OPX lamellae ‖ (100) opaque blades; twinned.			
Olivine	3.0-25.5	18.0	.2-1.5	Well-moderate	Subhedral-euhedral.	Cumulus, locally anhedral branching crystals.			FO=67.7-73.1	Serpentine, talc, magnetite.
Plagioclase	16.7-32.0	22.8	2-5		Anhedral-subhedral.	Postcumulus, poikilitic, interstitial, granular mosaic.			AN=64.7-78.3	Epidote, sericite.
Brown hornblende	0-5.3	1.5	>.5		do	Postcumulus, locally rims, biotite, rims spinels.				
Biotite	0-1.9	.52	.2-1.0		do	Postcumulus, rims opaques, interstitial.				
Spinels	0-13.9	6.8	>.1-1.0		Euhedral	Interstitial and inclusions.			Chromite.	
Sulfide minerals.			>.1-2.0		Subhedral-anhedral.	do			Pyrrhotite, pentlandite, chalcopyrite.	

Reactions inferred and observation:
1. Olivine resorbed by magma-anhedral branching grains.
2. Olivine + magma → orthopyroxene-subhedral, rounded OL against OPX.
3. Orthopyroxene+magma → clinopyroxene-subhedral, rounded in OPX, in CPX.

Variants:
1. Locally olivine occurs in clotty areas, some rimmed by CPX.
2. Olivine grains have reentrants and textures of resorbed quartz.

Crystallization sequence: OL and spinels, OPX, PL and CPX, BIO, HBN.

Rock name: Inverted pigeonite cumulate — **Number of sections examined: 2** — **Number of modes: 1**

Constituent minerals	Volume percent Range	Volume percent Average	Size range (mm)	Sorting	Crystallinity	Shape and texture	Internal features of crystals: Exsolution, twinning	Internal features of crystals: Zoning	Composition range	Alteration
Inverted pigeonite (orthopyroxene).	57.1				Subhedral-anhedral	Cumulus	Coarse, discontinuous lamellae, blebs; fine lamellae || (100).		EN=61.8	Chlorite, talc.
Clinopyroxene	10.8				Anhedral	Postcumulus.				
Plagioclase	23.8				do	do		Common	AN=77.4	
Brown hornblende	.9				do	do.				
Biotite	.1				do	do.				
Spinels and sulfides.	7.3									

Crystallization sequence: PIG, CPX, PL, HBN, BIO.

Rock name: Orthopyroxene-inverted pigeonite cumulate — **Number of sections examined: 2**

Constituent minerals	Volume percent Range	Volume percent Average	Size range (mm)	Sorting	Crystallinity	Shape and texture	Internal features of crystals: Exsolution, twinning	Internal features of crystals: Zoning	Composition range	Alteration
Orthopyroxene			1-2	Well-moderate.	Euhedral	Cumulus	CPX lamellae and blebs || (100).		EN=65.8-68.6	
Inverted pigeonite (orthopyroxene).			~1-2	do	Subhedral	do	Coarse, discontinuous lamellae and blebs.			
Clinopyroxene			2-5		Anhedral	Postcumulus, poikilitic, interstitial.	OPX lamellae || (100), twinned.			
Plagioclase			2-5		do	Postcumulus, poikilitic, vermicular intergrowth with QZ(?), KSPAR(?).			AN=67.5	
Brown hornblende.			>.5		do	Postcumulus, interstitial rims OPX, OPAQ.				
Biotite			>.3		do	Postcumulus, interstitial, inclusions, rims OPAQ.				
Spinels and sulfides.			>.1-4		Anhedral-subhedral.	Interstitial and inclusions.			Oxides, pyrrhotite, pentlandite, chalcopyrite.	

Reactions inferred and observation:
1. Orthopyroxene→brown hornblende, OPX irregular edge against HBN.
2. Orthopyroxene + magma→clinopyroxene; OPX irregular edges against CPX.

Crystallization sequence: PIG, OPX, CPX, PL, HBN, BIO.

Rock name: Clinopyroxene cumulate — **Number of sections examined: 3** — **Number of modes: 1**

Constituent minerals	Volume percent Range	Volume percent Average	Size range (mm)	Sorting	Crystallinity	Shape and texture	Internal features of crystals: Exsolution, twinning	Internal features of crystals: Zoning	Composition range	Alteration
Orthopyroxene	14.2		4-6		Anhedral-subhedral.	Postcumulus, poikilitic plates.	CPX lamellae || (100).			Serpentine.
Clinopyroxene	69.9		.5-2.0	Moderate	Euhedral-subhedral.	Cumulus	OPX lamellae || (100).			
Plagioclase	13.7		1-5		Anhedral	Postcumulus, interstitial, poikilitic.		Common.		
Biotite	.2		.1-.3		do	Postcumulus, rims on opaques.				
Spinels and sulfides.	2.0		>.1-.3		Subhedral	Interstitial and inclusions.			Oxides and pyrrhotite.	

Special features: Occurs in contact with hornfels.
Crystallization sequence: CPX, OPX, and PL, BIO.

TABLE 3.—*Generalized petrographic descriptions of cumulate rock types in the Basal zone*—Continued

Rock name: Inverted pigeonite cumulate — **Number of sections examined: 1**

Constituent minerals	Volume percent Range	Volume percent Average	Size range (mm)	Sorting	Crystallinity	Shape and texture	Internal features of crystals: Exsolution, twinning	Internal features of crystals: Zoning	Composition range	Alteration
Inverted pigeonite (orthopyroxene).	32.1	.....	.8-2.4 original. 2.0-6.9 overgrowth.	Moderate	Subhedral.....	Cumulus, locally shows poikilitic texture.	Broad, discontinuous lamellae and blebs.		EN=60.8	
Clinopyroxene....	1.5	.....	>1.0	.....	Anhedral.....	Postcumulus, interstitial.	OPX lamellae || (100).			
Plagioclase.....	44.4	.....	2.4-5.0	Moderate	Euhedral	Cumulus, tabular, stubby prisms.	Twinned.			
Quartz.....	.3	.....	.2-.5	.....	Anhedral.....	Postcumulus, interstitial.			AN=80.0	
Brown hornblende.	.1	.....	>.25	.....	do	do.				
Biotite.....	.3	.....	.12-.6	.....	do	do.				
Spinels and sulfides.	21.0	.....	2.0-5.0	.....	do	Pore filling			Pyrrhotite, pentlandite, chalcopyrite.	

Reactions inferred: After pigeonite accumulated and inverted had overgrowth of orthopyroxene to produce some grains with poikilitic texture.

Special features: Cordierite xenocryst, one grain.

Crystallization sequence: PIG and PL, OPX, CPX, HBN, BIO, QZ.

Rock name: Plagioclase-olivine cumulate — **Number of sections examined: 1**

Constituent minerals	Volume percent Range	Volume percent Average	Size range (mm)	Sorting	Crystallinity	Shape and texture	Internal features of crystals: Exsolution, twinning	Internal features of crystals: Zoning	Composition range	Alteration
Orthopyroxene (inverted pigeonite).	11.0	.....	1-2	.....	Anhedral.....	Postcumulus, irregular, interstitial.	CPX lamellae || (100) discontinuous, irregular blebs.		EN=70.8	
Clinopyroxene....	18.4	.....	1-2	.....	do	Postcumulus, poikilitic, interstitial.	OPX lamellae || (100).			
Olivine.....	14.2	.....	.5-1.5	Well	Subhedral-euhedral.	Cumulus, enclosed in OPX				Serpentine magnetite.
Plagioclase.....	55.1	.....	1-1.5	Well-moderate.	Euhedral-subhedral.	Cumulus, tabular		Common.	AN=72.4	
Brown hornblende.	.9	.....	>.5	.....	Anhedral.....	Postcumulus, interstitial, rims on OPAQ.				
Spinels and sulfides.	.2	.....	>.2	.....	do	Inclusions and interstitial.			Oxides sulfides, chromite (?).	

Special features: About one-tenth of OPX is inverted pigeonite.
Crystallization sequence: OL, PL, OPX, CPX, HBN.

Rock name: Clinopyroxene-olivine cumulate — **Number of sections examined: 1**

Constituent minerals	Volume percent: Range	Volume percent: Average	Size range (mm)	Sorting	Crystallinity	Shape and texture	Internal features of crystals: Exsolution, twinning	Internal features of crystals: Zoning	Composition range	Alteration
Orthopyroxene		11.0	2-3		Anhedral	Postcumulus, poikilitic plates	CPX lamellae || (100).		EN=92.4	
Clinopyroxene (1).		51.7	.5-2.0	Moderate	Euhedral-subhedral.	Cumulus, stubby prisms.	No exsolution or twins.		Low 2V+	
Clinopyroxene (2).			1-3		Anhedral	Postcumulus, poikilitic	OPX lamellae || (100), twinned inclusions or PL, CPX(1), BIO, OPAC.		Mod 2V	
Olivine		3.8	.9-1.2	Well	Euhedral-subhedral.	Cumulus, equidimensional				Talc, serpentine.
Plagioclase		20.4	.5-3.0		Anhedral-subhedral.	Postcumulus, poikilitic, granular, tabular.		Common.	AN=66.0	
Brown hornblende.		2.8	>.5		do	Interstitial, rims on ore.				
Biotite		.2	>.5		Anhedral	Rims on ores.				
Spinels and sulfides.	9.3		>.1-5.0		Anhedral-subhedral.	Interstitial, inclusions irregular.				

Special features: Traces of very highly birefringent brown mineral (sphene?) in CPX.
Crystallization sequence: OL, CPX(1), PL, CPX(2), OPX, HBN, BIO.

Rock name: Chromite cumulate — **Number of sections examined: 1**

Constituent minerals	Volume percent: Range	Volume percent: Average	Size range (mm)	Sorting	Crystallinity	Shape and texture	Internal features of crystals: Exsolution, twinning	Internal features of crystals: Zoning	Composition range	Alteration
Clinopyroxene			1.0-6.0		Anhedral-subhedral.	Postcumulus, poikilitic	OPX lamellae || (100)			Serpentine, chlorite, talc.
Plagioclase			.3-1.2		Anhedral	Postcumulus, granular, poikilitic.	Twinned.			
Chromite			.24-.60	Well to moderate.	Euhedral	Cumulus, octahedra.				

Special features: Bands of dominantly chromite-plagioclase, interbanded with highly altered silicate cumulate, possibly orthopyroxene cumulate.

gravity and (2) postcumulus material that crystallized later in the pores of the rocks. Cumulate terminology used in this report is that of Jackson (1967), who developed it for and applied it to other parts of the Stillwater Complex. Other cumulate terminologies exist, and cumulate processes in other complexes are well described (Wager and Brown, 1967). Modal or chemical compositions of cumulate rocks reflect the combined processes of accumulation and postcumulus deposition and are not equal to the composition of the magma from which they formed.

In the Basal zone, orthopyroxene, inverted pigeonite, clinopyroxene, plagioclase, olivine, spinel (chromite, magnetite), ilmenite, and sulfide phases are the cumulus minerals. For a particular rock, any one or as many as three of these minerals can be cumulus phases and the other minerals, postcumulus phases. Other important postcumulus minerals are brown hornblende, biotite, and quartz. As shown in table 3 and figure 5, various cumulates occur in the Basal zone. The Basal bronzite cumulate member consists of dominantly orthopyroxene cumulates, but locally thin lenses or layers of chromite and inverted pigeonite cumulates occur.

Table 3 summarizes the petrographic and mineralogic descriptions of the cumulate rocks observed in the Basal zone. Most of the terminology in the table is that commonly used in describing cumulate rocks. The material referred to as inverted pigeonite is now orthopyroxene and commonly has two sets of exsolution lamellae: (1) Thin lamellae (assumed to be clinopyroxene) parallel to the (100) plane of orthopyroxene, and (2) coarse discontinuous blebs and lamellae oriented on irrational planes in the orthopyroxene. The latter set is indicative of primary crystallization of pigeonite which, on cooling, exsolved augite and inverted to orthopyroxene (Poldervaart and Hess, 1951; Brown, 1957; von Gruenewaldt, 1970), which later exsolved clinopyroxene parallel to the (100) plane. It is important to distinguish this type of orthopyroxene which crystallized from the magma as pigeonite from the more abundant orthopyroxene which crystallized as orthopyroxene. Sorting is used to describe the spread in cumulate grain size in a particular rock (Jackson, 1961a, p. 28). Compositions of mineral phases were determined by X-ray techniques (Jackson, 1960, 1961b; Hotz and Jackson, 1963; Himmelberg and Jackson, 1967).

From figure 5 and table 3 it is apparent that orthopyroxene cumulates are most abundant and that plagioclase and plagioclase+orthopyroxene cumulates are next most abundant. The eight other cumulate types form only a small part of the rock sequence. Irvine's (1970a) listing of theoretical cumulate mineral combinations suggests that other unrecognized combinations of cumulate minerals may be present in the Basal zone.

The compositions of orthopyroxene and plagioclase in Basal zone rocks are summarized as histograms in figure 6. The average composition of orthopyroxene is $En_{68.9}$, and the plagioclase is $An_{77.8}$. Only five olivine compositions were obtained from the Basal zone with an average of $Fo_{70.7}$ and a narrow range of $Fo_{67.7}$ to $Fo_{73.1}$.

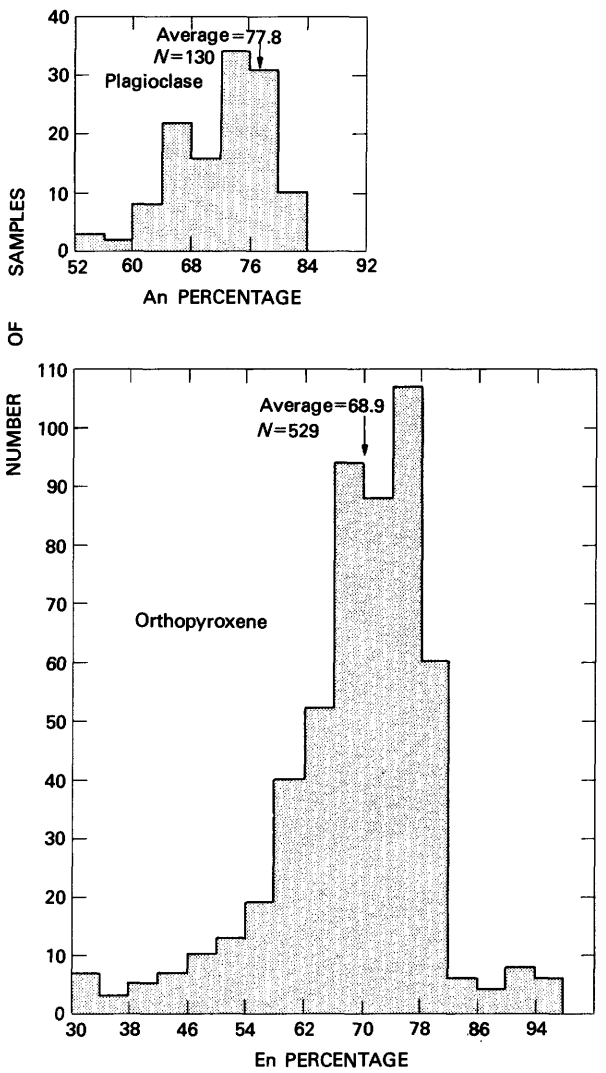

FIGURE 6.—Orthopyroxene and plagioclase compositions. N, total number of samples.

CUMULATE SEQUENCES

The relations of some cumulate rocks are shown in figure 5 for three sections of the Basal zone; plate 1 shows additional sections but in much less detail. In most layered complexes (Wager and Brown, 1967; Irvine, 1970a) and in the Ultramafic zone of the Stillwater Complex (Jackson, 1970), there are repetitive sequences of cumulate minerals and distinctive orders of appearance of cumulate rocks which are thought to be diagnostic of magma composition and conditions of crystallization in those complexes. All theoretical cumulate sequences (Irvine, 1970a, p. 468-472) begin with a one-phase cumulate rock which is followed by a two-phase cumulate rock. The theoretical sequence ends with a three- or four-phase cumulate. Such a sequence forms a cyclic unit. In the Stillwater Complex, an example of a

normal complete cyclic unit is the sequence of olivine, olivine+bronzite, and bronzite cumulates of the Peridotite member (Jackson, 1961a, 1963). Jackson (1970, p. 390-401) called cyclic units which lacked one or more members at the top of the sequences beheaded. Within this framework there are no recognizable complete cyclic units in the Basal zone, only parts of units. The partial sequences that are most important are (1) orthopyroxene, orthopyroxene + plagioclase, (2) olivine + orthopyroxene, orthopyroxene and, (3) plagioclase, plagioclase+orthopyroxene.

As pointed out by Irvine (1970a, p. 463), such short partial sequences of cumulates can represent several crystallization orders. In the Stillwater Complex several other pieces of evidence limit the choices of crystallization orders. First, the presence of olivine and plagioclase phenocrysts in the noncumulate igneous rocks indicates that olivine and plagioclase were the first minerals to crystallize from the magma, even though no olivine cumulates have been positively recognized in the Basal zone. Therefore, the crystallization order and cumulate sequence in the Basal zone must be such that either olivine or plagioclase form the first cumulates. Secondly, the order and sequence probably should be consistent with the order and sequence in the stratigraphically higher zones of the complex. Hess (1960), Jackson (1961a), and Page (1977) have established the crystallization order above the Basal zone as olivine, orthopyroxene, plagioclase, clinopyroxene, which produces the cumulate sequence olivine, olivine+bronzite, bronzite, bronzite + plagioclase, and bronzite + plagioclase + clinopyroxene. Two of the beheaded cumulate sequences in Basal zone—orthopyroxene, orthopyroxene+plagioclase and olivine+bronzite, bronzite—fall within this general scheme and probably account for more than three-fourths of the cumulates in the Basal zone.

The sequence plagioclase, plagioclase+orthopyroxene seems to represent another crystallization order and cumulate sequence. The probable order is plagioclase, orthopyroxene, clinopyroxene, and the sequence is plagioclase, plagioclase+orthopyroxene, plagioclase + clinopyroxene + orthopyroxene. Further evidence of this sequence will be presented in later sections of the report.

During study of the Basal zone, specific features were selected for study in anticipation that they would offer means of stratigraphic control. Selection was based on the assumption that the feature was controlled by a process operating over the whole magma chamber at, or nearly at, the same time. Size variation of cumulus phases, possible current structures, modal mineral variations, orthopyroxene compositional variations, and plagioclase compositions were examined. None of these features may be used for detailed stratigraphic correlation over distances of kilometers either by themselves or in combination with one another. However, over shorter distances they appear to be of some value in correlating stratigraphic horizons.

SIZE VARIATION OF ORTHOPYROXENE CUMULATES

In the Ultramafic zone, Jackson (1961a, 1970) demonstrated the importance of the variation in grain size of cumulus minerals in establishing cyclic units, and Page, Shimek, and Huffman (1972) showed that size-graded units within individual cumulate layers correlate with other physical and chemical parameters of the layer. Therefore, grain size was considered an important parameter early in the study, and two different approaches were used to record its variation in the Basal zone.

During core logging, visual estimates of average grain size were classified as fine-grained (less than 1 mm), medium-grained (1-5 mm), and coarse-grained (greater than 5 mm). Locally, terms such as "finer medium" and "coarser medium" were used to describe gradational changes in size-graded units, and where grain size varied over short distances (less than a foot) and apparently in a random manner, the grain size was recorded as randomly variable. Estimates of grain size were based mainly on orthopyroxene size, hence grain-size estimates were infrequent for the limited sections of other types of cumulates. Figure 7 summarizes some of these grain-size data for stratigraphic sections representative of the total strike length of the Basal zone.

One of the more striking aspects of the plots (fig. 7) is the repetition of the ascending sequence fine-, medium-, and coarse-grained cumulates, regardless of the stratigraphic section examined. The sequence is the same as that recorded for the cyclic units of the lower part of the Peridotite member (Jackson, 1961a, p. 22-23) and is similar to the repetitions found in a single layer of olivine cumulate (Page, Shimek, and Huffman, 1972). Attempts to correlate grain-size sequences laterally over long distances were not successful. Over short distances correlations have met with only limited success and suggest that lateral continuity for grain-size units is less than 1 km.

The second method of examining grain size was more quantitative and was restricted to a selected segment of the Basal zone in which no cumulate, composition, or grain-size units appeared to form repetitive cycles. The quantified data allow a check on the semiquantitative information and allow comparisons to be made with previously published grain-size studies in the Stillwater Complex (Jackson, 1961a; Page, Shimek, and Huffman, 1972). Length and width measurements of orthopyroxene were made in thin section for six samples spaced over about 56 m of core in the Basal bronzite cumulate from the upper Nye Basin section (fig. 7). The technique and limitations of this method were discussed by Jackson (1961a, p. 21).

The trend from finer to coarser grains expressed as arithmetic means, is apparent (fig. 7) and compares well with the qualitative data on grain-size changes made during core

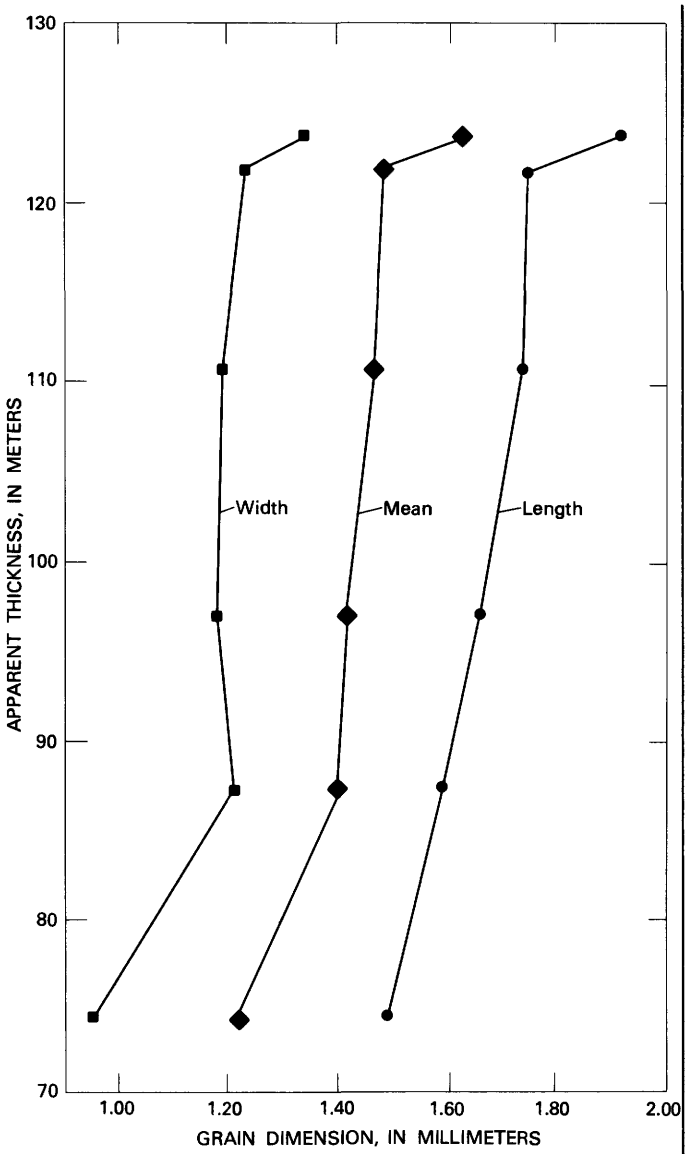

FIGURE 7.—Mean length, width, and average grain size of orthopyroxene versus stratigraphic position for a segment of Basal bronzite cumulate, upper Nye Basin.

logging. The range of average grain size, 1.22-1.63 mm, is mostly within the range of 1.3-2.3 mm reported by Jackson (1961a, p. 26) for orthopyroxene in the Ultramafic zone but is representative of the fact that slightly finer grain sizes are observed in the Basal zone. The width to length ratio of orthopyroxene remains fairly constant (0.64 to 0.76) throughout the section.

Size-frequency distributions of either lengths or widths of orthopyroxene for each sample are log-normal and similar to size-frequency distributions in other parts of the complex. All of the measurements for each sample were combined to examine the size-frequency distribution for this segment of the Basal zone. Because lengths, widths, and mean diameters of the orthopyroxene crystals vary in proportion, only

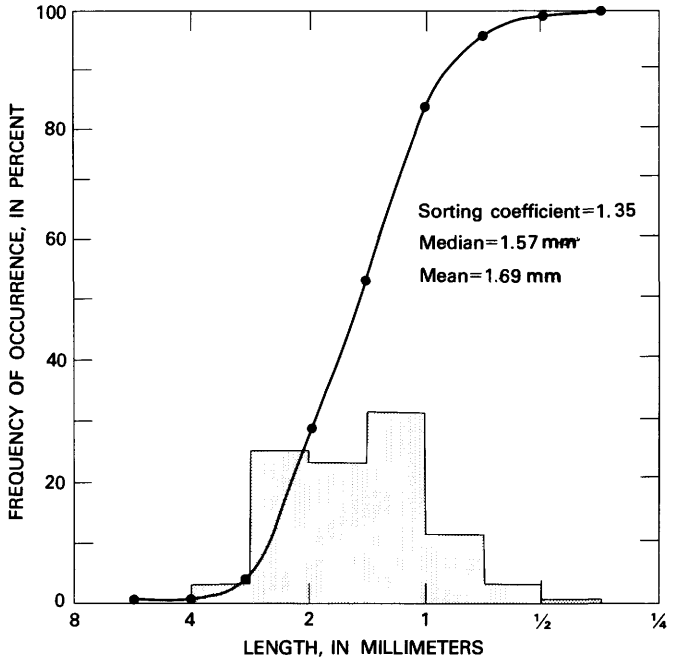

FIGURE 8. Length-frequency distributions of orthopyroxene crystals for a segment of Basal bronzite cumulate, upper Nye Creek Basin.

lengths were used. Figure 8 illustrates the length-distribution both as a histogram and a cumulative frequency curve. The orthopyroxene crystals are remarkably well sorted and have a low sorting coefficient. This is similar to the sorting of olivine, bronzite, chromite, and sulfide grains in the Ultramafic zone (Jackson, 1961a; Page, 1971b; Page, Shimek, and Huffman, 1972).

EVIDENCE FOR CURRENT STRUCTURES

Current structures are apparently rare, or at least not easily detectable in the Ultramafic zone; Jackson (1961a, p. 29) discusses one example of scour and local unconformity in olivine and olivine-chromite cumulates and implies that the smaller chromite grains were winnowed out in that example. Where evidence for magmatic currents is well demonstrated, strongly lineated fabrics of the elongate minerals are found (for example, the Skaergaard Intrusion, Wager and Brown, 1967). In the petrofabric studies (Hambleton, 1947; Jackson, 1961a) and fieldwork in the Ultramafic zone lineated rocks appear to be rare. The apparent rarity of current structures in the Ultramafic zone may in part be due to the poor color contrasts of the minerals that compose most of the zone. In order to overcome this difficulty, more than 1200 samples of core and surface specimens were prepared with flat ground surfaces and etched with hydrofluoric acid. Etching attacks the plagioclase, giving it a chalky white color that may be preserved by spraying the specimen with plastic. Etching provides a background that highlights grain-size distributions, shapes, and packing of the orthopyroxene.

Even with this technique no structures that could be ascribed to magmatic currents were observed in the Basal

bronzite cumulate member, although such structures were found in the Basal norite member. Most discernible structures consist of scours or cuts and local unconformities; many are similar to the ones shown in figure 9. Typically these structures are found at the contacts between orthopyroxene cumulates and either plagioclase or plagioclase+orthopyroxene cumulates. Some show what appear to be truncated layers with up to 35° of apparent angular discordance (fig. 9*A*). Others display small basins, furrows, and hills in the underlying rock that are filled in by the immediately overlying cumulate without the shape being reflected in the next cumulate layer (fig. 9*B*).

In table 2, orthopyroxene cumulates were subdivided into two groups, planar and linear. The terms refer to the apparent orientation of orthopyroxene when the orthopyroxene crystals have a shape other than equidimensional. In planar cumulates, the long dimensions of individual orthopyroxene crystals tend to lie randomly in planes parallel to ratio, phase, and form layering. Jackson (1967) termed this planar lamination. This fabric has been explained (Jackson, 1961a) as due to settling of crystals in a magma without currents. In linear cumulates, the long axes of orthopyroxene crystals also lie in planes parallel to layering but in addition show a linear orientation in that plane. Petrofabric studies of the degree of preferred orientation have not yet been made. Linear fabrics are interpreted to be the result of magmatic currents.

MODAL MINERAL VARIATION IN CUMULATES

Variations in the proportion of mineral constituents of the cumulates in the Basal zone are given in table 3 as ranges and averages. In figure 10, modes of individual samples are plotted in terms of clinopyroxene, orthopyroxene, and plagioclase. This projection was chosen because the bulk modal composition for most samples could be adequately represented even though some rocks contain olivine. Cumulus and postcumulus minerals are combined in the diagram, but the cumulus minerals are indicated in the rock name adjacent to the appropriate symbol. The orthopyroxene and plagioclase cumulates cluster in distinctive groupings near their respective corners of the diagram (fig. 10), and the plagioclase+orthopyroxene cumulates fall between the single-phase cumulates in a somewhat restricted area. Examination of other two-phase cumulates in the Stillwater Complex and Great Dyke (Jackson, 1970, p. 394, 409) suggests that percentages of each cumulate mineral in a two-phase cumulate vary from 10 to 45 percent, a fairly restricted range.

Mineralogical differences between the Basal and Ultramafic zone cumulates are shown by comparison of the averages in table 3 and an average of 132 modes of Ultramafic zone rocks (Jackson, 1961a, p. 5). The Basal zone contains (1) less olivine and correspondingly more orthopyroxene, (2) more plagioclase, generally more than the 7.8 percent average for rocks from the Ultramafic zone,

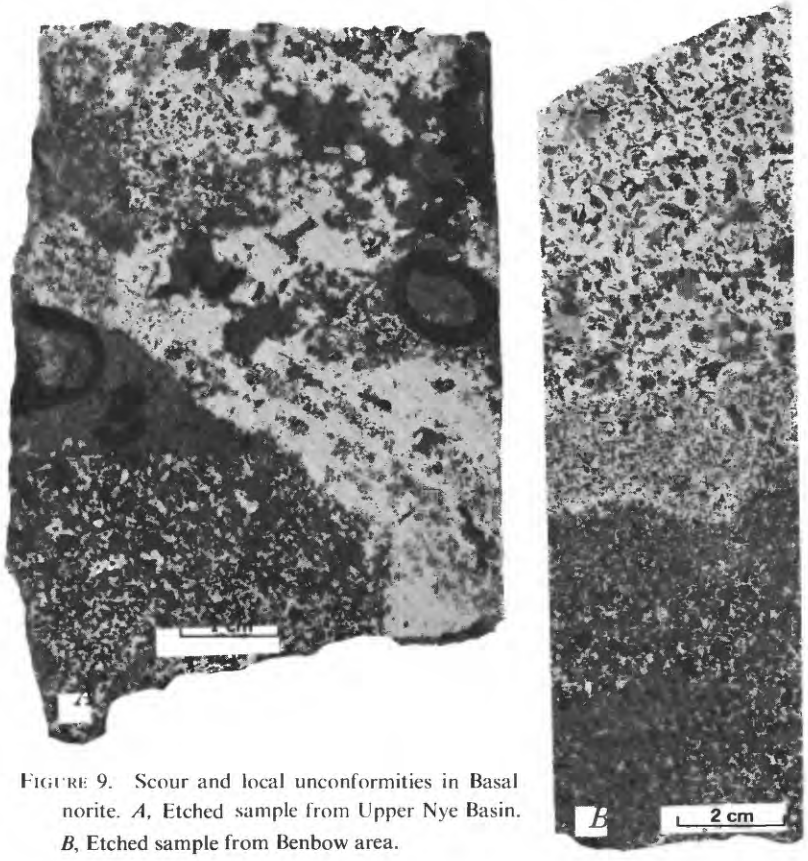

FIGURE 9. Scour and local unconformities in Basal norite. *A*, Etched sample from Upper Nye Basin. *B*, Etched sample from Benbow area.

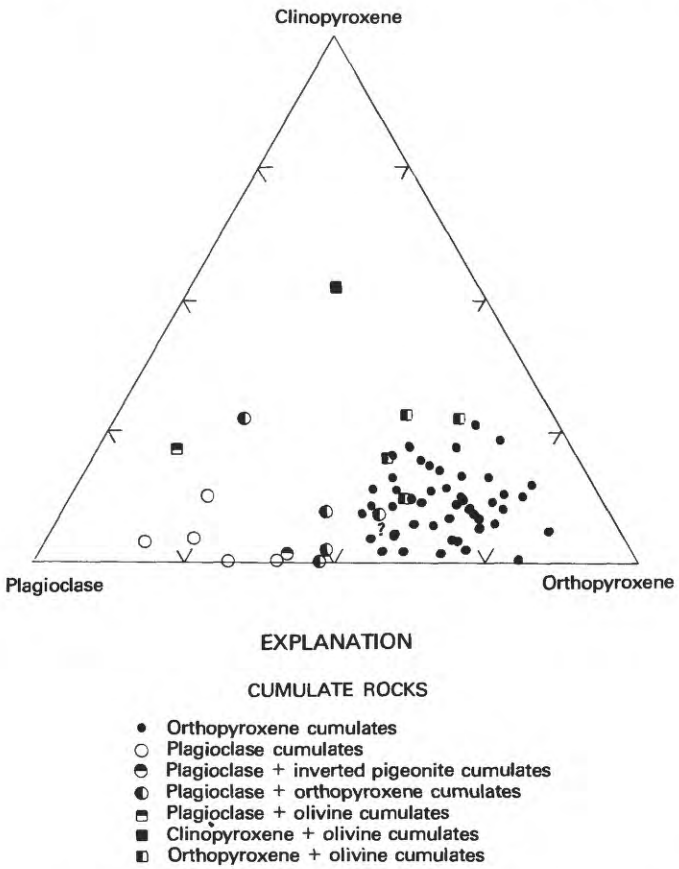

FIGURE 10.—Modes of cumulates from Basal zone projected on the triangular diagram clinopyroxene, orthopyroxene, and plagioclase in volume percent.

and (3) more clinopyroxene in all cumulates except for the plagioclase cumulates. Brown hornblende, biotite, and quartz also appear to be more abundant in the Basal zone than in the Ultramafic zone. The relative abundance of plagioclase and clinopyroxene in the orthopyroxene cumulates (fig. 11) reflects the tendency for the proportion of postcumulus materials to be greater in the Basal zone than in the Ultramafic zone. This relation implies that the cumulus minerals are less tightly packed and have a smaller amount of secondary overgrowth on the average than rocks from higher in the complex. On the basis of four samples, Jackson (1961a, p. 61) argued that secondary enlargement or overgrowth was considerably less in the Basal zone than in the Ultramafic zone.

A segment of core from the Benbow West Golf Course section was selected for more detailed examination of modal variation in the Basal zone. It was chosen because the segment contains two breaks in orthopyroxene compositions and several repetitions of grain-size units. Modes based on at least 1000 points were determined on 41 thin sections representing samples between core depths 62 and 280 m. The volume percentage of orthopyroxene is plotted against stratigraphic position for this segment in figure 11.

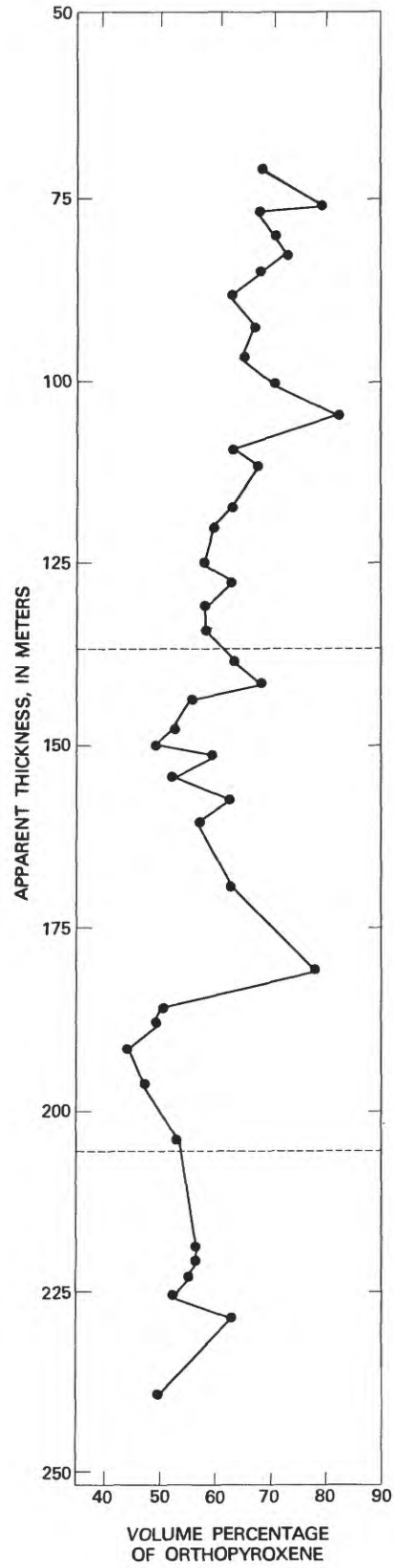

FIGURE 11.—Volume percentage of orthopyroxene in Basal zone plotted against stratigraphic position, Benbow West Golf Course section. Dotted lines represent orthopyroxene compositional units.

The diagram shows that, on the average, the volume percentage of orthopyroxene increases from the bottom to the top of the section. Within the section there are two or three sharp maxima in orthopyroxene content. If the maxima reflect breaks in the accumulation process and are assumed to represent either the bottom or top of a unit, then there are several units in the section marked by a fairly regular increase in the volume of orthopyroxene. These repeated units could be correlated neither with repeated units defined by grain size nor with those defined by orthopyroxene compositions. As orthopyroxene is the only cumulate mineral, the volume of orthopyroxene in the section could reflect relative accumulation rates or varying rates of solidification of the postcumulus material.

LATERAL AND VERTICAL VARIATION OF ORTHOPYROXENE COMPOSITION

Orthopyroxene is the dominant and most widespread mineral in the Basal zone, and because it usually is a cumulus mineral, it has the potential of offering the most information regarding the behavior of the parent magma. Himmelberg and Jackson (1967) developed an X-ray method for determining the ionic percent of magnesium in orthopyroxene based on Stillwater samples. This method yields the value for MgX100/total octahedral cations in orthopyroxene, which will be referred to in this report as the En (enstatite) content of orthopyroxene. Determinations of the En content of orthopyroxene have been made on 529 core and surface specimens from the Basal zones. Fifteen fairly complete stratigraphic sections were selected from this data and are shown on plate 2. Determinations in other sections are not reported because they represented short, incomplete segments of the Basal zone. The precision of these measurements ranges from ±0.05 to ±3.0 percent of the En content and averages ±0.51 percent, which is well within the two-sigma deviation of ±1.3 percent assigned to the determinative survey by Himmelberg and Jackson (1967).

The cross sections and data on plate 2 are fairly representative of the strike length of the complex; all except the Bluebird, Forge Creek, Unnamed Creek, and Boulder River sections are based on drill core. Unfortunately, none of the sections are complete either because of lack of outcrops, limitations in drill core, or inadequate sample collection. All section thicknesses represent true thickness adjusted for the local attitude of the Basal zone and the attitude of the drill hole or traverse section. Schematic rock logs are given for each cross section, and grain-size logs are included where they were available. The contact between the Basal and Ultramafic zones is used as the reference horizon, and the location of each section is illustrated on plate 2. Most of the En contents for orthopyroxene have been connected by lines to emphasize the changes, but the connecting lines do not indicate compositions for intervening orthopyroxenes. The presentation of the data in the form of plate 2 allows lateral and vertical correlations of rock type, grain size, and orthopyroxene composition to be readily visualized.

Several generalizations can be derived from the data. Orthopyroxenes range in En content from 30 to 98, but most En contents for the Basal zone fall between 54 and 82, comparable with the range 50-90 reported for the whole complex (Hess, 1960; Jackson, 1961a). Individual specimens from each stratigraphic section (pl. 2) show a similar gradual increase in En content from the base to the top of the section. The rate of increase in each section is not the same and short-range fluctuations in orthopyroxene composition are superimposed on the gradual increasing trend of En content. Many of the sections show compositional units within the individual trends as defined by sharp increases and decreases in En content.

Well-defined and inferred or suspected unit boundaries are shown on plate 2 as dotted lines. Three to five orthopyroxene composition units can be distinguished in more detailed stratigraphic sections. In the Benbow West Golf Course section the units were numbered sequentially from the lowest unit upward. In three of the adjoining sections, unit correlations appear possible based on the orthopyroxene composition changes, rock types (specifically the presence of plagioclase cumulates), and grain size. For the middle and upper Nye Basin and Benbow East Golf Course sections, tentative unit numbers were assigned. However, the present data do not permit positive correlation with other sections.

COMPOSITIONAL VARIATION OF PLAGIOCLASE

Three textural varieties of plagioclase have been recognized in the Basal zone. By far the most abundant is postcumulus plagioclase. The next most abundant is the cumulus plagioclase of plagioclase and plagioclase+orthopyroxene cumulates. The least abundant variety is plagioclase phenocrysts in noncumulate rocks and phenocrysts as scattered crystals in thin layers but usually not in crystal contact with one another as in other cumulate rocks (pl. 2). Many estimates of plagioclase compositions were made during examination of thin sections, but all compositions reported were determined by the X-ray method of Jackson (1961b) developed specifically for plagioclase from the Stillwater Complex. The uncertainty for the determinative curve is ±2.1 percent An (anorthite) in the range of about An_{65-80} and otherwise is +2.4 percent An (Jackson, 1961b, p. C287). Precision of the measurements made in this study is within these limits. The composition of all varieties of plagioclase in the Basal zone ranges from An_{57} to An_{83}; most compositions fall between An_{65} and An_{80} (fig. 6). These compositions are comparable to the range of An_{69} to An_{77} reported by Jackson (1967) for postcumulus plagioclase in the Ultramafic zone and the range of An_{63} to An_{86} reported for the whole Stillwater Complex (Wager and Brown, 1967, p. 303).

Postcumulus plagioclase compositions were examined in detail for the upper Nye Basin section, but for other sections more or less random samples were checked by the X-ray method. The trends of plagioclase composition with stratigraphic position (fig. 12) are very similar to the trends of orthopyroxene compositions (pl. 2). The overall trend of plagioclase composition in the Basal zone is one of generally increasing An content from the base to the top of the zone. Superimposed on this trend are several sharp fluctuations in An content (fig. 12). Some of the sharp fluctuations in An content coincide with the sharp fluctuations in orthopyroxene compositions in the same section. Postcumulus plagioclase compositions apparently form repeating compositional units which may coincide with those based on orthopyroxene compositions.

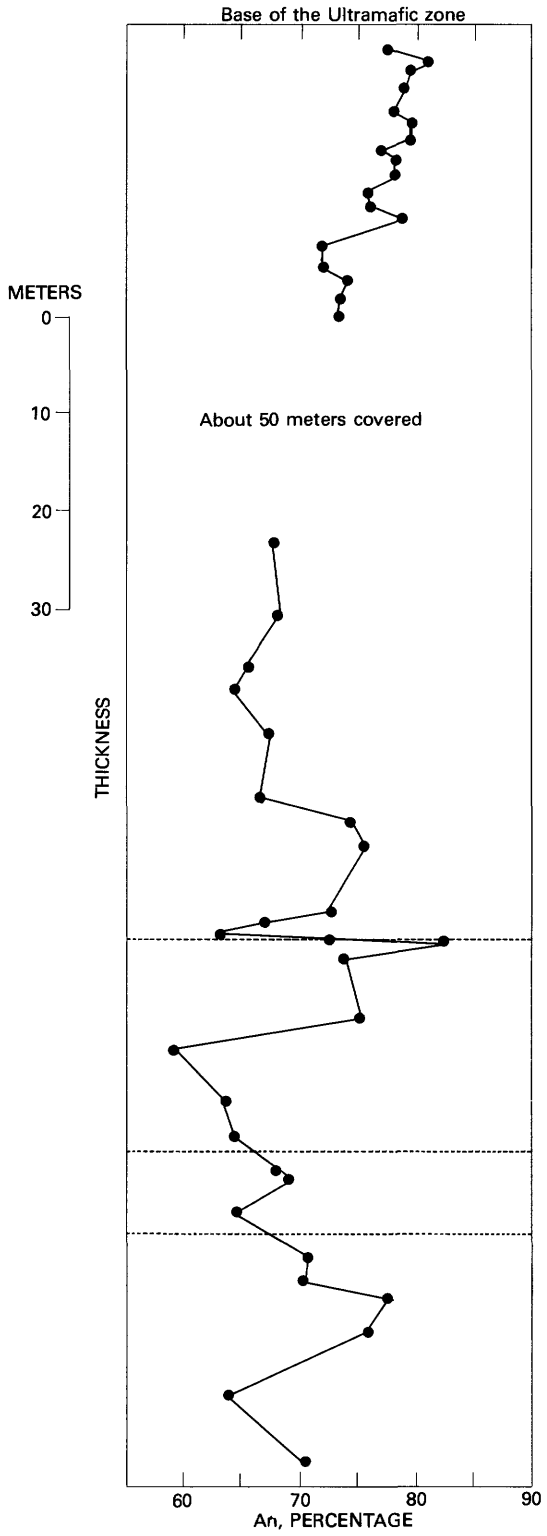

FIGURE 12.—Plagioclase composition plotted against stratigraphic position, upper Nye Basin section. Dotted lines represent orthopyroxene compositional units.

Samples in which both the An content of the plagioclase and the En content of orthopyroxene were determined are plotted in figure 13. Increasing An content shows weak to moderate correlation with increasing En content. The correlation was not expected to be strong because the two minerals originated in different ways. Orthopyroxene is a cumulus mineral and settled under the influence of gravity through some of the magma from which it crystallized, whereas plagioclase is a postcumulus mineral and crystallized in place from magma that was trapped in the cumulus pore spaces. Only if the plagioclase crystallized from trapped magma of the same composition as that which precipitated the orthopyroxene would there be a strong correlation between their compositions. Several processes have been suggested that would modify the composition of the trapped magma. These include chemical diffusion between trapped magma and the main magma (Hess, 1939, 1960), intercumulus convection (Hess, 1972), and crystallization-differentiation (Jackson, 1961a, p. 85). Such processes are probably responsible for the spread in the

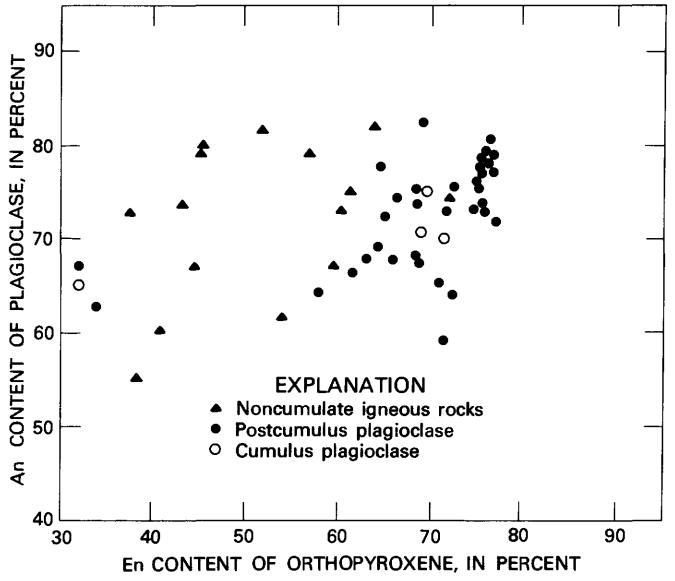

FIGURE 13. Coexisting plagioclase and orthopyroxene compositions in Basal zone.

composition plot. In addition, the spread may indicate a variation in accumulation rates of orthopyroxene if the postcumulus processes are assumed to take place at approximately constant rates.

DISCUSSION OF CUMULATE ROCKS IN THE BASAL ZONE

Although consistent mineralogic, petrologic, and stratigraphic patterns in cumulate rocks in the Ultramafic zone allow correlation over relatively long distances, similar patterns in the cumulate rocks in the Basal zone tend to have relatively little continuity along strike. Thus, a basic distinction between cumulate rocks of the Basal zone and the Ultramafic zone concerns the ratios of thickness to breadth of the tabular units. The chemical processes that formed lithologic and mineral compositional patterns in the Ultramafic zone operated over great lateral distances at the same time, in the same batch of magma, whereas the same processes active during the accumulation of the Basal zone occurred at different times, possibly in different batches of magma, and within localized areas. Cumulate sequences and possibly compositions of cumulus minerals may tentatively be correlated within individual basinlike structures, but because such sequences are not the same between the basinlike structures (compare fig. 4 and pl. 2), correlation of minor units within the Basal zone along the strike of the complex does not appear to be possible with the present data. For example, plagioclase cumulates are abundant in the Nye Basin-Benbow area and appear typical of this basinlike structure but are not abundant in the Mountain View area, another basinlike structure. This suggests that each basinlike structure had its own convection pattern and its own chemical and physical controls, at least through its early history of accumulation.

The fact that grain-size sequences do not correlate, even over short distances and within similar cumulate rock sequences or mineral compositional sequences, indicates that some type of mechanical differentiation was active. The vertical fine- to coarse-grained repetitive sequences are regular throughout the Basal zone and must be the results of the same process. One possible explanation can be based on an analogy to turbidite deposition described by Bouma (1962). In general, deposition from a turbidity current results in a decrease in thickness and grain size away from its source, so that sediments vary laterally in grain size from coarse to fine within the same physical unit. If small batches of magma begin to crystallize within the basinlike structures, become unstable relative to other magma because of the density contrast due to cumulus crystals, travel across the basin in a manner analogous to turbidity currents, and deposit their crystal content, the lateral grain-size variations may be plausibly explained. The variation upward from fine to coarse may be explained by continued crystallization during deposition. Thus, those cumulus crystals at the upper part of the postulated magma mass continued to grow relative to those crystals already deposited at the base of the mass.

IGNEOUS-TEXTURED (NONCUMULATE) ROCKS OF THE BASAL ZONE

Noncumulate igneous-textured rocks of the Basal zone include rocks that may or may not contain phenocrysts but that crystallized virtually in place. These noncumulate rocks have intrusive contacts with the country rocks, and approximate the magma composition from which they formed (table 2). Neither crystal settling under the influence of gravity nor any of the postcumulate processes is considered to have greatly altered the rock compositions or textures.

The noncumulates are subdivided into groups with ophitic, subophitic, and ragged textures (fig. 5). The term "ophitic" as used in this report refers to rocks that contain subhedral to anhedral ortho- or clinopyroxene, which totally encloses lath-shaped plagioclase. Ophitic is not used to suggest the dominance in amount of either plagioclase or pyroxene. Rocks that contain lath-shaped plagioclase partly enclosed in either ortho- or clinopyroxene are termed "subophitic." Ragged-textured rocks are composed of anhedral, very irregularly shaped phenocrysts of pyroxenes, olivine, or plagioclase set in poikiolitic, subophitic, or mosaic-textured groundmasses. Locally, the ragged phenocrysts are closely packed and are surrounded by interstitial material. Ragged-textured rocks appear to be gradational between ophitic and subophitic rocks at one textural extreme and cumulate rocks at the other. These three subdivisions may be further divided on the basis of the mineralogy of the phenocrysts, by the presence of inverted pigeonite or orthopyroxene, and by the presence of absence of quartz. Plagioclase phenocrysts range in An content between 63.4 and 77.2 and average 71.2; olivine phenocrysts have a composition of approximately Fo_{70}.

The proportions of the noncumulate rocks in the Basal norite are difficult to estimate because of the variability in texture over relatively short intervals in outcrop and drill core. Qualitative estimates made during surface mapping suggest that ragged-textured rocks are most abundant, but examination of core and thin section study suggests that the ophitic and subophitic types may be more abundant.

A generalized sequence of noncumulate rocks has been synthesized. This textural sequence from the base upward is ophitic texture, subophitic texture, ragged texture, and cumulate. However, not all rocks need be present, but if more than one type is present, they fit this sequence. As has been shown in figure 5, igneous rock sequences may repeat several times in any particular section, as do cumulates.

MODAL VARIATION OF NONCUMULATE ROCKS

Changes in the proportions of plagioclase, clinopyroxene, and orthopyroxene, representing the major variations in the modal composition of the noncumulate rocks, are illustrated in figure 14. Modes for some of the specimens upon which this diagram is based, those that are chemically analyzed, are

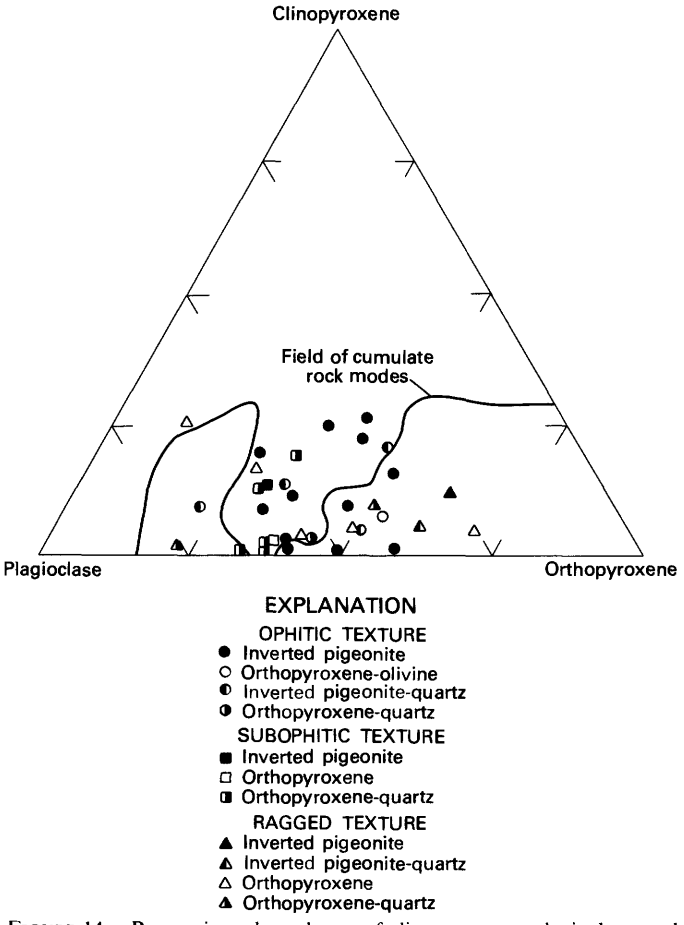

FIGURE 14.—Proportions, by volume, of clinopyroxene, plagioclase, and orthopyroxene in noncumulate rocks.

given in table 4. Each mode was determined by counting 1,000 points in thin section. Two difficulties in gathering the modal data are how to treat alteration products, and how to count exsolution lamellae in the ortho- and clinopyroxenes. Alteration products were counted as primary minerals if the original mineral was readily suggested by shape and texture; if not, the material was counted as alteration. Exsolution lamellae in either orthopyroxene or clinopyroxene were counted as the host pyroxene phase in which they occurred.

There is substantial variation in the modal compositions of the noncumulate rocks, and textural subdivisions are not represented by well-defined clusters in modal composition (fig. 14). Comparison of modal data for noncumulate rocks with those given in figure 10 for cumulate rocks shows some overlap in mineral proportions for most of the ragged-textured rocks and some ophitic-textured rocks. Yet, a large part of the ophitic and subophitic rocks have proportions of pyroxenes and plagioclase that differ from cumulate rocks and form a cluster between the groupings for plagioclase and orthopyroxene cumulates. The overlap in modal proportions of the ragged-textured cumulate rocks reinforces the idea that ragged-textured rocks are indeed gradational between ophitic and cumulate rocks, whereas the separation of subophitic and ophitic from cumulate rocks implies that they originated by different processes.

CHEMICAL COMPOSITION OF THE NONCUMULATE IGNEOUS-TEXTURED ROCKS

In the past, the major interest in the chemical composition of the noncumulate igneous-textured rocks has been related to attempts to determine the composition of the parental magma for the Stillwater Complex. On the basis of field occurrence and mineralogical characteristics, Hess (1960) and Jackson (1971) selected a limited number of samples believed to be possible parents, three of which were analyzed and the results were published. These analyses were presented as representative of the chilled border of the Stillwater Complex, and both authors suggested that the analyses represent the original melt or magma composition for the complex. Hess (1960) also estimated the composition of the parent magma by attempting to calculate the bulk composition of the whole complex and found some agreement between this calculation and the composition of border rocks.

The approach in this study was to select for analysis representative samples of ophitic, subophitic, and ragged-textured rocks which in hand specimen and thin section showed little alteration or contamination with metasedimentary rocks. The purpose was more to determine the extent of chemical variation in the igneous-textured rocks than to find the original parent magma composition. Each ophitic and subophitic rock analyzed is assumed to represent a melt or magma composition at the time and place the rock crystallized.

Table 4 gives chemical and semiquantitative spectrographic analyses, CIPW norms, modes, mineral compositions, and locations of ophitic, subophitic, and ragged-textured rocks. The data demonstrate the variability in composition of noncumulate igneous-textured rocks and emphasize the difficulty of selecting any particular rock to be a parent magma. Analytical data reported by Hess (1960) and Jackson (1971) for their chilled border rocks are listed for comparison. Hess' (1960) two specimens have the highest Al_2O_3 content of any analyses presented, and it should be noted that Hess called sample EB89 a "contaminated hypersthene dolerite or hornfels" (Hess, 1960, p. 53). Jackson (1967, p. 25) criticized Hess' other sample (463G70) as not representing the parental magma on the basis of its high Al_2O_3 content. Therefore, neither of Hess' (1960) samples appears to be an acceptable representative of the parental magma. The analyses in table 4 show a fairly wide range of compositions, but all, including Hess' samples, fall within the range for basalts. Table 5 summarizes the chemical analyses in table 4 and compares them with average tholeiitic basalt compositions from other basaltic provinces. Jackson's (1971) specimen approaches the average of all the analyses in table 4 and can be considered fairly representative of a parental magma. It is immediately apparent that

TABLE 4.— *Chemical, spectrographic, normative, and modal analyses of ophitic, subophitic, and ragged-textured rocks of the Basal norite, Basal zone, Stillwater Complex, Montana, with some mineral compositions*

[Chemical analyses by P. Elmore, J. Glen, H. Smith, and J. Kelsey performed in the Rapid Rock Analysis Laboratory under the direction of Leonard Shapiro. X-ray fluorescence analyses of S and Cl by B. P. Fabbi. Quantitative spectrographic analyses of Cr, Cu, and Ni by R. E. Mays and Chris Heropoulos. Fire-assay spectrochemical analyses of Pd, Pt, and Rh by W. D. Goss, A. W. Haubert, and Joseph Haffty. Semiquantitative six-step spectrographic analyses by Chris Heropoulos and R. E. Mays. Looked for but not detected at the limit of detection: As, Au, B, Be, Bi, Cd, La, Mo, Nb, Pd, Pt, Sn, Te, U, V, Zn, Ce, Hf, In, Li, Re, Ta, Th, Tl, Eu, Tr, element present but below limit of determination; N, not detected; H, interference from other elements]

Sample number	2NB68	1MV71	M17 1091	387-339 411	387-339 416	387-339 481	56BF69	67MV69	M17 1116	38CM71	32CM71	NB12 349	M19A 594	NB1, 386.5	64BE69	EB89	463G70	Jackson (1971)
Chemical Analyses, Weight Percent																		
SiO_2	48.7	47.4	48.7	52.4	48.9	53.3	48.8	48.7	48.9	50.3	51.4	48.8	44.5	48.0	46.6	47.34	50.68	49.41
Al_2O_3	15.2	13.5	15.0	14.5	13.8	14.9	13.9	16.6	16.2	13.7	12.1	14.9	10.8	14.2	16.0	17.12	17.64	15.78
Fe_2O_3	2.8	1.2	.92	1.3	1.6	.79	3.9	4.0	.50	.73	.36	1.7	1.9	1.7	.57	2.51	.26	2.11
FeO	12.2	14.5	13.8	12.8	14.1	14.1	10.2	11.4	16.0	8.7	10.4	12.8	21.1	13.0	15.3	12.05	9.88	10.25
MgO	6.7	7.0	6.4	6.9	7.1	3.9	7.6	7.1	6.4	14.9	10.9	7.0	9.4	6.4	7.6	8.23	7.71	7.36
CaO	10.6	10.3	10.6	8.2	10.5	6.1	10.6	6.3	7.5	9.7	11.3	11.0	9.0	10.0	8.7	9.79	10.47	10.88
Na_2O	1.5	.45	1.8	.77	.77	2.2	1.7	2.6	1.3	.65	1.3	1.1	.88	1.2	.50	.76	1.87	2.19
K_2O	.24	.89	.17	.49	.24	.28	.15	.32	.19	.08	.15	.32	.33	2.2	.42	.21	.24	.16
H_2O+	.00	1.7	.61	1.2	1.1	.11	1.1	.70	.56	.79	.41	.55	.60	.76	1.2	.73	.42	.23
H_2O-	.12	.08	.16	.03	.24	.24	.18	.07	.10	.07	.09	.10	.11	.34	.12	.04	.06	.07
TiO_2	1.4	1.5	1.4	.88	1.2	3.3	1.4	1.7	1.4	.13	.45	1.4	.87	1.6	1.6	.52	.45	1.20
P_2O_5	.17	.22	.19	.08	.08	.52	.16	.20	.24	.04	.09	.07	.12	.19	.07	...	.09	.11
MnO	.26	.27	.26	.24	.23	.24	.26	.27	.27	.21	.30	.27	.23	.28	.33	.17	.15	.20
CO_2	<.05	<.05	<.05	.12	<.05	<.05	<.05	<.05	<.05	<.05	.27	<.05	.08	.17	.02	...	...	...
Total	100	99	100	100	100	100	100	100	100	100	100	100	100	100	99	...	99.92	99.95
F	.01	.01	.00	.00	.00	.02	.00	.01	.01	.00	.00	.00	.02	.00	.00	...	...	...
S	.12	.14	.17	.44	1.76	.01	.00	.17	.39	.05	.00	.19	4.66	.17	.61	...	...	...
Cl	.0055	.0136	.0067	.0080	.0042	.0300	.0022	.0043	.0062	.0141	.0221	.0016	.0085	.0110	.0073	...	...	...
Cr	.170	.150	.190	.170	.210	N2	.210	.090	.200	.700	.700	.190	.067	.0125	.0030	...	...	...
Cu	.210	.080	.200	.480	.700	.036	.100	.100	1.40	.170	.070	.380	.120	.0145	.0560	...	...	...
Ni	.210	.100	.085	.290	.950	.015	.100	.140	.260	.250	.240	.100	.220	.028	.011	...	...	...
Pd (ppb)	.8	<4	...	Tr	...	...	<4	<4	...	32	14	<4	...	...	...	...	...	...
Pt (ppb)	<10	<10	...	<10	...	...	<10	<10	...	19	19	<10	...	...	...	...	...	...
Rh (ppb)	<5	<5	...	<5	...	...	<5	<5	...	<5	<5	<5	...	...	...	...	...	...
Semiquantitative six-step spectrographic analyses, parts per million																		
Mn	1,500	1,500	1,500	1,500	1,500	1,500	1,500	1,500	1,500	1,000	1,500	1,500	1,500	1,500	1,500	...	...	...
Ag	N	N	N	N	2	N	N	N	3	N	N	N	N	N	N			
Ba	70	150	70	150	70	150	70	100	70	15	70	70	70	100	30	...	...	...
Co	50	50	30	30	50	30	30	50	30	50	50	50	150	70	70	...	...	...
Cr	150	100	150	150	150	N	200	70	150	700	700	150	1,000	150	30	...	...	...
Cu	200	100	200	500	1,000	20	150	200	3,000	200	100	500	1,500	150	700	...	...	...
Ni	200	150	100	300	1,000	15	150	150	300	300	200	150	2,000	300	200	...	...	...
Pb	N	N	N	20	15	15	N	N	20	N	N	N	10	N	N	...	...	...
Sc	50	50	30	30	50	15	50	30	50	50	50	50	50	50	50	...	...	...
Sr	150	200	150	100	100	300	150	200	200	100	100	150	100	150	300	...	...	...
V	500	500	300	200	500	150	500	300	300	150	200	500	200	300	500	...	...	...
Y	30	30	30	10	10	30	20	20	20	N	20	15	10	30	N	...	...	...
Zr	30	70	70	20	15	150	15	50	N	N	15	15	30	50	N	...	...	...
Ga	15	20	15	15	15	20	15	20	15	10	10	15	10	15	15	...	...	...
Yb	3	3	3	2	2	3	2	2	2	1	1	2	H	3	H	...	...	...
CIPW norms, constituents normalized to 100 percent																		
Q	2.35	2.58	...	10.02	4.15	...	2.27	1.99	3.46	...	1.16	2.37	...	...	...	1.26	...	...
Or	1.42	5.31	1.00	2.89	1.42	...	.88	1.89	1.12	0.47	.89	1.89	...	...	...	1.24	1.42	0.94
Ab	12.71	3.84	15.24	6.52	6.53	...	14.41	22.01	11.05	5.50	11.06	9.31	...	...	...	6.46	15.84	18.55
An	34.09	32.51	32.37	34.70	33.60	...	29.90	29.64	35.49	34.23	26.89	34.78	...	...	...	42.92	39.08	32.79
Di	14.24	14.49	15.66	3.95	14.87	...	17.52	...	...	10.73	22.21	15.82	...	...	...	4.80	10.17	16.88
Di-Wo	7.16	7.23	7.80	1.98	7.44	...	8.94	...	...	5.56	11.35	7.94	...	...	...	2.47	5.15	8.57
Di-En	3.37	3.07	3.23	.87	3.23	...	4.98	...	...	3.64	6.44	3.64	...	...	...	1.23	2.63	4.51
Di-Fs	3.69	4.17	4.61	1.09	4.20	...	3.60	...	...	1.52	4.42	4.23	...	...	...	1.17	2.39	3.80
Hy	27.93	34.26	29.59	36.68	33.39	...	24.07	33.02	43.31	44.84	35.15	29.85	...	...	...	37.81	31.38	23.52
Hy-En	13.33	14.53	12.19	16.32	14.51	...	13.97	17.69	16.01	31.60	20.85	13.79	...	...	...	19.37	16.43	12.75
Hy-Fs	14.59	19.72	17.40	20.35	18.88	...	10.10	15.33	27.29	13.24	14.30	16.06	...	...	...	18.44	14.94	10.76
Ol	...	...	.95	...	...	...	...	...	...	1.91	...	...	...	...	...	.....	.22	1.46
Ol-Fo	...	...	.36	...	...	...	...	...	...	1.30	...	...	...	...	...	...	.11	.75
Ol-Fa	...	...	.58	...	...	...	...	...	...	.60	...	...	...	...	...	...	.11	.70
Mt	4.06	1.75	1.33	1.88	2.32	...	5.66	5.80	.72	1.05	.52	2.46	...	...	...	3.66	.37	3.06
Il	2.66	2.87	2.66	1.67	2.28	...	2.66	3.23	2.67	.24	.86	2.66	...	...	...	.99	.85	2.28
Ap	.40	.52	.45	.19	.19	...	.38	.47	.57	.09	.21	.16	...	...	...	...	.21	.26
Cc	.11	.11	.11	.27	.11	...	.11	.11	.11	.11	.61	.11	...	...	...	.....	...	...
C	...	...	...	...	...	...	...	1.11	.91	...	...	...	...	...	...	...	...	...

TABLE 4.—*Chemical, spectrographic, normative, and modal analyses*—Continued

Sample number	2NB68	1MV71	M17 1091	387-339/411	387-339/416	387-339/481	56BI69	67MV69	M17 1116	38CM71	32CM71	NB12 349	M19A/ 386.5	NBI 386.5	64BE69	EB89	463G70	Jackson (1971)
Modes, volume percent																		
Quartz	...	6.1	...	11.4	6.5	5.1	...	1.1	7.9	...	1.3	1.6	0.2	...	...	...	...	...
Plagioclase	49.2	49.6	51.0	36.3	26.1	56.5	56.8	57.2	41.4	49.3	45.4	48.1	25.9	50.8	47.1	...	...	49.7
Inverted Pigeonite	...	...	28.5	41.4	39.2	...	...	...	...	...	...	31.2	32.9	25.2	45.7	...	...	
Orthopyroxene	24.7	27.3	...	...	...	28.4	10.8	28.5	33.3	46.2	31.6	...	...	...	...	...	...	...
Clinopyroxene	14.7	11.4	12.3	4.0	16.7	.5	23.2	...	2.3	2.1	18.2	12.6	20.9	18.7	.8	...	...	19.9
Brown hornblende	...	1.2	5.3	3.0	4.2	.1	...	...	4.3	2.0	Tr	...	3.1	...	.3	...	...	...
Biotite	1.2	.4	.3	.3	.3	.3	Tr	1.3	.9	.3	1.3	.1	1.3	Tr	.1	...	...	...
Opaques	5.7	4.0	2.5	3.6	5.7	7.8	9.2	11.9	7.5	Tr	2.2	6.4	16.2	5.2	5.5	...	...	8.6
Olivines	...	...	...	...	...	...	...	...	...	...	...	Tr	...	...	...	...	...	.6
Apatite	.1	...	...	...	...	...	...	Tr	...	...	...	...	...	...	...	...	...	Tr
Alteration[1]	4.4	...	0.1	...	1.3	1.3	...	...	2.7	...	...	...	...	.1	1.3	...	...	...
Mineral compositions																		
Normative An	72.84	89.44	67.99	84.18	83.73	...	67.48	57.39	76.26	86.16	70.86	78.88	...	...	...	86.92	71.16	63.86
Normative En	47.74	42.42	41.20	44.51	43.46	...	58.04	53.57	36.97	70.47	59.32	46.20	...	...	...	51.23	52.37	54.23
Normative Di-Wo	50.35	49.97	49.87	50.25	50.03	...	51.03	...	...	51.87	51.10	50.22	...	...	...	50.72	50.64	50.77
Normative Di-En	23.70	21.22	20.65	22.08	21.72	...	28.42	...	...	33.96	29.00	23.02	...	...	...	25.26	25.86	26.72
Normative Fo	...	...	38.30	...	...	...	...	...	...	68.42	...	...	...	...	...	...	50.00	51.72
Mgx100/ Σ cations	44.3	...	40.7	45.1	45.4	38.3	54.0	61.1	37.8	68.0	...	43.1	51.0	30.7	64.0	...	...	...
An (X-ray)	67.2	...	60.5	79.6	80.1	55.4	61.9	53.0	72.7	82.5	...	73.8	...	70.9	82.1	...	...	...

Sample description and location:

2NB68, ragged-textured gabbro; Nye Basin.
1MV71, subophitic-textured gabbro; Mountain View area.
M17/1091, subophitic-textured gabbro; Mountain View area.
387-339/411, ophitic-textured gabbro; Mountain View area.
387-339/416, subophitic-textured gabbro; Mountain View area.
387-339/481, ophitic-textured gabbro; Mountain View area.
56BE69, ragged-textured gabbro; Benbow area.
67MV69, subophitic-gabbro; Mountain View area.
M17/1116, ophitic gabbro; Mountain View area.
38CM71, ragged-textured gabbro or plagioclase-orthopyroxene cumulate; Iron Mountain area.
32CM71, subophitic gabbro; Iron Mountain area.
NB12/349, ophitic gabbro; Nye Basin area.
M19A/594, subophitic gabbro; Mountain View area.
NB1/386.5, ophitic gabbro; Nye Basin area.
64BE69, ophitic-textured gabbro; Benbow area.
EB89, contaminated hypersthene dolerite or hornfels; analyst, A. H. Phillips, alkalies by R. B. Ellestad (Hess, 1960, table 12, col. 2, p. 53); East Boulder Plateau.
463G70, hypersthene dolerite border facies, collected by Peoples; analyst, R. B. Ellestad (Hess, 1960, table 12, col. 1, p. 53); East Boulder Plateau.
Jackson (1971), chilled border rock; analyst, Faye H. Neuerburg (Jackson, 1971, table 1, p. 132), Nye Basin.

[1]Includes blue-green clinoamphibole, clear amphibole, chlorite, serpentine, talc, and epidote.

except for Hess' two analyses (1960), the Stillwater noncumulate igneous-textured rocks resemble neither oceanic tholeiitic basalts nor alkali basalts. The average compositions of the noncumulate igneous-textured rocks fall between the Hawaiian and Thingmuli averages. The chemical characteristics of Stillwater noncumulate igneous-textured rocks—low K_2O, Na_2O, TiO_2, and high FeO—are similar to those of chilled border rocks from the Bushveld, Muskox, and Great Dyke stratiform intrusions as pointed out by Jackson (1971, p. 131).

The variation in composition of noncumulate igneous-textured rocks is illustrated by the spread of data along the iron-magnesium side of an alkali-iron-magnesium diagram (fig. 15). Hess' (1960) calculated liquid trend is superimposed upon the diagram as a reference line. Comparison of the spread in compositions with the liquid trend line illustrates the difficulties of establishing a single unique parent magma composition. Moreover, the analytical data, as well as the presence of two crystallization sequences and olivine and plagioclase phenocrysts in the Basal zone, suggest that no single unique parent magma will be established by analyzing ophitic and subophitic rocks. At best, an average composition and the deviation from it may be established by this technique. Because the causes of variation from a parent composition, are numerous, a definition of the variation may be more important to the development of models for the crystallization of the Basal zone and the whole complex than the actual parent composition. Processes that may cause local variation in compositions of parent magma include (1) contamination by and reaction with country rocks either within the magma chamber or conduits leading to the chamber, (2) fractional crystallization and winnowing of crystals in either the magma chamber or conduits, (3) initial variation in magma compositions due to generation processes or incomplete mixing in the magma chamber, (4) alteration by diffusion or metamorphic processes at or near magmatic temperatures, and (5) lower temperature alteration.

Figure 15 also illustrates that the compositions of noncumulate igneous rocks and cumulate rocks from all

TABLE 5.—*Comparison of the range and average chemical analyses of noncumulate igneous-textured rocks from the Stillwater Complex with Hawaiian basalt, Thingmuli basalt, average oceanic tholeiitic basalt, and alkali basalt*

	Stillwater Complex[1]		Hawaii[2]	Thingmuli[3]	Oceanic[4]	Alkali[5]
	Range	Average				
SiO_2	44.5-53.3	49.05	49.84	48.75	49.34	47.41
Al_2O_3	10.8-17.64	14.77	14.09	13.12	17.04	18.02
Fe_2O_3	.26-4.0	1.60	3.06	4.64	1.99	4.17
FeO	8.7-21.1	12.92	8.61	9.61	6.82	5.80
MgO	3.9-14.9	7.70	8.52	5.46	7.19	4.79
CaO	6.1-11.3	9.53	10.41	9.71	11.72	8.65
Na_2O	.45-2.6	1.31	2.15	2.85	2.73	3.99
K_2O	.08-2.2	.39	.38	.49	.16	1.66
H_2O+	.0-1.2	.71	.....	.85	.69	.79
H_2O-	.04-.34	.12	.....	.79	.58	.61
TiO_2	.13-1.7	1.24	2.52	2.85	1.49	2.87
P_2O_5	.04-.52	.16	.26	.48	.16	.92
MnO	.15-.30	.25	.16	.25	.17	.16
CO_2	.02-.17	.....	.....	.....	.....	.....

[1]Range and average of analyses from table 4 of noncumulate igneous-textured rocks from the Stillwater Complex, Mont.
[2]Average of 181 tholeiites and olivine tholeiites from the Hawaiian Islands (Macdonald and Katsura, 1964, table 9, p. 124).
[3]Average of 10 analyses olivine tholeiite and tholeiite lavas and dikes from the Thingmuli volcano, Iceland (Carmichael, 1964, table 2, p. 439).
[4]Average oceanic tholeiitic basalt (Engel and others, 1965, table 2, p. 721).
[5]Average alkali basalt from seamounts and islands (Engel and others, 1965, table 2, p. 721).

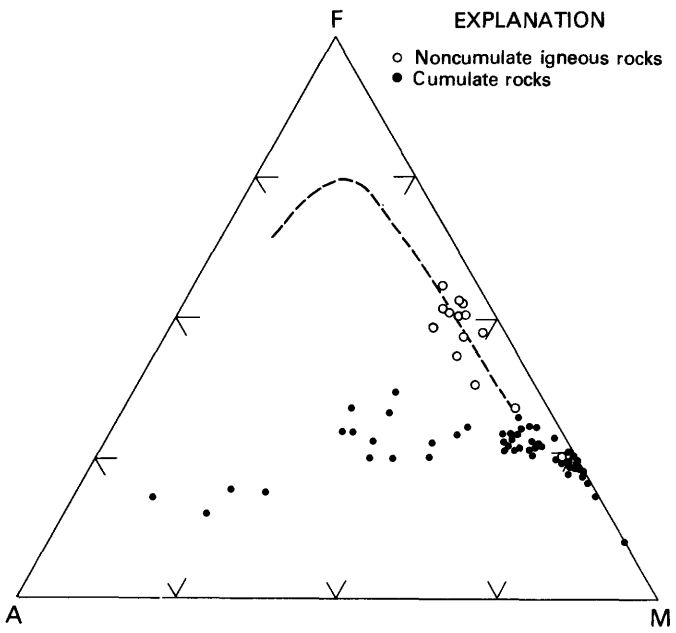

FIGURE 15.—Noncumulate igneous-textured rock compositions compared with cumulate rock compositions. A=Na_2O+K_2O, F=FeO+MnO, M=MgO. Cumulate rock coordinates calculated from analytical data of Bowes, Skinner, and Skinner (1973). Line is Hess' (1960) calculated liquid trend.

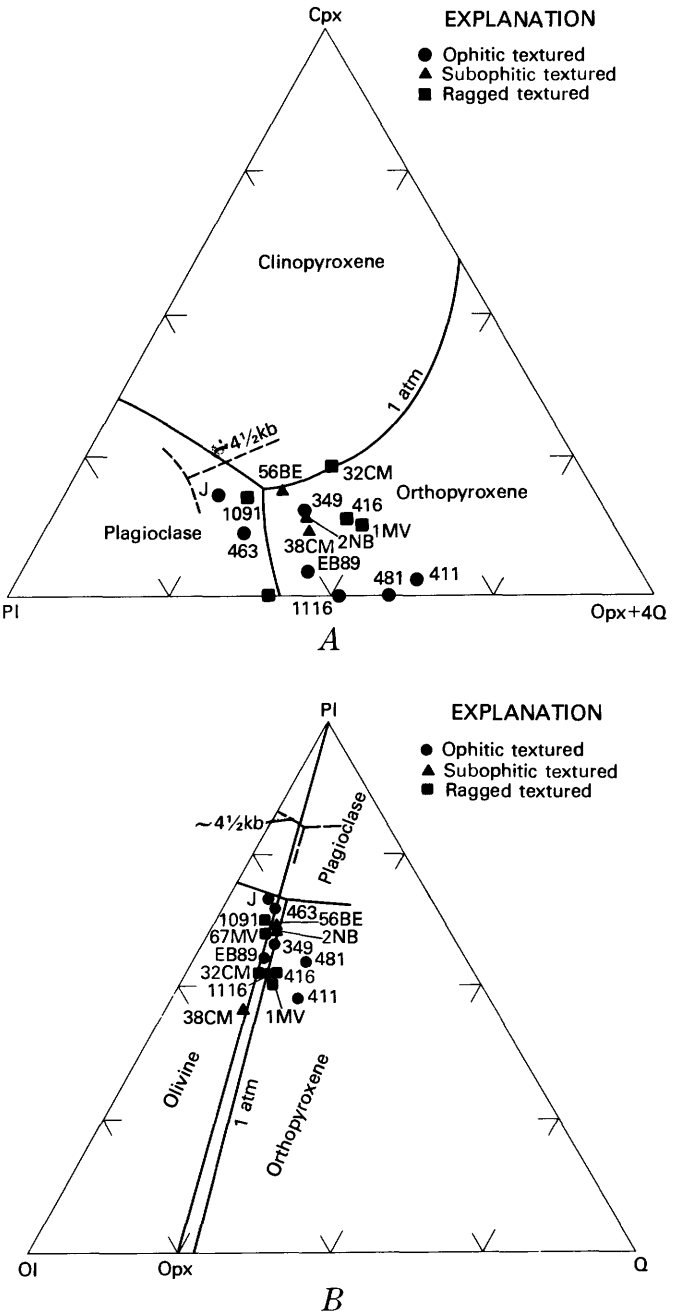

FIGURE 16.—Projections of analyses of noncumulate igneous-textured rocks in the system olivine-clinopyroxene-plagioclase-silica. *A*, Plagioclase (Pl)-clinopyroxene (Cpx)-orthopyroxene (Opx)+4SiO_2 (4Q). *B*, Olivine (Ol)-plagioclase (pl) SiO_2 (Q). Data are plotted as cation equivalents. Numbers refer to identifiable parts of sample numbers in table 4. Solid lines represent liquidus boundaries after Irvine (1970a) for average basaltic liquids at one atmosphere. Dashed lines represent liquidus boundaries inferred after Irvine (1970a) for 4½ kb.

parts of the complex are different. Cumulate rock compositions plotted in figure 15 were calculated from 61 chemical analyses of samples collected along three traverses across the complex (Bowes and others, 1973). Nine of the analyzed samples showed secondary alteration mainly to serpentine minerals. For these samples, the Fe_2O_3 content was converted to FeO and combined with FeO and MnO for the F coordinate of the diagram. If actual volumetric proportions of these analyzed rocks within the complex could be determined, it might be possible to determine a parent magma composition. Obviously an arithmetic

average does not yield the parent composition. Unfortunately the Upper and Banded zones of the complex are too poorly known at the present time to justify a volumetric calculation.

Interpretation and diagrammatic projections developed by Irvine (1970a) for the system olivine-clinopyroxene-plagioclase-silica allow the analytical data from table 4 to be examined with respect to possible crystallization paths. Ophitic, subophitic, and ragged-textured rock compositions have been plotted on two of these projections in figure 16. The calculations follow those of Irvine (1970a). In general, most of the noncumulate igneous-textured rock compositions would first crystallize small amounts of olivine followed by plagioclase or orthopyroxene, or first orthopyroxene followed by other phases.

More detailed examination leads to the following observations. Magmas represented by samples projected into the olivine volume of figure 16*B* would first crystallize small amounts of olivine at 1 atmosphere and similarly at about 4 1 2 kb. Samples such as J would next crystallize plagioclase followed by clinopyroxene and then orthopyroxene; in others such as 463 the crystallization sequence would be olivine, plagioclase, orthopyroxene, clinopyroxene. Samples such as 56BE would crystallize in the order olivine, orthopyroxene, clinopyroxene, plagioclase; others such as 2NB in the order olivine, plagioclase, orthopyroxene, clinopyroxene. Magmas represented by samples projected in the orthopyroxene volume of figure 16*B* would first crystallize orthopyroxene. With this model all of the crystallization sequences of cumulates in the Basal zone can be accounted for by the various magma compositions except for the sequence olivine, olivine+orthopyroxene, orthopyroxene.

Irvine (1970a, p. 470-472) proposed a phase-diagram model to give this sequence by fractional crystallization. His model involves postulating a particular shape and position for the olivine-orthopyroxene liquidus boundary to allow coprecipitation of olivine and orthopyroxene. If his model is accepted, all of the cumulate rocks (see compositions projected on fig. 16) within the complex can be accounted for by fractional crystallization. Cumulate rocks in the Basal zone reflect local variations in magma compositions; the rocks in other zones perhaps reflect a more homogeneous composition caused by more complete mixing of magma over a longer time span.

VISCOSITY, DENSITY, AND SETTLING VELOCITIES

Estimates of the variation in viscosity and density of the Stillwater magma and of the probable settling velocities within it are the basis for evaluation of accumulation processes in the Basal zone. Both the viscosity and density of magmatic liquids are strongly dependent upon chemical composition, hence their variation may be more important than their absolute values in interpreting features in the Basal zone and the processes responsible for them. Estimates of these properties were made in the past by Hess (1960) and Jackson (1961a, 1971), but recent studies of the viscosity of basaltic rocks (Shaw and others, 1968; Shaw, 1969; Murase and McBirney, 1973) and the development of techniques to calculate viscosities of magmatic silicate liquids of varying composition (Bottinga and Weill, 1972; Shaw, 1972) and their densities (Bottinga and Weill, 1970) allow these properties to be quantified with more confidence than in the past. Viscosity and density ranges have been calculated from the theoretical models for the possible liquid compositions represented by chemically analyzed noncumulate, ophitic, and subophitic rocks.

Bottinga and Weill (1970) calculated and approximated partial molar volumes of the major constituents of basaltic magmas from binary and ternary silicate melt data and presented compositional coefficients and a model from which densities of melts in the range of 1,200° to 1,600°C may be calculated. Using their method, densities of possible dry (without water) magmas represented by compositions of the noncumulus ophitic and subophitic rocks in table 4 were calculated for a temperature range of 1,200°-1,400°C as shown in figure 17. The density calculations were extrapolated below 1,200°C but probably do not represent true densities because below 1,200°C crystalline phases would be present that would tend to increase the bulk density. Water was not included in the calculations because its effect is

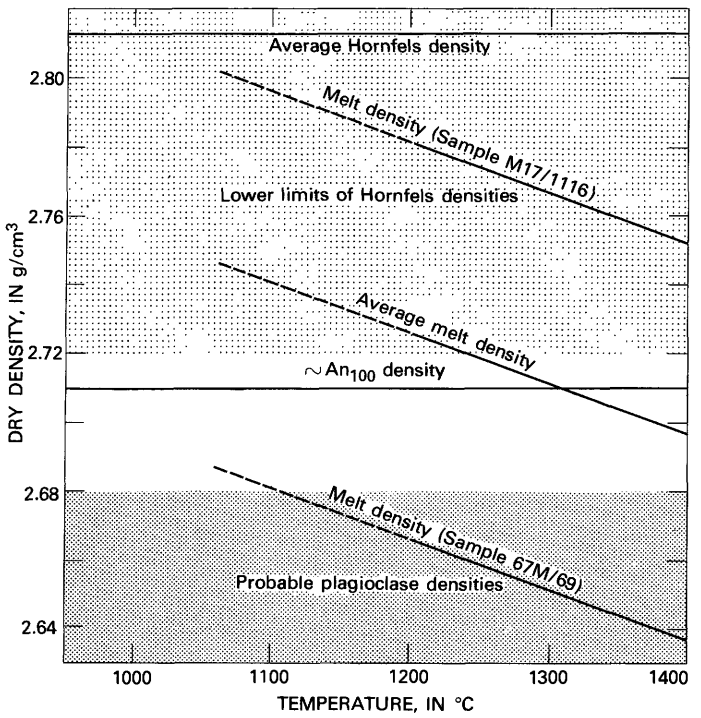

FIGURE 17. Calculated dry density-temperature curves of possible Stillwater magmas. Sample M17/1116 (table 4) represents highest and sample 67MV69 represents lowest densities. Densities of samples NB-12 349 and 463G70 are near average. Solid lines indicate densities calculated after Bottinga and Weill (1970); dashed lines indicate extrapolations.

sensitive to the total pressure on the system and the pressure on the Stillwater magma is unknown. As shown by Bottinga and Weill (1970, p. 179), the density difference between dry and wet magmas depends upon the amount of water present and the total pressure.

In general the calculated densities are slightly higher than the densities for the Stillwater magma estimated in previous studies. For example, Jackson (1971, p. 138) and Hess (1972, p. 505) used a density of 2.60 g/cm^3. The calculations emphasize the variation in magma densities as a function of small composition and temperature changes and point out the impropriety of assigning one density to the whole magma.

The magma density calcuations show that in most of the possible Stillwater magma compositions plagioclase (An_{83} to An_{55}) could have floated (fig. 17) if it was a primary phase. However, stratigraphic and petrologic observations (fig. 5) indicate that some plagioclase was a cumulate phase. Assuming that the range of plagioclase density (An_0 to An_{100}) at 1,200°C is 2.53 to 2.71 g/cm^3 (Bottinga and Weill, 1970, p. 180) it is possible for plagioclase to have been cumulus in some of the lower density compositions of the magma in the Basal zone. Previous problems of interpretation concerning magma composition and the behavior of plagioclase (Jackson, 1961a; Bottinga and Weill, 1970) can be eliminated by suggesting that plagioclase could sink or float depending upon the local composition and physical conditions of the magma.

The appearance of hornfels inclusions in the Basal zone, both as isolated fragments and as groups of fragments in lenses or layers, raises the question of whether they represent pieces of country rock that floated upward from the base, or roof rocks that sank to their present position. Measured bulk densities range from 2.720 to 2.924 and average 2.813 g/cm^3 (Page, 1977). Thus, hornfels inclusions may have either sunk or floated depending on local magma composition, although most of the hornfels probably sank.

H. R. Shaw (1972) simplified calculation techniques for prediction of viscosities of silicate liquids and extended them to treat hydrous compositions. Shaw's (1972, p. 881) data indicate that his method yields smaller mean differences from measured viscosities of silicate liquids than does the more cumbersome technique of Bottinga and Weill (1972). Hence Shaw's method of calculation was used to estimate viscosities for magmas corresponding to the compositions in table 4 over a temperature range from 1,300° to 1,000°C. The results of these calculations are shown in figure 18 as a plot of ln η, where η is the viscosity in poises, against reciprocal temperature in kelvins. Sample 463G70 (table 4) would yield the most viscous magma, similar to those measured for a Hawaiian tholeiitic basalt (Shaw, 1969; sample 1MV71 (table 4) would yield the least viscous magma. Calculated viscosities for samples M17/1091, 67MV69, and 32CM71 are close to the average calculated for all the Basal zone rocks over the chosen temperature range. The mean slopes for each composition were used to calculate the viscosity-temperature curves by the equation

$$\ln \eta = S(10^4/T)\text{-}1.50S\text{-}6.40,$$

where S=slope and T=temperature in kelvins (Shaw, 1972, p. 873). The viscosities in figure 18 were calculated assuming that no crystals or gas bubbles are present in the magma. It is more likely that the magma contained crystals in the chosen temperature range; if so, the viscosities would be higher, depending upon the proportion of crystals present (Shaw and others, 1968, p. 257). Previous viscosity estimates of $3X10^3$ poises (Hess, 1960) and 300 poises (Jackson, 1971) fall within the range of calculated magma viscosities. The most probable range of viscosity, from 36 to 909 poises, is shown in the stippled area of figure 18. It is important to emphasize that the slight variations in rock composition represented in table 4 lead to variations in calculated viscosities of almost an order of magnitude.

Many scientists have calculated Stokes law settling velocities of olivine, orthopyroxene, and plagioclase grains of different sizes in basaltic magmas under stagnant conditions for various viscosity conditions and particle shapes. Jackson (1971, p. 138) showed that in a magma with a

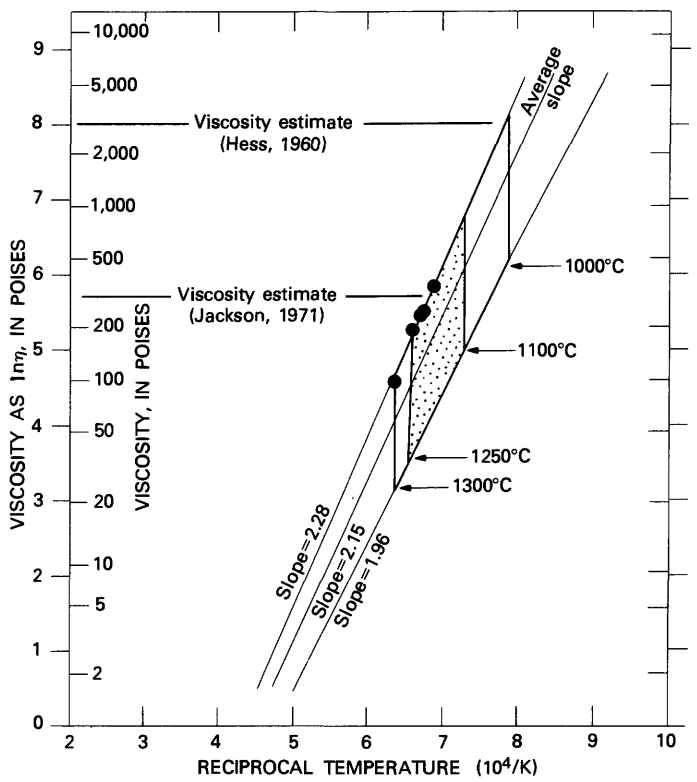

FIGURE 18. Calculated viscosities (η) of possible parent magmas for the Stillwater Complex plotted against reciprocal temperature. Stippled area is the most likely viscosity range for Stillwater magmas. Black dots show measured viscosities of Hawaiian basalts (Shaw, 1969). Two horizontal lines show viscosity estimates of Hess (1960) (upper line) and of Jackson (1971) (lower line).

viscosity of 300 poises, extreme prismatic shapes of plagioclase and pyroxenes settled nearly as rapidly as ideal spherical shapes. Shaw (1965) demonstrated that if a cumulus crystal is assumed to grow continuously while settling it will travel only about one-third as far as a crystal of fixed size in the same amount of time. It also can be shown that the density contrast between crystal and magma is not changed enough through the range of compositional solid solution of olivine, orthopyroxene, and plagioclase of the Basal zone to greatly alter settling velocities of individual mineral species. Settling velocities for minerals in the Basal zone are shown in figure 19. The conditions correspond to a magma with a density of 2.712 g/cm^3 and a viscosity of 59.1 poises at 1,300°C and a density of 2.726 g/cm^3 and a viscosity of 149.9 poises at 1,200°C, the average ranges of the preceding density and viscosity calculations. For orthopyroxene a density of 3.36 g/cm^3 representing En_{80} was used at 1,200°C and a density of 3.58 (En_{50}) at 1,300°C. This allows a maximum range of settling velocities to be shown. Similarly at 1,200°C a density of 3.47 (Fo_{74}) and at 1,300°C a density of 3.57 (Fo_{67}) was used for olivine. A plagioclase density of 2.68 corresponding to a composition of about An_{85} at 1,200° C was used in the calculations. One must conclude from figure 19 that settling velocities in the Basal zone were from 25 to 61,000 meters per year.

Throughout the lithologic and stratigraphic descriptions of the Basal zone, the abrupt variation in grain size along the trend of the zone and within individual hand samples has been emphasized. One explanation for this phenomenon is that grain-size distributions are controlled by magma density and viscosity which in turn are dependent upon composition. The slight variation in composition of possible magmas, represented by ophitic and subophitic rocks in table 4, appears to be large enough to change viscosity in the temperature range of interest by an order of magnitude and to change the density by 4 or 5 percent. These variations could locally affect settling velocities by as much as 70 percent. Therefore, if there were local volumes of magma with varying compositions, it is reasonable to expect abrupt changes in grain size. This explanation does not consider the existence of currents or local convection, which were certainly present as evidenced by textures and structures. Movement of masses of magma could probably increase the observed irregularities without contributing to rapid mixing.

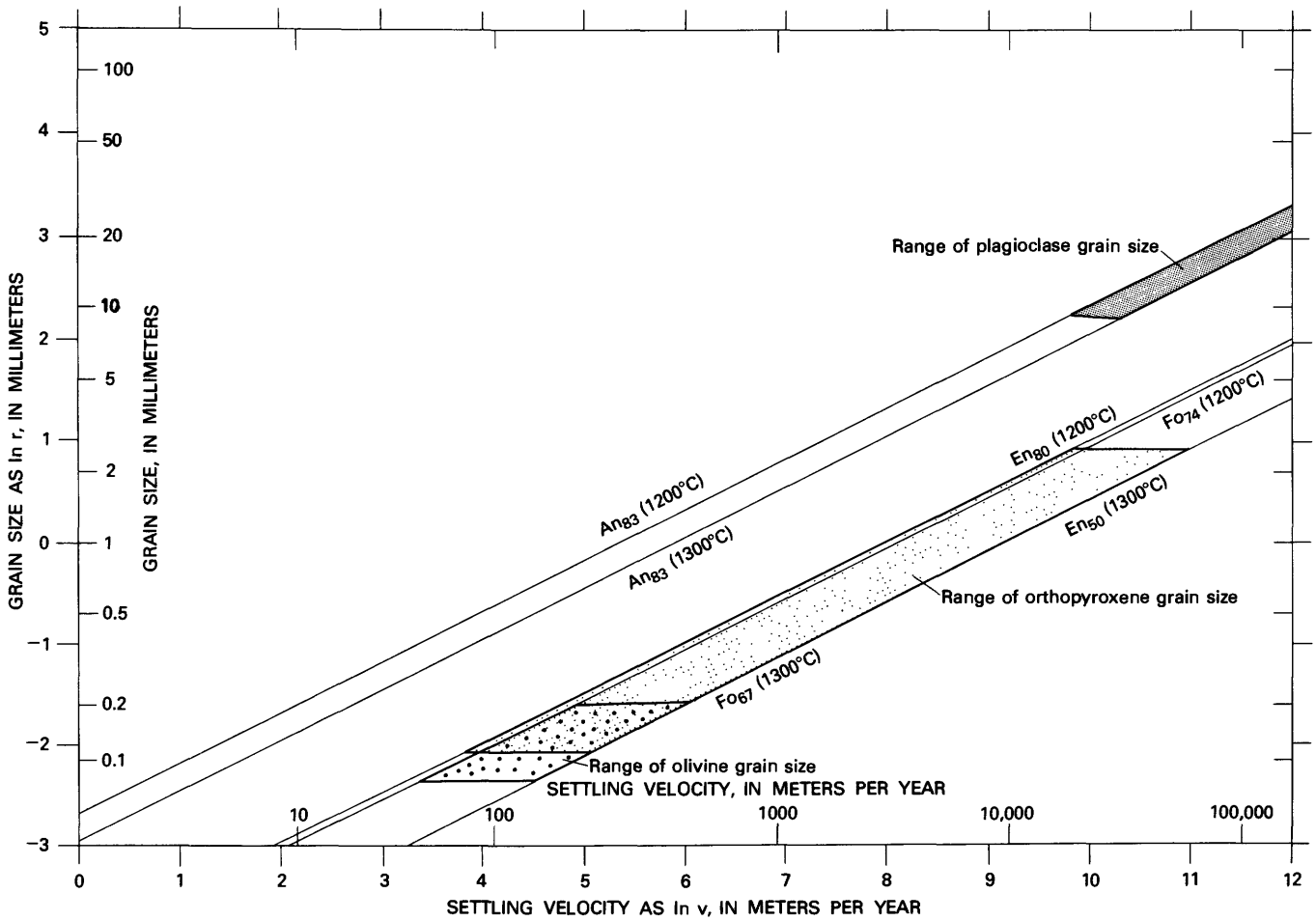

FIGURE 19.—Settling velocities of plagioclase, orthopyroxene, and olivine in a possible Stillwater magma. r, grain size; v, settling velocity.

CONTAMINATED IGNEOUS ROCKS

Contaminated igneous rocks or rocks of mixed origin are found locally in contact zones between metasedimentary rocks and either cumulate or noncumulate igneous-textured rocks of the Basal norite. Inclusions of metasedimentary rocks are sparse throughout the Basal bronzite cumulate and in the lower part of the Peridotite member as well as in the Basal norite. In the Basal zone, at least two types of contaminated igneous rocks may exist. The first type consists of cumulate and noncumulate igneous-textured rocks that crystallized from magma whose composition had been changed by addition or subtraction of components. The second type consists of rocks of mixed origin formed by reaction of metasedimentary rocks with magma. The first type is recognized by chemical features such as unique trace element contents, mineral compositions, or crystallization sequences; the second type is recognized on the basis of textures, mineralogy, and relation to the metasedimentary rock. Recognition of the first type of contaminated igneous rocks in the Basal zone is difficult; this discussion is therefore restricted to those contaminated rocks that can be unquestionably distinguished on mineralogical, textural, and petrologic criteria. They have been observed only in contact with metasedimentary rocks that occur either as inclusions or at the lower margins of the Basal norite. Mixed rocks are present along the strike length of the Basal zone but are concentrated in areas where there are abundant inclusions of metasedimentary rocks.

TYPES, TEXTURES, AND MINERALOGY OF THE CONTAMINATED IGNEOUS ROCKS

The more common variants of the mixed rocks contain large (0.2 to 0.5 cm), anhedral, interlocking poikilitic crystals. These crystals occur within the igneous rock and also extend across the contact and into the metasedimentary rock where they enclose relict mineral grains from the metasedimentary rock. Table 6 summarizes the textures and mineralogy of the mixed rocks. Where mixed rocks occur between metasediments and orthopyroxene cumulate, plagioclase cumulate, ophitic norite, subophitic norite, or ragged norite, they contain relict poikilitic plagioclase and varying amounts of relict orthopyroxene, cordierite, biotite, and magnetite from the pyroxene hornfels facies metasedimentary rocks. Figure 20 shows examples of this type of contaminated rock and their contacts with the igneous and metasedimentary rocks. Orthopyroxene in mixed rocks is distinguished from either euhedral cumulus orthopyroxene or ophitic orthopyroxene by its shape, texture, and internal characteristics. It occurs as fine (less than 1 mm diameter), anhedral, locally branching grains that contain neither the fine clinopyroxene exsolution lamellae parallel to the (100) plane of orthopyroxene nor the coarser discontinuous blebby exsolution bodies typical of inverted pigeonite. These characteristics are typical of the orthopyroxene in the hornfelses (Page, 1977) and orthopyroxene of this form and structure is therefore considered relict from the hornfelses. Cordierite in the mixed rocks retains the characteristics it has in the hornfels but locally has rounded or subrounded grain shapes where enclosed in plagioclase, instead of the sharp, distinct corners it has in the cordierite grain mosaics in the hornfelses. Biotite and magnetite have similar shapes in the mixed rock and in the hornfels. Green spinel (possibly hercynite) occurs in the hornfelses (Page, 1977), but is not common. In the mixed rocks, green spinel usually forms fine (<0.x mm diameter) inclusions in the center of cordierite crystals or occurs as inclusions in poikiloblastic orthopyroxene in positions normally occupied by cordierite.

The contacts between the rocks listed in table 6 tend to be gradational and irregular rather than sharp, although contacts between metasedimentary rocks and mixed rocks with poikilitic plagioclase are generally no thicker than the

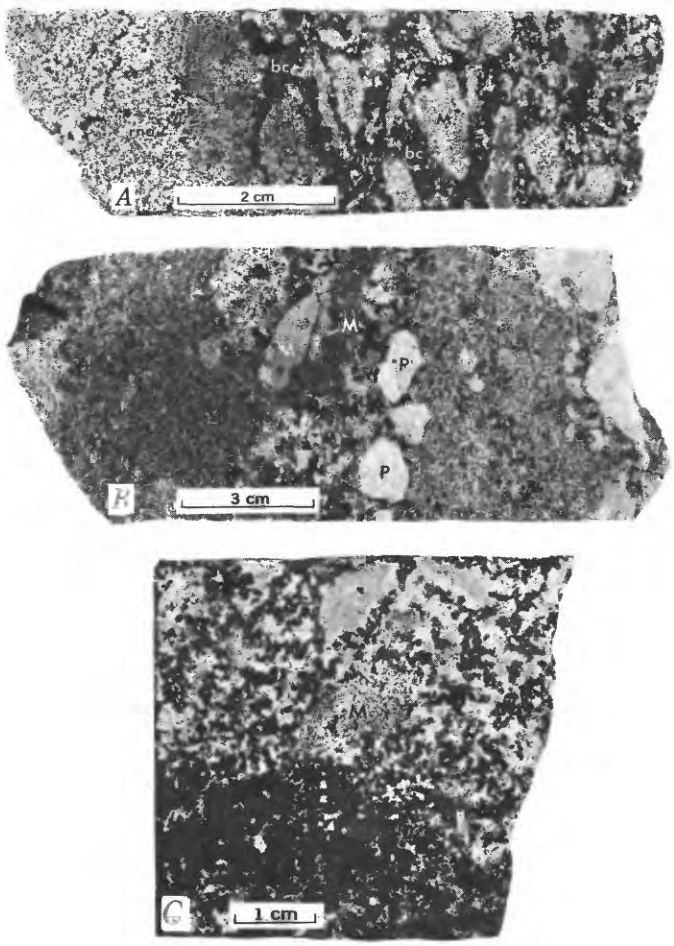

FIGURE 20.—Etched slabs of contaminated igneous rocks. *A*, Fragments of partly reacted metasedimentary rocks (M) in orthopyroxene cumulate (bc) and in ragged-textured norite (rno). Sample 387-339/240. *B*, Reacted fragment of metasedimentary rock (M), plagioclase phencryst (P) at the grain-size boundary and within two orthopyroxene cumulates. Sample NB-1/194.5. *C*, Almost completely reacted fragment (M) in orthopyroxene cumulate. Sample NB-13/490.

TABLE 6 *Summary of types, textures, and mineralogy of contaminated igneous rocks and their relation to igneous and metasedimentary rocks*

Igneous rocks	Contaminated or mixed rocks		Metasedimentary rocks
Orthopyroxene cumulate	Large, anhedral poikilitic plagioclase, enclosing anhedral orthopyroxene (irregular grain shapes of orthopyroxene).		Cordierite+ orthopyroxene+ biotite+ magnetite (+quartz or plagioclase).
Plagioclase cumulate	Large, anhedral, poikilitic plagioclase enclosing anhedral orthopyroxene, minor cordierite, biotite, magnetite.		
Ophitic norite	Large anhedral poikilitic plagioclase enclosing cordierite and green spinel.	Cordierite with green spinel inclusions, minor orthopyroxene, biotite, magnetite poikilitic plagioclase.	
Subophitic norite Ragged norite	Large, anhedral poikilitic plagioclase enclosing green spinel.	Large, anhedral poikilitic plagioclase enclosing green spinel and cordierite.	
Orthopyroxene cumulate Ragged clinopyroxenite (possible cumulate).	Ophitic gabbro, clinopyroxene enclosing tabular plagioclase		Locally layered with orthopyroxene or cordierite enriched bands.
Orthopyroxene cumulate, matrix of graphically intergrown plagioclase and quartz, biotite, and ores.	Graphically intergrown plagioclase and quartz enclosing minor cordierite.		
Orthopyroxene cumulate, matrix of micrographic plagioclase and quartz.	Plagioclase forms micrographic intergrowths in quartz grains of metaquartzite.		Metaquartzite 99 percent quartz, minor chlorite, magnetite.

crystals of plagioclase. The mineralogic composition of the contaminated rocks is gradational from typical igneous rock to metasedimentary rock, which makes it difficult to derive average compositions for the mixed rock. Table 7 lists modes of two mixed rocks and the adjoining hornfelses. The data illustrate the predominance of plagioclase over cordierite in the mixed rock and the reverse in the hornfelses. The accuracy of the modes may be questioned because of the relatively small number of points counted and the gradational properties of the rock, but the consistency of modes suggests that they represent reasonable approximations.

The lower three types of mixed rocks in table 6 apparently occur sparsely but are interesting in that plagioclase is an important constituent of two of them. Figures 20*B* and *C* illustrate the textures of these two variants. The replacement of quartz in the metaquartzite is similar to textures at the contact of dikes and quartzite near the Dufek intrusion in Antarctica (A. B. Ford, oral commun., 1969), and textures described where the Mashaba igneous complex in Rhodesia comes in contact with leucocratic granitic rocks (Wilson, 1968, p. 76). Ragged clinopyroxenite and ophitic gabbro rich in clinopyroxene were observed near hornfels inclusions only a few times; the mineral assemblages are strikingly different elsewhere in the Basal zone. Although there is no textural evidence that these mixed rocks formed by contamination, their unique mineral association suggests this origin.

TABLE 7. *Modes of contaminated or mixed rocks and the immediately adjacent hornfels*

[Determined by point counting in a single thin section per pair with a grid 1.3 mm x 1.6 mm; variable number of points counted because of limited areas available for counting]

Rock type	Sample number ...	M17 441		NBI 149.2	
		Hornfels	Mixed	Hornfels	Mixed
Plagioclase		.....	71.8	.....	74.6
Cordierite		74.5	.....	70.0	12.3
Orthopyroxene		17.2	26.5	22.0	6.8
Green spinel		.8	.....	1.2	2.5
Opaque minerals		4.7	1.7	1.8	1.4
Biotite		2.8	.....	5.0	2.4
Total		100.0	100.0	100.0	100.0
Number of points		640	355	323	796

M17 441: Drill core, Mountain View.
NBI 149.2: Drill core, Nye Basin.

RELATION OF MIXED ROCKS TO INCLUSIONS OF METASEDIMENTARY ROCKS

Most of the contaminated igneous rocks observed in this study occur around inclusions of metasedimentary rocks, therefore it is necessary to digress and describe the inclusions at least with respect to their sizes and volumes. Inclusions of hornfels range in size from less than a centimeter across to approximately 60 by 300 m (exposed on the surface in the Benbow area). Larger inclusions possibly occur, especially if the east-west-trending outcrop in the Mountain View area (pl. 1) is interpreted as an inclusion and not a spine or block attached to the basement hornfels. Estimates of the volume of included material in the Basal zone are uncertain, but the following method offers one approximation. Surfaces of drill core amounting to about 6.34 X 10^6 cm^2 of drill core were examined and logged and samples with an area of about 39 140 cm^2 were collected. Within the area of the samples, 69 inclusions were identified and their sizes, including recognizable zones of mixed rock, measured. The inclusions range in size, expressed as the average of the extreme dimensions, from 0.2 to 6.0 cm. Figure 21 illustrates

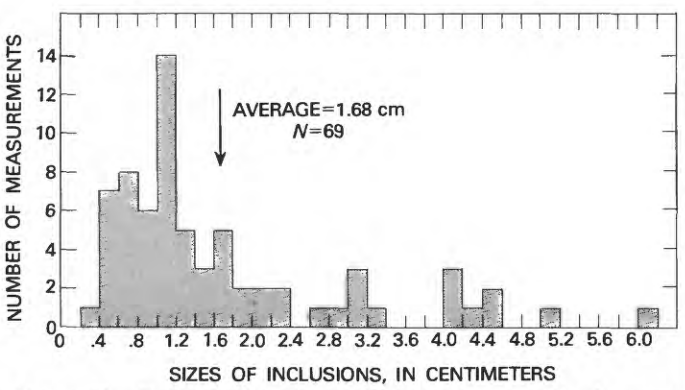

FIGURE 21.—Sizes of metasedimentary inclusions, expressed as the average of maximum length and minimum width. Based on etched core samples, maximum core width about 6 cm. N, number of measurements.

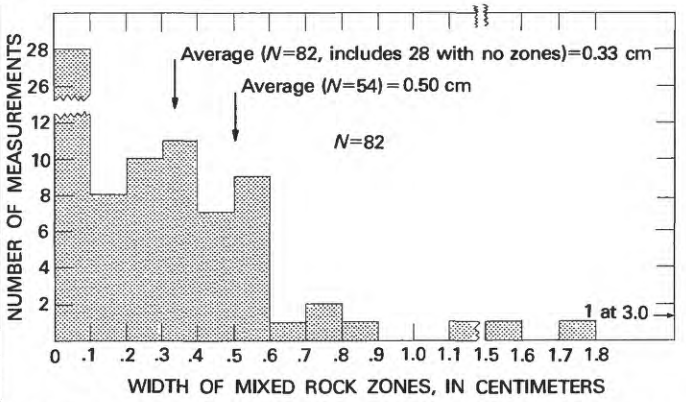

FIGURE 22.—Widths of mixed rock zones adjacent to inclusions. N, number of measurements.

the size, range, and number of occurrences by size intervals of the inclusions in the samples of drill core. Larger inclusions than these were probably intersected during drilling but, because of the limitations of core widths, are not included in this estimate. The average size is 1.68 cm; assuming a circle of this diameter as an average for 69 inclusions yields an area of about 153 cm^2. By area or volume the Basal zone contains at least 0.4 percent inclusions.

Of the 69 inclusions, 28 showed mixed rock zones less than 0.1 mm wide; the others contained rims of mixed rock ranging in width from 0.1 to 3.0 cm; 13 additional zones of mixed rock were measured at other contacts. Figure 22 shows the distribution of the widths of the zones of mixed rock. Two different average widths were calculated: One average includes those with mixed rock zones less than 0.1 mm wide, the other, only those with zones wider than 0.1 mm. It appears that on the average about 0.5 cm of the margins of metasedimentary rocks is involved in making mixed rocks. Figure 23 illustrates the relation of inclusion size and the width of the mixed rock zone.

PROCESSES FOR FORMING MIXED OR CONTAMINATED ROCKS

The mineralogic, textural, and petrologic observations discussed above demonstrate that the position occupied by cordierite in the metasedimentary inclusion is filled by plagioclase in the mixed rock or contaminated rock. Because the metasedimentary rocks are low in CaO and Na_2O (Page, 1977), these constituents must have been derived from the magma from which the igneous rocks crystallized. In turn the cordierite in the hornfels must have given up MgO and FeO to the magma. All the other hornfels constituents appear to remain in the mixed rock. This reaction is similar to one suggested by Subramaniam (1956) for the formation of cordierite xenoliths in the anorthosites of the Sittampundi Complex, India. More recently, Willemse and Viljoen (1970, p. 364-365) proposed calcification of pelitic rock inclusions and addition of MgO and FeO to the Bushveld magma on a local scale. Such reactions could eventually change the composition of the original magma.

To evaluate the magnitude of this process a model was developed for the exposed part of the Stillwater Complex. Assuming a model volume of magma to form the complex of 8.2X1.0X42 km^3 and using a specific gravity of 2.72, calculated from Bottinga and Weill (1970), the weight of magma is about $9.4X10^{17}$ grams. This magma would contain about $7.2X10^{16}$ grams of MgO (see table 5 for average value of MgO). If we assume that the total surface area of the base of the complex reacted over a thickness of 0.5 cm, and that the basal rocks have an average density of 2.81, then $5.9X10^7$ grams of hornfels would be used to make mixed rock. Of this only about 6.4 percent is MgO, and therefore $3.8X10^6$ grams of MgO would be added to the magma. This amounts to adding about 0.04 parts of MgO per billion to the magma by this reaction. The other possible additions and subtractions

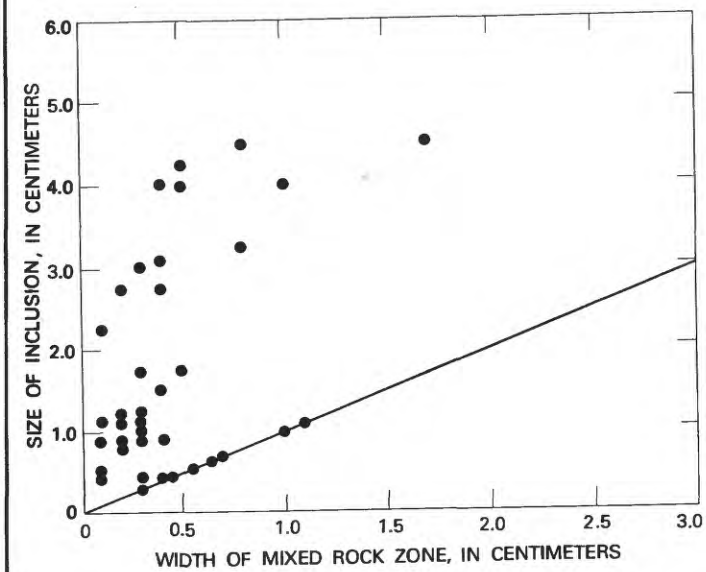

FIGURE 23.—Inclusion size (maximum length plus minimum width times one-half) plotted against width of mixed rock zone. Plotted line represents hornfels totally converted to mixed rock.

to the original magma would be of the same order of magnitude. With complete mixing, the production of mixed rocks would not produce an easily recognizable change in the original magma composition. On the other hand, without complete mixing, the basaltic magma would be locally enriched with MgO and FeO and depleted in CaO. This would force the magma to precipitate more pyroxene, iron oxides, or possibly sulfide minerals.

If there is only limited mixing, the surface area of metasedimentary rocks exposed to the original magma is an important factor because an increase in surface area would increase the amount of MgO and CaO available for reaction and exchange. Processes associated with the Basal zone that increase the surface area of metasedimentary rocks exposed to the magma include brecciation, formation of dikes and sills, and incorporation of inclusions. Figure 24 shows the percentage of hornfels of different sizes that would be consumed in reacting with an original magma. For construction of this diagram it has been assumed that: (1) Inclusions are spheres, the shape that presents a minimum surface area for contact with the magma; and (2) zones of mixed rock from 0.5 to 3.0 cm thick form from the sphere margins. These widths are the average and maximum widths observed in the Basal zone. Figure 24 illustrates that as the size of inclusion decreases, especially below radii of 20-30 cm, the volume percentage of mixed rock derived or contamination per inclusion increases rapidly. Although the diagram was constructed for the average and maximum widths observed in the Basal zone, there is a family of curves of similar shape for other widths.

ROCKS DERIVED BY PARTIAL MELTING

OCCURRENCE

Wisps, clots, lenses, discontinuous veins, and irregularly shaped volumes of quartz norite occur within hornfelsed metasedimentary rocks immediately below the Basal norite member and within the larger inclusions and attached blocks of the hornfelses. These quartz norite masses consist of orthopyroxene, plagioclase, quartz, biotite, and opaque minerals and occur in bodies commonly between 2 and 10 mm wide, but occasionally as wide as about 5 cm. Most of the wisps, lenses, and discontinuous veins have a length five

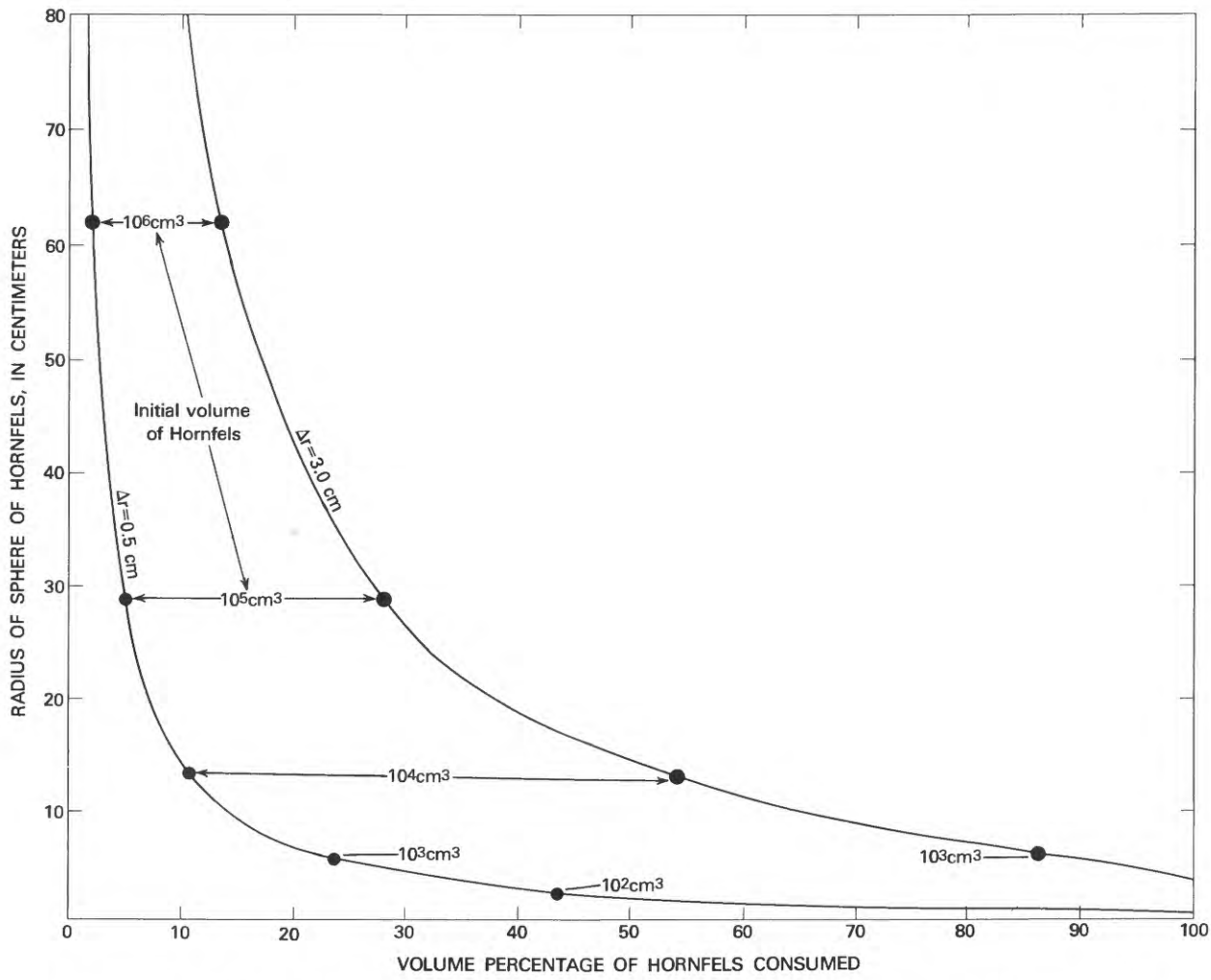

FIGURE 24.—Percentage of hornfels that would be consumed to form mixed rocks for various sizes of hornfels inclusions.

to ten times their width. Many have tabular shapes, but others are more like flattened ellipsoids. Figure 25 shows several sketches and photographs of lenses, wisps, and veins taken from etched slabs. The sketches illustrate that a series of elongate lenses and discontinuous veins may have a semiparallel arrangement but that clots and irregularly shaped volumes appear to have no organization. Examples of quartz norite veins and lenses that are semiconcordant to layering as well as those that crosscut layering have been found. Locally the irregular patches, clots, and lenses merge and form slightly larger volumes. The quartz norite appears to have been mobilized and shows intrusive features in some areas.

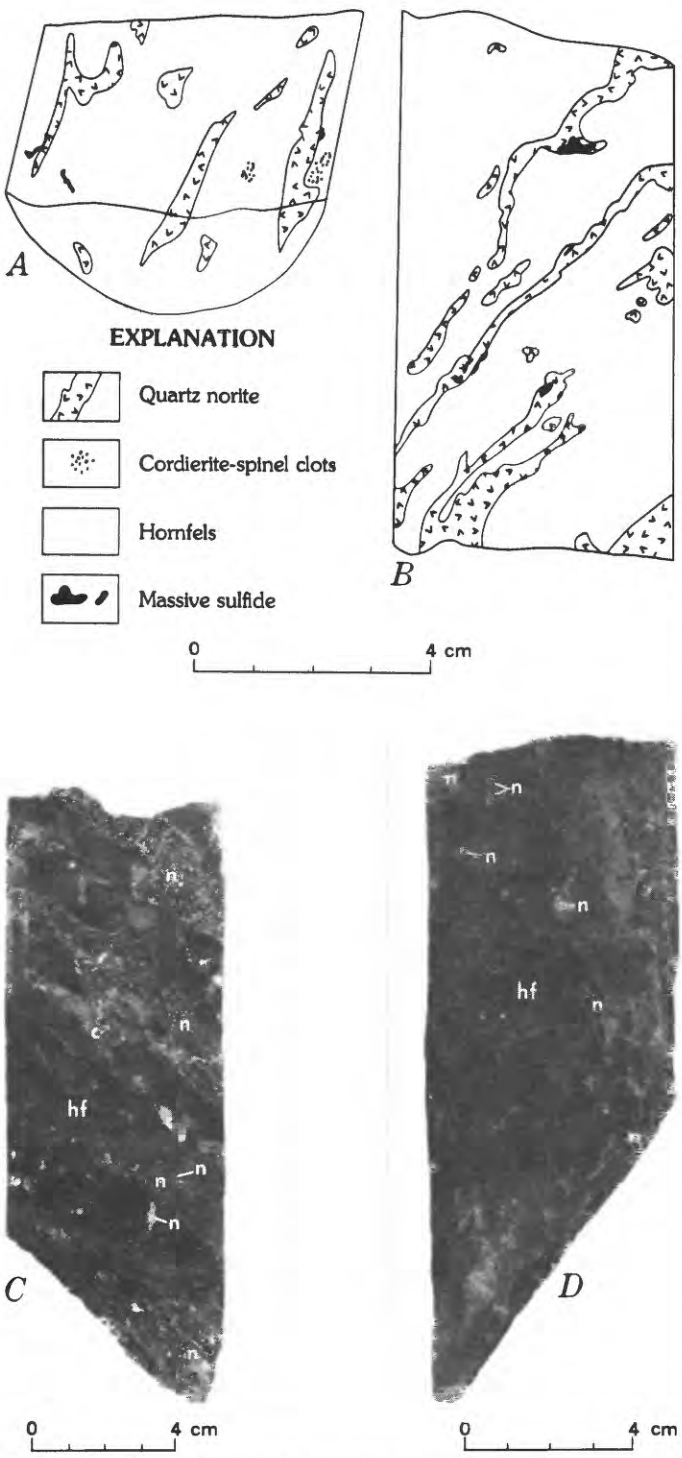

FIGURE 25.—Wisps, lenses, and discontinuous veins of quartz norite. *A* and *B*, Sketches of hand specimen of hornfels showing quartz norite lenses. *C*, layered hornfels (hf) with veins of quartz norite (n) and rock fragments rich in cordierite (c). *D*, Hornfels (hf) with irregular patches of quartz norite (n).

Quartz norite veins and lenses were found both in hornfels inclusions and in the country rocks in the Benbow, Nye Basin, Mountain View, and west of Chrome Mountain areas and thus appear to have a widespread areal development in practically all the areas in which country rocks and the Basal zone are exposed. Within individual sections of hornfels, between 5 and 30 percent of the total section contains recognizable concentrations of quartz norite veins and lenses. Within these segments or areas, the quartz norite veins and lenses compose between 1 and 10 percent of the country rock. Reconstruction of the geology suggests that the quartz norite veins and lenses in hornfels may extend from the nearest Basal norite contact for 120-180 m. As the distance from the Basal zone increases, the volume and extent of quartz norite decreases.

PETROGRAPHY AND MINERALOGY

Textures of all the quartz norites are very similar and the mineralogy simple. The lenses and veins are composed of euhedral to subhedral equidimensional orthopyroxene phenocrysts (1-3 mm in diameter) set in a matrix of intergrown quartz and plagioclase with scattered biotite flakes. Other phases present are pyrrhotite, chalcopyrite, pentlandite, and iron oxides. Potassium feldspar occurs in the matrix, usually in micrographic intergrowths with quartz, but it is not a common constituent in most of the lenses and veins. Some of the orthopyroxenes contain extremely fine exsolution lamellae parallel to the (001) plane. The locally zoned plagioclase occurs in the matrix as euhedral to subhedral crystals intergrown with or surrounded by quartz, as graphic, micrographic, or vermicular intergrowths with quartz, and as poikilitic crystals that enclose orthopyroxene. Quartz may be interstitial or intergrown with plagioclase. Within one lens or patch of quartz norite, orthopyroxene, quartz, and plagioclase frequently are uniformly distributed. In a few of the discontinuous veins, plagioclase is the matrix material in one side or part of the vein and quartz in another. Sulfide minerals generally form clots or discontinuous disseminations at the contact of the quartz norite and the hornfels (fig. 25). Apatite and clinopyroxene were found in one lens. The textures and mineralogy described above indicate that the rock is igneous and crystallized from a melt.

Modes of the quartz norites are difficult to obtain because of the small areas of quartz norite. Table 8 lists the range and

TABLE 8.—*Range and average volume percentage of minerals in quartz norite in lenses, clots, and discontinuous veins*

Mineral	Range	Average (11 samples)
Orthopyroxene	29.6-89.4	65.7
Plagioclase	0-51.0	12.6
Quartz	4.0-19.0	12.0
Potassium feldspar	0-15.9	2.3
Biotite	0-3.1	1.0
Clinopyroxene	0-1.8	1.0
Apatite	0-.3	
Spinels and sulfide minerals	0-25.1	6.1

average of 11 modes; four based on 400-500 points using a one-third millimeter grid and seven on 800-1100 points. The average mode of the quartz norites demonstrates dominance of orthopyroxene over approximately equal volumes of quartz and plagioclase. Figure 26 compares the modes of quartz norite rocks with modes of the noncumulate igneous-textured rocks. Almost all of the quartz norites have different compositions than other noncumulate igneous-textured rocks and are enriched in the orthopyroxene constituents. There are not enough data to determine whether the orthopyroxene-rich quartz norites form a gradational series with the noncumulate igneous-textured rocks.

Orthopyroxene compositions from six quartz norite veins determined by the method of Himmelberg and Jackson (1967) average $En_{62.1}$ and range from $En_{59.4}$ to $En_{67.6}$. This is comparable with the range of compositions in the hornfels of En_{50}-En_{70}. Quartz norite plagioclase compositions estimated from optical properties and X-ray techniques range from An_{75} to An_{80}.

CHARACTERISTICS OF HORNFELSES ADJACENT TO QUARTZ NORITE

The most frequently occurring mineral assemblage in hornfelsed metasedimentary rocks near the Basal zone is cordierite+plagioclase + orthopyroxene + biotite+opaque minerals with or without quartz. Near and adjacent to quartz norite lenses and discontinuous veins the most frequently occurring assemblages are cordierite+orthopyroxene +biotite+opaque minerals, cordierite+orthopyroxene +opaque minerals, cordierite+orthopyroxene+biotite, and cordierite + biotite + opaque minerals. Assemblages containing quartz or plagioclase are extremely sparse. Where quartz or plagioclase occurs in the hornfels adjacent to quartz norite it is poikilitic and appears to extend outward from the quartz norite. However, in one sample of cordierite + plagioclase + orthopyroxene + biotite + opaque minerals, the plagioclase formed subhedral to anhedral grains in a mosaic texture. In addition, near several of the quartz norite bodies, there are lenses of the assemblage cordierite+green spinel+biotite+opaque minerals. The lack of development of the assemblage cordierite+plagioclase +orthopyroxene+biotite +opaque minerals with or without quartz near the quartz norites and the development of green spinel suggest that near the quartz norite lenses and veins,

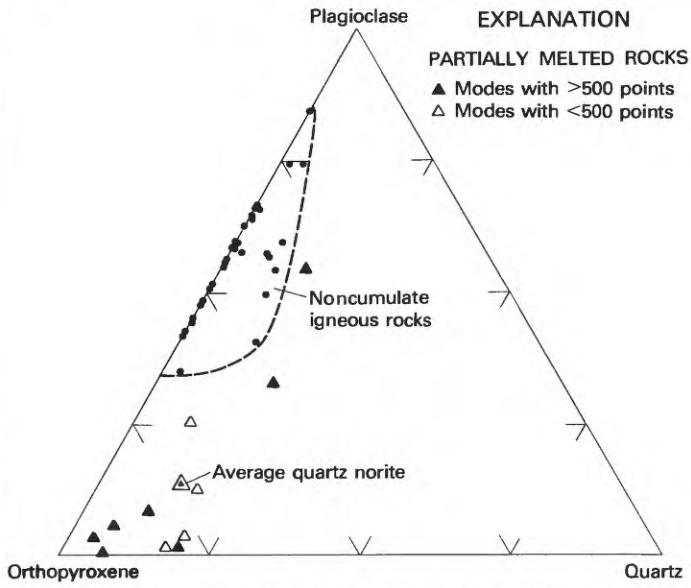

FIGURE 26.—Modal compositions in volume percent of quartz norites and noncumulate igneous rocks.

the metasedimentary rocks responded differently to metamorphic and igneous conditions.

ORIGIN OF THE QUARTZ NORITES

The simple consistent textures and mineralogy of the quartz norite and its widespread but sparse occurrence in isolated unconnected patches spatially related to the bottom of the Basal norite suggest that it was formed by a single process. Moreover, the change in mineral assemblages of the hornfelses to ones of fewer phases adjacent to the quartz norite suggests that the metasedimentary rocks were involved in the process that formed the quartz norite. Two reasonable possibilities are presented to explain the origin of the quartz norites. The first is that igneous material was injected into the hornfelses along fractures; the second is that the metasedimentary rocks partially melted to produce isolated pockets of liquid, which subsequently crystallized as quartz norite.

Injection of basaltic melt, or of magma of quartz norite composition produced by differentiation from the Stillwater magma, would require a pervasive fracture system within the metasedimentary rocks through which the melt could have traveled and would require that the fractures healed, possibly by annealing, after the melt was injected. The restriction of quartz norite volumes to small size, the distribution of these volumes as much as 150 to 180 m from the base of the complex, and the decrease in abundance of quartz norite away from the complex suggest that the process was not fracture-controlled. The injection origin also requires that either an extreme differentiate of the Stillwater magma was formed or that one of the known variants of the magma reacted with the metasedimentary rocks upon injection to produce magma of the quartz norite

composition. The fact that no similar compositions are known from noncumulate igneous-textured rocks of the Basal norite suggests that no differentiated magmas of this composition existed. Because of the widespread distribution of the quartz norite material, such an event would have affected a large volume of the chamber. There is little or no evidence that the hornfelses near the quartz norite lenses were involved in reactions with a basaltic magma similar to those reactions discussed for the mixed rocks. For these reasons, an origin by magmatic injection seems unlikely.

Partial melting or fusion of the metasedimentary rocks to derive a relatively small amount of quartz norite melt seems the only likely means for creating small lenses and pods that are not interconnected. The Stillwater magma is a logical heat source, although it is difficult to understand the distribution of heat outward from the complex in light of heat balance studies by Jaeger (1959), Hess (1972), and Irvine (1970b) of tabular intrusive bodies and their country rocks. The occurrence of the quartz norite in lenses and clots is what might be expected if partial fusion occurred where the appropriate number of phases were in contact to produce a composition that could melt. The distribution and decrease in abundance away from the complex also fit the expectation.

The metasedimentary rocks available for melting are composed mainly of SiO_2, Al_2O_3, MgO, and FeO with minor amount of CaO (Page, 1977). The amounts of K_2O and Na_2O are relatively low. Figure 27 shows the compositions of the metasedimentary rocks projected onto various planes in the tetrahedron CaO-MgO-Al_2O_3-SiO_2 and demonstrates the high proportion of SiO_2 in the hornfels relative to MgO, Al_2O_3, and CaO. The projections also show that the quartz norite rocks have a composition distinct from the hornfelses and the noncumulate igneous rocks and that liquids of quartz norite composition could crystallize to form the observed mineral assemblages. The average composition of the quartz norite was calculated from average mode (table 8) and determined mineral compositions.

Several low-temperature invariant points exist in the systems K_2O-MgO-Al_2O_3-SiO_2 (Schairer, 1954) and CaO-MgO-Al_2O_3-SiO_2 (Hytonen and Schairer, 1960; Chinner and Schairer, 1962; Schairer and Yoder, 1970). Both systems contain phases relevant to the hornfelses and

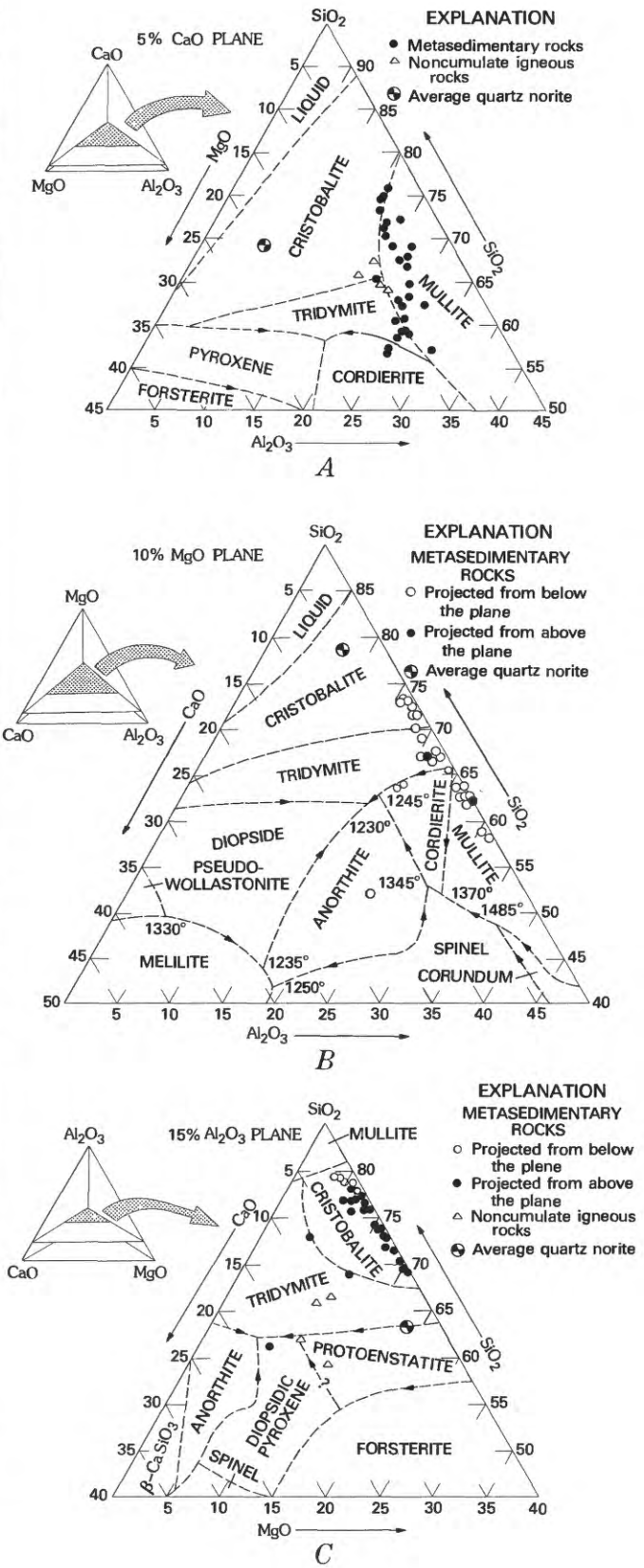

FIGURE 27.—Comparison of compositions of metasedimentary rocks, noncumulate igneous rocks, and estimated compositionof quartz norite in the tetrahedron CaO-MgO-Al_2O_3-SiO_2. *A*, The 5 percent CaO plane. Projection of approximate liquidus surfaces derived from data of Osborn, Devries, Gee, and Kraner (1954) and Prince (1954). *B*, The 10 percent MgO plane. Projection of approximate liquidus surfaces after Prince (1954). *C*, The 15 percent Al_2O_3 plane. Projection of approximate liquidus surfaces after Osborn, DeVries, Gee, and Kraner (1954).

the quartz norite compositions. Consideration of the lower temperature invariant points at which liquids would be produced in conjunction with the hornfels compositions, based on Presnall's (1969) geometrical analysis of fractional fusion, shows that only small amounts of melt of uniform composition could be produced. This is in agreement with the observed amounts of quartz norite. At least three invariant points in these systems could correspond to the production of partial melts: (1) The eutectic point at 960°±20° C at which enstatite-tridymite-potassium feldspar-cordierite-liquid coexist (Schairer, 1954), (2) the invariant point at 1150°±10° C at which enstatite-anorthite -diopside-tridymite-liquid coexist (Hytonen and Schairer, 1960; Schairer and Yoder, 1970), and (3) the invariant point at an undetermined temperature at which enstatite-anorthite-tridymite-cordierite -liquid coexist. The liquid produced at the second invariant point relates most closely with the minerals present in the quartz norites. Such liquids could eventually crystallize as the assemblage plagioclase+quartz+orthopyroxene with diopsidic augite exsolution lamellae. As partial fusion continued, one or more phases in the adjacent hornfels would be consumed.

Elsewhere, features ascribed to partial fusion of country rocks associated with mafic intrusive rocks have been described. Gribble (1966, 1967, 1968, 1970) and Gribble and O'Hara (1967) interpreted the cordierite norites in northeastern Scotland as having originated by fusion; other examples of partial fusion have been reported by Wyllie (1959) and Argell (in Chinner and Schairer, 1962, p. 633). Gribble and O'Hara (1967) used the invariant point enstatite-anorthite-tridymite-cordierite-liquid to explain the composition of their rocks from Scotland. Their analytical data on the material to be melted, the interpreted partial melts, and the residual materials show higher amounts of K_2O and Na_2O than in the Stillwater example, which would explain the dissimilarities between the rocks in Scotland and the Stillwater example in which quartz norites were produced.

OTHER SILICATE ROCKS

Two other types of rocks composed mainly of silicate minerals were recognized in the Basal norite. Discussion of their distribution, abundance, texture, and mineralogy is limited by the few samples found. One type, which exhibits textures and mineralogy resembling ultramafic xenoliths and basalts or rocks from alpine ultramafic masses, was found only in samples of drill core of the lower part of the Basal norite in the Iron Mountain and Chrome Mountain areas. The other type, which has compositions similar to the Basal norite and exhibits granoblastic textures imprinted upon cumulate or ophitic textures, locally occurs intermixed with cumulates and noncumulates of the Basal norite from the Benbow area to and including the Mountain View area and in the area west of the Boulder River. The first type is tentatively labeled ultramafic xenoliths and the other type, autohornfelsed Basal zone. It is not known whether the xenoliths have an origin cognate or external to the Stillwater Complex.

ULTRAMAFIC XENOLITHS

Rocks classified as ultramafic xenoliths occur as discrete fragments that are distinguished from the enclosing orthopyroxene cumulate matrix by texture and mineralogy. Three groups of xenoliths are present: (1) Websterites composed of orthopyroxene and clinopyroxene, (2) dunites composed of olivine and minor amounts of orthopyroxene, and (3) orthopyroxenites composed of orthopyroxene and plagioclase. The host rock for all known xenoliths is orthopyroxene cumulate composed of euhedral to subhedral orthopyroxene with $En_{63.3}$ to $En_{66.5}$ surrounded by post-cumulate plagioclase, minor clinopyroxene, biotite, and opaque minerals. These are similar to all other orthopyroxene cumulates (table 3) in appearance, mineralogy, texture, and composition. They also seem to fit into any trends established in the section of the Basal norite in which they occur.

The websterites (fig. 28*A*) typically contain orthopyroxene crystals that are 6 to 11 mm in diameter, anhedral, and interlocking, show undulatory extinction in thin section, and extinguish in domains that appear to have been rotated or moved slightly in relation to one another. Rims of larger grains generally lack exsolution lamellae, and exsolution

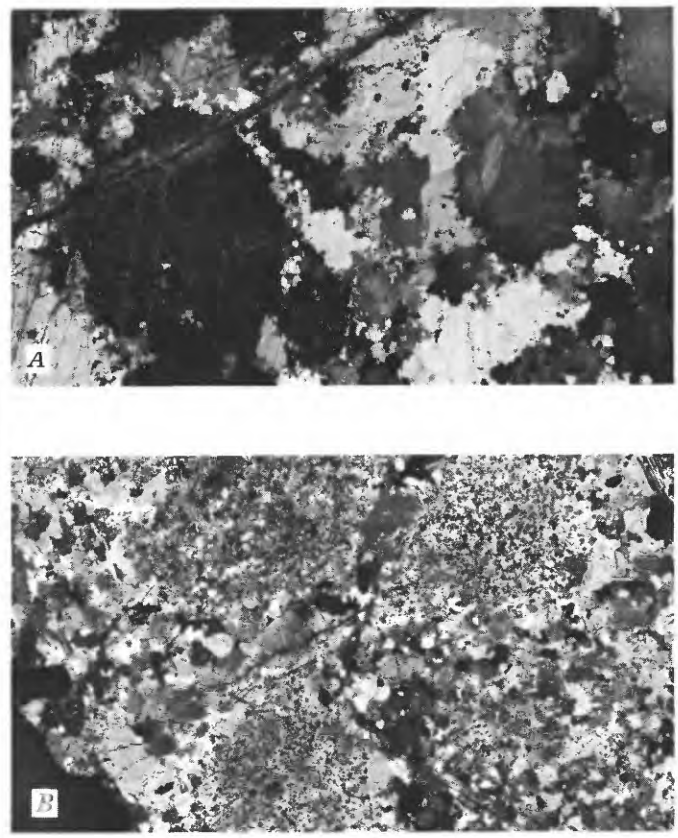

FIGURE 28. Photomicrographs of ultramafic xenoliths. *A*, Websterite showing large strained orthopyroxene with a necklace of smaller orthopyroxene. *B*, Dunite in orthopyroxene cumulate.

lamellae parallel to the (001) plane of orthopyroxene are irregularly developed throughout single crystals. Larger orthopyroxenes are partly to totally surrounded by necklaces of smaller (0.15 to 0.5 mm diameter) subhedral to anhedral orthopyroxene grains without exsolution lamellae. The orthopyroxene necklaces are several grains wide and, where developed in patches, show a granoblastic or mosaic closely packed texture. Clinopyroxene makes up 5-20 percent of the xenolith and occurs in the necklaces as small anhedral grains without exsolution lamellae. Plagioclase makes up 1-5 percent of the xenolith, occurs as interstitial material, and has altered to epidote where it is near fractures. A clear clinoamphibole occurs near fractures where it replaces both clino- and orthopyroxene. The opaque minerals make up less than 1 percent of the xenolith and are dominantly sulfides that occur along grain boundaries or at grain junctions.

The texture of the websterites is interpreted as metamorphic, with strained and possibly granulated orthopyroxene that recrystallized along with clinopyroxene to form necklaces. Such textures are similar to those in xenoliths from basalts (White, 1966; Jackson, 1968b) and in alpine ultramafic rocks (Loney and others, 1971). Their formation within the Stillwater magma chamber would require a peculiar sequence of events, and I suggest that the websterite xenoliths may have had an external source.

The dunite xenoliths contain 70-90 percent by volume subhedral olivine (0.5-0.8 mm in diameter) with a granoblastic texture. Most of the olivine is altered to serpentine, talc, and iron oxides and thus internal features of the olivine grains have been destroyed. Other constituents of the xenoliths are 5-20 percent plagioclase, 5-15 percent anhedral to subhedral orthopyroxene, less than 1 percent biotite, and 3-5 percent opaque minerals. The dominant opaque phase is subhedral to euhedral spinel, the thinner edges of some grains showing brown or green colors. Inside the xenoliths the plagioclase is interstitial to the mafic minerals but is most abundant near the margins of the xenoliths where it has a poikilitic texture enclosing olivine grains. Poikilitic plagioclase crystals near the margins of the xenoliths extend into the orthopyroxene cumulate.

Clots of olivine and single crystals of olivine from the Basal norite in the eastern sections of the complex show undulatory extinction in thin section. Some olivine crystals contain parallel bands of slightly different extinction position called kink bands (Raleigh, 1965a, b). Although kink bands are not observable in the olivine of the dunite xenoliths because of serpentinization, their presence in olivine xenocrysts suggests that there was a source of deformed olivine. It is possible that the xenoliths are this source.

The orthopyroxenite xenoliths have a granoblastic mosaic texture and contain 80-90 percent by volume of granular anhedral orthopyroxene (average diameter 0.5 mm), interstitial plagioclase, opaque minerals, and a few flakes of biotite. The orthopyroxene contains no visible exsolution lamellae and shows no evidence of having been strained. Margins of the xenoliths are similar to those of the dunite xenoliths in that they have poikilitic plagioclase extending both inward and outward from their contact with the orthopyroxene cumulate host.

Two possible origins for the dunite and orthopyroxene xenoliths are suggested. First, the xenoliths represent ultramafic material from a source external to the Stillwater magma that was caught up in the magma and reacted with it to form poikilitic plagioclase. Second, the xenoliths are cognate and crystallized elsewhere in the magma chamber, were mechanically incorporated in the magma crystallizing the cumulate host rock, and reacted with it to form the poikilitic plagioclase. The granofelsic mosaic texture in either type of inclusion only implies some annealing and rearrangement of the grain boundaries and is consistent with either hypothesis. Although ultramafic xenoliths are rare in tholeiitic basalts, they have been reported in the norite near the base of the Sudbury Nickel Irruptive in the Strathcona ore deposit (Naldrett and Kullerud, 1967).

AUTOHORNFELSED BASAL ZONE ROCKS

About a dozen samples of the Basal norite collected from drill core and outcrops megascopically appear to be typical cumulate or noncumulate rocks but in thin section have quite a different aspect, in that the plagioclase forms a granoblastic mosaic regardless of whether its texture was originally ophitic or poikilitic. In some of the rocks the ortho- and clinopyroxenes are granulated along their margins and appear to have recrystallized. These recrystallized textures are similar to those in the metadolerite dikes from the Beartooth terrane (Page, 1977). Comparison of the textures in the metadolerite dikes and in the hornfelsed metasedimentary rocks with these textures in the Basal zone suggests that the granoblastic mosaic feldspar and the granulated pyroxene were derived by a metamorphic process. It is suggested that these textures result from autometamorphism of precrystallized rocks (cognate xenoliths) mechanically transported and annealed by the Stillwater magma, or local annealing of rocks that crystallized in place.

SULFIDE-BEARING ROCKS

OCCURRENCE, GENERAL TERMINOLOGY, AND DISTRIBUTION

All rocks within the Basal zone contain sulfide minerals. By far the majority of Basal zone samples contain less than 1 percent sulfide, although higher concentrations, even 100 percent, are not uncommon. To cover this wide range of sulfide content, a terminology was developed on the basis of natural divisions, resulting in three types of sulfide concentrations: Disseminated sulfide, matrix sulfide, and massive sulfide rock.

The occurrence and distribution of sulfide mineralization in and adjacent to the Basal zone are difficult if not impossible to determine on the basis of surface exposures and must await extensive studies of subsurface information. However, several generalizations about the distribution of mineralization can be made from the extent and development of gossans, sulfide rock exposures, and early prospecting. (1) The mineralization is not homogeneously distributed within nor is it limited to the Basal zone. Locally, sulfide concentrations occur within the metasedimentary rocks and within the lower part of the Peridotite member of the Ultramafic zone. (2) The amount of mineralization varies along the strike of the complex and, as shown by surface exposures and gossans, is concentrated in the following areas (pl. 1): Benbow, Nye Basin, Mountain View, Initial, Crescent Creek, between Blakely and the unnamed creek to the south, and west of the Boulder River. Other areas with fair exposure appear to contain less sulfides, but many areas that may contain mineralization are not exposed, owing to either thrusting or covering Quaternary deposits. (3) The amount of mineralization varies vertically in the Basal zone; stratigraphically lower parts of the section, mainly the Basal norite, tend to have higher concentrations of sulfide minerals. (4) Areas believed to represent depositional basins (fig. 4) tend to have higher concentrations of sulfides than the interbasinal areas. Moreover, sulfide mineralization appears to increase toward the centers of the basin areas. (5) Sulfide concentrations in metasedimentary rocks occur as pods and lenses, usually associated with rocks of noritic mineralogy and composition. (6) No sulfide concentrations have been shown to be localized by faulting. (7) Some areas in the Basal norite that are characterized by mixed rocks, hornfels inclusions, and intrusive breccias tend to contain relatively more mineralization.

An example of the vertical distribution of sulfide mineralization in the Basal zone is given in figure 29. The section shows estimates of maximum sulfide amounts present within about a meter of section, a measure easier to judge than average sulfide content. Even though this section may not be typical of the Basal zone, several generalizations which appear valid for the whole zone may be made from figure 29. (1) Within the Basal zone, the Basal norite is enriched in sulfide minerals relative to the Basal bronzite cumulate. (2) Noncumulate, igneous-textured, ophitic and subophitic rocks tend to have relatively small amounts of sulfide minerals but commonly are followed stratigraphically upward in the section by concentrations of sulfide minerals in the cumulate rocks. (3) No particular cumulate rock lithology appears to have more sulfide minerals than another, suggesting that the accumulation process is not closely related to a specific magma chemistry. (4) Increases and decreases in maximum sulfide mineral content appear to form cycles which may be related to repetitions of noncumulate and cumulate lithologies. (5) Massive sulfide layers tend to be relatively thin—about a meter thick.

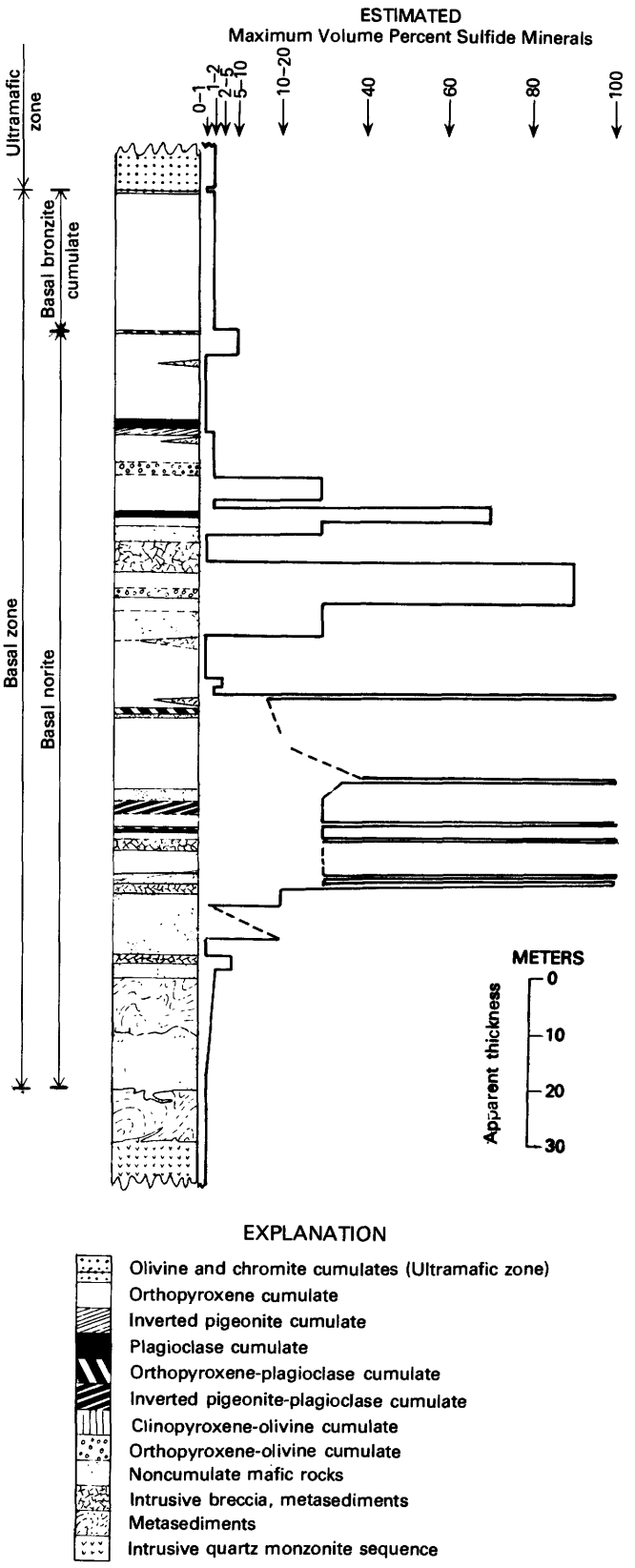

FIGURE 29.—Estimated maximum volume percentage of sulfide minerals in a stratigraphic section of the Basal zone in the Mountain View area.

DEVELOPMENT OF TERMINOLOGY FOR SULFIDE-BEARING ROCKS

Various names and terms such as massive sulfide ore, matrix sulfide (Ewers and Hudson, 1972), net-textured ore (Naldrett, 1969), and disseminated sulfide have been used by other authors to describe the range in proportions of sulfide and silicate minerals in mafic and ultramafic rocks. Consideration of the variation in the amount of sulfide minerals present and their degree of interconnection suggested that there might be a set of natural boundaries upon which to base a terminology for sulfide mineralization in the Stillwater Complex.

To examine this possibility, modal volume percentages of sulfide minerals were determined by point-counting on ground rock slabs or polished sections. On the same sections or slabs the electrical resistance (conductivity) was measured between numerous sulfide grains (Kanehira, 1966) to determine the extent of interconnection among them. In selecting specimens for this analysis, relatively few samples were chosen whose visual estimates indicated less than 5 percent or more than 95 percent sulfide minerals present. Thus, the data are most representative in the intermediate concentration ranges and should not be considered to represent the natural frequency of sulfide mineral occurrence in the Basal zone. As noted, the natural frequency distribution would have a very large maximum in the 0 to 5 percent range. Figure 30 illustrates that sulfide-bearing rocks can be broken into three distinct groups, separated by the minima between 5 and 10 and 55 and 70 percent sulfide minerals.

Measurements of electrical resistivity between sulfide grains indicate that in all the samples that contain more than 10-15 volume percent sulfides, the sulfide minerals are continuously interconnected at least within the volumes represented by the slabs. At sulfide concentrations below 10 percent, sulfide minerals are interconnected within volumes from less than 1 mm to 1-2 cm in diameter (Page, 1971b). Ewers and Hudson (1972, p. 1079) reported a somewhat higher level for sulfide continuity; rocks with more than 20 percent sulfide minerals showed electrical continuity. The break between continuous sulfide interconnection over indeterminate volumes and the much smaller continuous areas of 1-2 cm and less, appears to be a natural break which is useful for developing a terminology. Rocks containing less than 10 percent sulfide minerals are called by their rock name and are said to contain disseminated sulfide minerals.

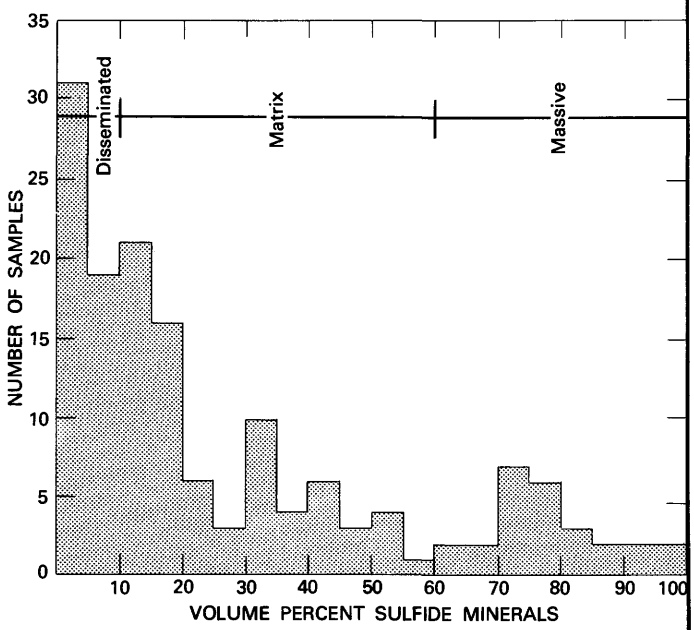

FIGURE 30. --Modal volumes of sulfide minerals in 150 selected samples.

Rocks containing between 10 and 60 volume percent sulfide minerals are called by their rock name and said to contain matrix sulfide minerals. In these rocks the sulfide minerals occupy interstices in the cumulus silicate phases in an exactly analogous texture to that of postcumulate silicate phases in normal cumulate rocks. The silicate minerals enclosed in the sulfide matrix have the same appearance and properties as cumulus phases in typical cumulate rocks. Estimates of initial porosity of cumulates range from 20 percent (Wager and Deer, 1939) to 45 percent (Wager and others, 1960). Jackson (1961a) reported porosities between 15 and 50 percent with an average of 35 percent in the Stillwater Complex, depending on the cumulate rock type. Measurements of beach sand porosities (Fraser, 1935) are in accord with the estimates of initial porosities of cumulate rocks, and calculations of ideal porosities for various packing arrangements of spheres range from 25.9 to 47.6 percent (Graton and Fraser, 1935). The lack of rocks with 55 to 70 percent sulfides appears to be correlated with a similar lack of normal cumulate rocks with these initial porosities, and it appears that the silicate host fixes a natural upper limit for the matrix sulfides. The lack of rocks with 20 to 30 percent sulfides may also be related indirectly to porosity. Cumulate rocks containing relatively small amounts of interstitial silicate or sulfide minerals frequently show extensive overgrowths on the cumulus minerals that tend to decrease the initial porosity. Overgrowth on silicate minerals requires an adequate supply of silicate magma and abundant diffusion paths. Such conditions imply a correspondingly small amount of sulfide liquid at the sites of postcumulus development, with the implication that conditions in this range of porosity of cumulate rocks do not allow concentrations of sulfides.

Rocks containing between 70 and 100 volume percent sulfide minerals are termed massive sulfide rocks because the framework of these rocks is composed of sulfide minerals. Because silicate minerals or rock fragments are not essential components in the massive sulfide rocks, their formation and sulfide content are not directly related to processes of silicate crystallization.

TEXTURES OF SULFIDE-BEARING ROCKS

The large number of apparent textural varieties displayed by the sulfide-bearing rocks in the Basal zone and probably

throughout the entire Stillwater Complex can be divided into two major groups. The first group, composed of disseminated and matrix sulfide rocks, has textures controlled by the shapes of interstices between cumulus minerals in cumulate rocks or interstices in the ophitic and subophitic noncumulate rocks. The second group consists of the massive sulfide rocks and has the texture of the sulfide framework; the silicate minerals or rock fragments enclosed by sulfide are incidental to the texture. This section of the report considers only the textures formed by the sulfide content—regardless of the mineralogy—and the silicate fraction; textural relations between various sulfide minerals are considered in the section entitled, "Mineralogy of the sulfide-bearing rocks."

DISSEMINATED AND MATRIX SULFIDE TEXTURES

Textures of disseminated and matrix sulfide-bearing rocks are controlled by the shapes of the interstices between cumulus minerals. Interstices take the shape of branching concave polygons whose sides are formed by the crystal faces of the cumulus minerals. Cross sections of the interstices, as viewed in polished sections, approximate the cuspoid shapes of the voids resulting from the systematic packing of spheres (Graton and Fraser, 1935, p. 810, 815, 852-857). Jackson (1961a, p. 65 and following pages) discussed the interstitial shapes in rocks from the Ultramafic zone, and his discussion is applicable to the Basal zone. Jackson demonstrated that the shapes of the interstices are altered wherever secondary enlargement or overgrowth of cumulus phases occurs or when there has been reaction replacement of the cumulus phases. No evidence for reaction, replacement, or overgrowth textures involving sulfide minerals has been observed, however; disseminated or matrix sulfides tend to preserve the original polygonal shapes of the interstices, unless the whole rock was involved in later alteration. Figure 31 depicts in photographs and tracings from slabs the typical textures exhibited by disseminated and matrix sulfide minerals in cumulate rocks. The dashed circles superimposed on figure 31*A* show areas within which the disseminated sulfide minerals are continuously interconnected.

Considered within the framework of processes for forming cumulate rocks, the textures exhibited by the disseminated sulfide minerals suggest possible methods of deposition. The occurrence of sulfides in polygonal shapes, molded onto cumulus minerals, implies that sulfide minerals crystallized after the cumulus silicates and that most of the sulfide crystallization history must be a postcumulus process. A similar argument based on common grain boundaries with most postcumulus silicates implies that the sulfide minerals crystallized after most postcumulus silicates. Experimental evidence on crystallization temperatures of silicate and sulfide minerals supports these inferences.

The sulfide minerals that appear as clots or groups of grains in two dimensions but that prove to be continuously interconnected in three dimensions suggest concentration of sulfide material prior to postcumulus crystallization. At least two possible models for concentration can be envisioned: (1) A postcumulus process in which sulfide material accumulates by diffusion from the magma above the cumulus crystal pile into pore spaces; and (2) a mainly cumulus process in which an immiscible sulfide liquid forms droplets and coalesces into masses of liquid large enough to settle as a cumulus liquid phase which displaces the interstitial silicate magma in the crystal pile before the postcumulus silicate crystallizes. The postcumulus process requires intricate timing of events—the sulfide must accumulate before postcumulate silicate crystallization—and it requires a variable amount of sulfide in solution in the magma to account for the volume variation of sulfide mineral. The cumulus process requires only a variable supply of droplets, possibly controlled by the time taken to coalesce into masses that could settle. Evidence for diffusion processes has not been found, and the timing of the event suggests that such evidence should be available. Therefore the hypothesis of a cumulus process is preferred for the origin of disseminated sulfides.

Figures 31*D-H* show the textures exhibited by cumulate rocks with a range of matrix sulfide content from 13 to about 50 volume percent. All matrix sulfides fill interstices with continuity over large volumes. Figures 31*E* and *H* illustrate the irregular contacts between barren rocks and cumulates with matrix sulfides; the slabs in figures 31*F* and *G* show comparable pore-filling textures between sulfide and silicate material in orthopyroxene and plagioclase cumulates. It is thought that the processes responsible for the textures exhibited by the matrix sulfides are the same as for the disseminated sulfide minerals except that the supply of sulfide material was much larger than for the disseminated ores. Any model of origin of the matrix sulfides must be constrained by the following observations: (1) There is no noticeable relation between the volume of sulfide matrix and

FIGURE 31.—Textures of disseminated and matrix sulfide minerals in cumulate rock slabs. *A*, Disseminated sulfide minerals in medium-grained orthopyroxene plagioclase cumulate (BB-3/378.5). Sulfide minerals, black; dashed circles enclose continuously interconnected sulfide minerals. Traced from ground and etched slab. *B*, Disseminated minerals (NBI3347). Width of sulfide grain 2 mm; po, pyrrhotite; pn, pentlandite. *C*, Part of rock slab with matrix sulfide minerals in orthopyroxene cumulate (387-339/228). Black, sulfide minerals. *D*, Rock slab of orthopyroxene cumulate containing about 13 percent matrix sulfide minerals (368-307A/561). Light gray, sulfide minerals. *E*, Rock slab of orthopyroxene cumulate containing 46 percent matrix sulfide minerals (368-307A/772.5). Light gray, sulfide minerals. *F*, Rock slab of plagioclase cumulate containing matrix sulfide minerals (NB13/295); s, sulfide; o, orthopyroxene; p, plagioclase. *G*, Rock slab of orthopyroxene cumulate containing 48 percent matrix sulfides in right half of the section (368-307A/542). Specimen shows irregular contact between matrix sulfide-bearing cumulate and silicate interstitial material. Light gray, sulfide minerals.

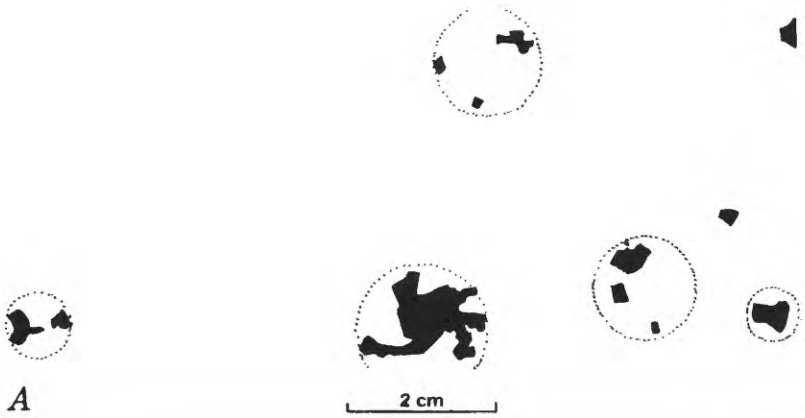
A
2 cm

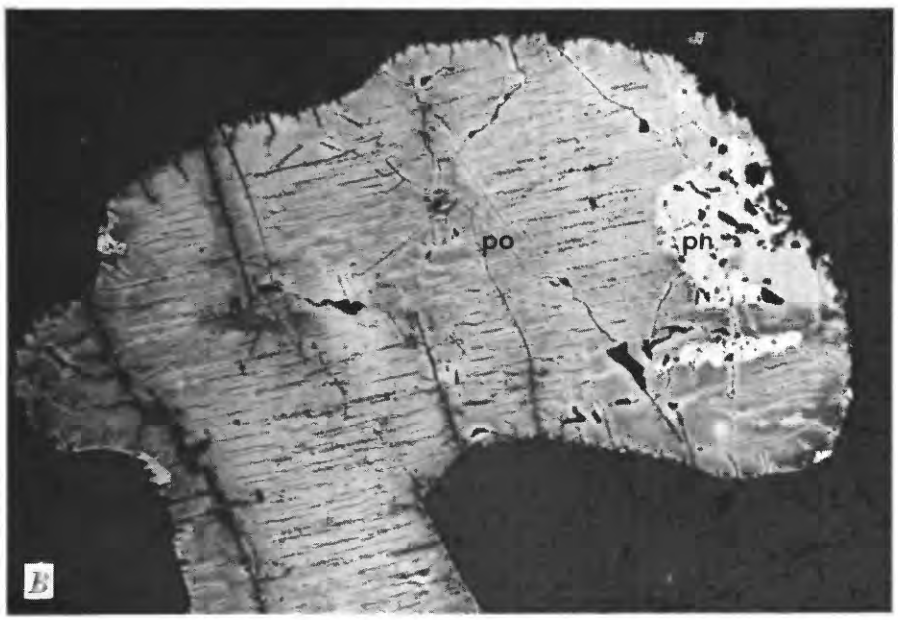
po
ph
B


D
2 cm


E
2 cm


C
2 cm

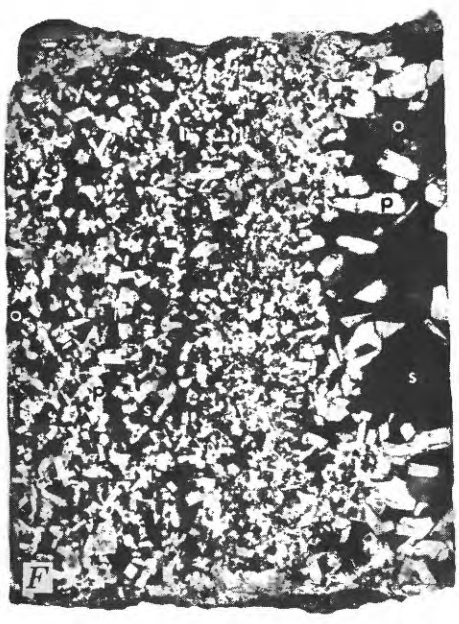
p
s
F
2 cm

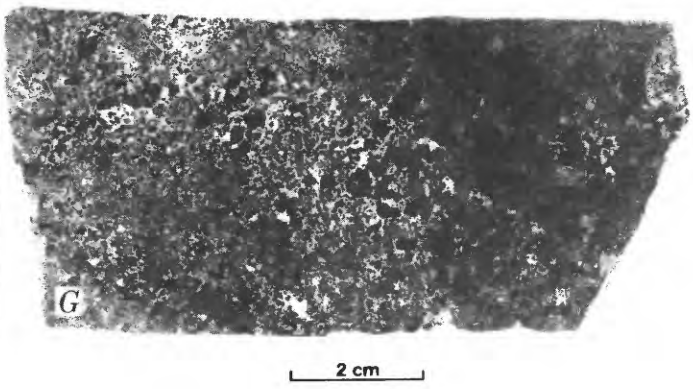
G
2 cm

the type of cumulate mineral or minerals forming the framework; (2) there is no evidence of reaction between the sulfide matrix and postcumulus silicate minerals or at the margins of lenses or layers of matrix sulfide; and (3) the matrix sulfides are molded tightly to the cumulus silicate minerals—generally there are no intervening rims of postcumulus silicate phases.

TEXTURES OF MASSIVE SULFIDE ROCKS

A variety of textural features are found in the massive sulfide rocks (fig. 32), which generally contain cumulus silicate minerals, rock fragments, or both. Orthopyroxene and plagioclase occur in the massive sulfide rock as euhedral to subhedral phenocrysts that resemble silicate crystals of cumulate rocks (figs. 32*A* and *B*). Rock fragments of metasedimentary rocks, orthopyroxene cumulates, or both are engulfed and surrounded by massive sulfide material (fig. 32*D*). Both types of rock fragments appear to have been mechanically incorporated. One process by which fragments of hornfelses were incorporated into the massive sulfide rock appears to have been brecciation (figs. 32*E* and *F*). Hornfels fragments in these samples have margins against sulfide that on adjacent hornfels fragments approach puzzle-shaped pieces of one another, and it appears that the original metasedimentary rock could be put back together without the massive sulfide. In other instances fragments produced by such brecciation appear to have been moved or mixed by magmatic currents and gravity to their present positions.

As figure 32*A* illustrates, the only difference between massive sulfide rocks and cumulates with matrix sulfide minerals is in the amount of sulfide present. The contact between types of sulfide-bearing rocks may be sharp and irregular (fig. 32*A*) or gradational (lower part of specimen in fig. 32*B*). The layering of the samples (fig. 32*A*, *B*) is typical of many of the massive sulfide rocks. Hornfelsed metasedimentary rock fragments engulfed or enclosed by massive sulfides may have irregular shapes (upper part of specimen in fig. 32*B*), lensoid shapes with tapering tails (fig. 32*C*), or angular to subangular blocky shapes (figs. 32*D* and *F*). Many of the metasedimentary fragments are enriched in cordierite, but others have mineralogic features like the underlying metasedimentary rock basement. Locally sulfide material tends to penetrate some of the rock fragments along fractures or foliation planes of the metasedimentary rock. Fragments of cumulate rocks tend to be angular to subangular (fig. 32*D*).

Any model of the origin of the massive sulfide must be constrained by the following observations: (1) Generally no other silicate material separates the massive sulfide and the phenocrysts or rock fragments, (2) there are no observable reactions between silicate minerals and the sulfides at the edges of massive sulfide lenses and layers, and (3) massive sulfide rocks usually have sharp contacts with matrix sulfide cumulates but may have contacts that appear to consist merely of a change in sulfide content.

TEXTURAL RELATIONS BETWEEN SILICATE AND SULFIDE MINERALS

Little evidence of replacement of primary igneous silicate minerals by sulfide minerals has been observed in the three sulfide-bearing rocks. The silicate minerals, around which the sulfides are molded, retain the characteristic euhedral to subhedral crystal margins that they exhibit in unmineralized rocks. Sulfide veins rarely cut silicate minerals, and where they do the sulfide minerals appear to be fracture fillings because the margins of the fractures generally match. The regular and smooth margins of sulfide masses against silicate minerals, whether the silicate is a cumulus, postcumulus, or noncumulate igneous phase, are evidence that replacement of primary silicate minerals by sulfide minerals probably did not occur.

In mixed rocks where sulfide minerals are present, replacement of silicates and oxides is more common. Pyrrhotite forms pseudomorphs after magnetite and spinels of the metasedimentary part of the mixed rock, and sulfide minerals, mainly pyrrhotite and chalcopyrite, penetrate silicate minerals along fractures whose margins do not match. However, these types of replacements are minor.

MINERALOGY OF THE SULFIDE-BEARING ROCKS

The overall mineralogy of the sulfide-bearing rocks is relatively simple, and except for samples from surface exposures the sulfides in specimens of sulfide-bearing rock are not altered. Locally where silicate minerals are altered to amphiboles, serpentine, and other silicate minerals, the primary assemblages of sulfide minerals appear to have been remobilized, possibly changing the compositions of the phases but not altering the primary phase to another species. The following table lists the minerals present in the sulfide-bearing rocks. Because the sulfide minerals do not appear to vary in number or kind, but only in amount and proportions, the sulfide minerals from all three texture types can be considered together. Pyrrhotite, pentlandite, and

FIGURE 32.—Rock slabs of massive sulfide rocks. *A*, Sharp, irregular boundary between massive sulfide rock, lower right side, and orthopyroxene cumulate with matrix sulfide. Sulfide minerals have continuity throughout entire sample (389-339/303.5). *B*, Massive sulfide rock, containing hornfels inclusion, and showing layering of massive sulfide and orthopyroxene phenocrysts (387-339/53.5). *C*, Massive sulfide rock enclosing hornfelsed metasedimentary rocks and orthopyroxene phenocrysts (387-339/49). *D*, Massive sulfide rock enclosing fragments of hornfelsed metasedimentary rocks and orthopyroxene cumulates. Adjacent tracing shows distribution of larger hornfels and cumulate fragments (M20/355.0). *E*, Massive sulfide rock engulfing fragments of brecciated hornfelsed metasedimentary rock (387-339/398.5). *F*, Massive sulfide rock engulfing fragments of brecciated hornfelsed metasedimentary rock. Upper part of massive sulfide is rich in chalcopyrite (368-307A/595).

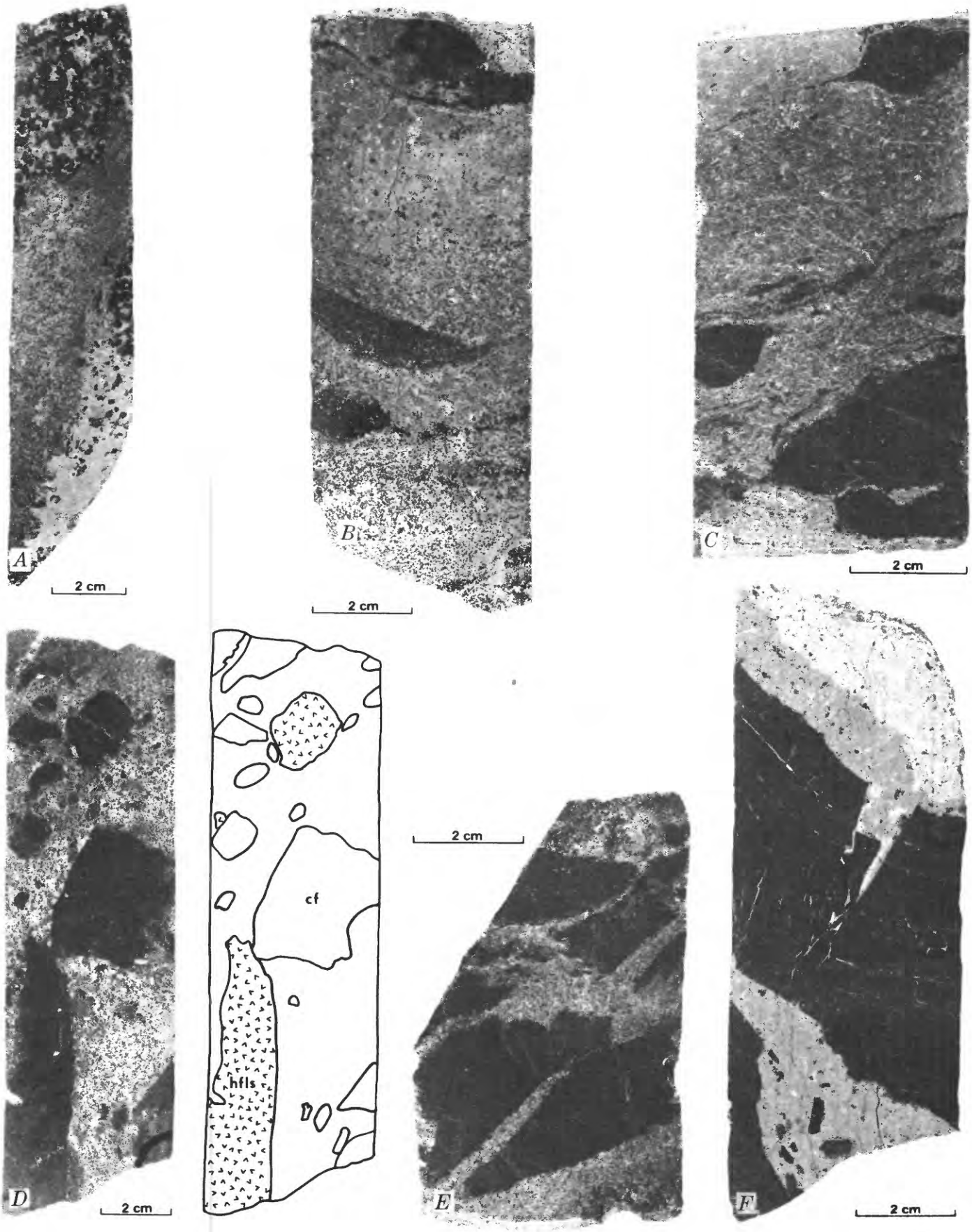
A
2 cm
B
2 cm
C
2 cm
D
2 cm
cf
hfls
2 cm
E
F
2 cm

chalcopyrite are the dominant primary sulfide minerals. Local alteration has produced small amounts of bravolite, violarite, mackinawite, marcasite, pyrite, cuprite, and native copper. Earlier mineralogic studies by Howland (1933) established the presence of most of the phases; this report documents their occurrence in the Basal zone. Oxide minerals are primarily magnetite with exsolved ilmenite, ilmenite, chromite, and local goethite.

Sulfides		Oxides	
Primary			
Pyrrhotite	Pentlandite	Magnetite	Chromite
Monoclinic	Chalcopyrite	Ilmenite	
Hexagonal	Gersdorffite	Magnetite-ilmenite intergrowths	
		Ilmenite-hematite intergrowths	
Alteration			
Bravolite	Marcasite	Magnetite	Cuprite
Violarite	Pyrite	Goethite	Native copper
Mackinawite			

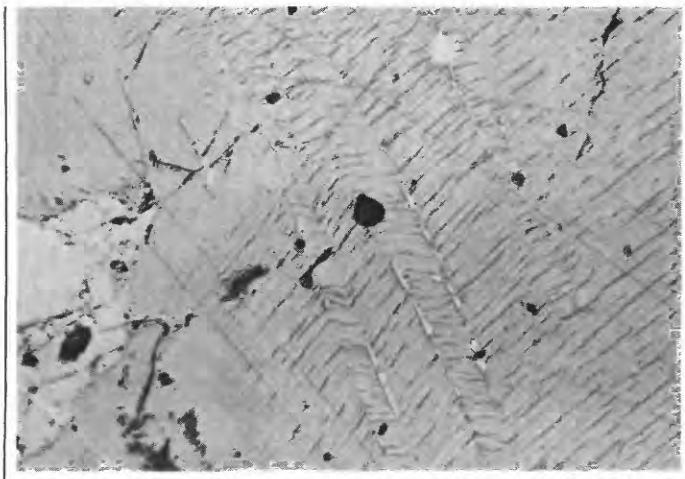

FIGURE 33.—Monoclinic and hexagonal pyrrhotite. Etched in 57 percent hydriodic acid. M14/434.5. Lamellae approximately 10μm across.

PYRRHOTITE

Both hexagonal and monoclinic pyrrhotite are present in all the specimens of sulfide-bearing rocks from the Basal zone. This might have been expected based on Desborough and Carpenter's (1965, p. 1437) previous report of both phases in one sample from the Mouat mine area, but in the context of studies by Cowan (1968) on the Strathcona ore deposit and Haynes and Hill (1970) on the Renison Bell deposit, the consistent proportions and relations of the phases to one another in the Basal zone are unexpected. The hexagonal phase is dominant in all the sections examined, but it is everywhere accompanied by the monoclinic phase (10-20 percent of total pyrrhotite).

In well-prepared polished sections, both phases can be observed without etching. The more reflective lighter hexagonal phase is the host for fine (10-15μm in width) lamellae of the less reflective darker monoclinic phase. Immersion in a 57-percent solution of hydriodic acid for 15-30 seconds increases the contrast between the phases by etching the hexagonal phase (Vaughn and others, 1971, p. 1135) and makes it possible to distinguish the phases in poorer polished sections (fig. 33). Finely ground magnetite applied as a suspension adhered to the unetched lamellae, demonstrating the ferromagnetic properties of the monoclinic phase. Diffractograms over the "$d_{(102)}$" reflection (Desborough and Carpenter, 1965) for bulk pyrrhotite samples generally contain only the reflection of the hexagonal phase, although a few samples showed a low-intensity peak for the monoclinic phase. This confirms the identification and supports the estimates of the monoclinic phase present as intergrowths.

Page (1972) reported electron microprobe analyses of some pyrrhotites from the Basal zone (C-395½, table 1, p. 815) and obtained values of atomic percent metals between 46.2 and 47.5. Some of the variation in composition may be ascribed to the possibility that the analyses represent mixtures of hexagonal and monoclinic phases. The compositions of pyrrhotite from samples showing no monoclinic reflections were determined for the hexagonal phase at a number of localities using the X-ray diffraction method of Arnold (1962, 1967), Arnold and Reichen (1962) and Toulmin and Barton (1964). Glass-slide smear mounts were oscillated at ¼° per minute through two cycles between the "$d_{(102)}$" and the halite (220) reflections (halite annealed for 3 days at 500°C. a_0=5.6400 Å) on a diffractometer using Ni filtered Cu K_α radiation. The smear mounts were rotated 180° between cycles. The results of this study are shown in table 9. The compositions given are of hexagonal pyrrhotites after their inversion to the hexagonal-monoclinic mixture.

Consideration of compositions of hexagonal pyrrhotite given in table 9 and the range of compositions of natural

TABLE 9.—*Compositions of hexagonal pyrrhotite determined by X-ray diffraction*

[Atomic percent metals read from Arnold and Reichen's (1962) curve]

Sample number	$d_{(102)}$ (°±0.0005°)	Atomic percent metals (±0.05-0.075 percent)	Sample number	$d_{(102)}$ (°±0.0005°)	Atomic percent metals (±0.05-0.075 percent)
M14/226	2.0697	47.61	BB-3/233	2.0677	47.5
M14/253.5	2.0695	47.59	BB-3/259	2.0668	47.38
M14/260	2.0686	47.51	BB-3/352	2.0655	47.25
M14/262.3	2.0696	47.60	355-1/141.2	2.0672	47.4
M14/275	2.0705	47.67	355-1/177A	2.0663	47.25
M14/287	2.0701	47.64	355-1/177	2.0663	47.25
M14/292.5	2.0694	47.58	355-1/286	2.0672	47.4
M14/339.5	2.0705	47.67	355-1/389.4	2.0672	47.4
M14/391	2.0705	47.67	355-1/555.5	2.0641	47.15
M14/434.5	2.0702	47.66	355-8/190	2.0681	47.48
M14/463.2	2.0701	47.64	355-12/240	2.0681	47.48
M14/491.5	2.0702	47.66	355-14/226	2.0681	47.48
BB-7/819	2.0646	47.18	368-307A/595	2.0686	47.5
BB-7/855	2.0672	47.4	368-307/773.5	2.0695	47.6
BB-7/860	2.0632	47.35	368-507/561	2.0708	47.7
BB-7/863	2.0663	47.3	387-339/49	2.0708	47.7
BB-7/884	2.0655	47.25	387-339/53.5	2.0699	47.62
BB-7/914	2.0637	47.1	387-339/303.5	2.0681	47.48
BB-7/937	2.0681	47.48	389-339/398.5	2.0677	47.5
BB-3/183	2.0659	47.23			

pyrrhotite summarized by Misra and Fleet (1973, p. 530) allows an estimation of the pyrrhotite composition before inversion if the relative amounts of hexagonal and monoclinic phases are known. In figure 34, atomic percent of metals in pyrrhotite is plotted against percent of the hexagonal phase present. All bulk pyrrhotite compositions must lie between the sloping lines for the compositions of hexagonal pyrrhotite in table 9 and monoclinic pyrrhotite (Misra and Fleet, 1973). Estimates of the percentage of the hexagonal pyrrhotite range between 10 and 20 percent, and therefore the bulk composition of pyrrhotite before exsolution is estimated to fall within the stippled area of figure 34. This approach lends support to the supposition that the microprobe analyses of Page (1972) were done on mixtures of the hexagonal and monoclinic phases.

Pyrrhotite is usually the most abundant sulfide mineral present in all three types of sulfide-bearing rocks, and it occurs in four distinctive textures. In the most common texture, the shapes of the pyrrhotite grains in contact with silicate minerals are controlled by the crystal shapes of the silicate minerals and may be straight, gently curving, or irregular. Grains of pyrrhotite in contact with one another (observed under crossed nicols) generally form equigranular to inequigranular mosaic textures in which mutual grain boundaries form triple points. Grain diameters range from 0.05 to 40 mm and average about 17 mm. The fine wavy lamellae of monoclinic pyrrhotite are the major internal features of the grains.

Locally near fault and shear planes deformation twins, kink bands, and combinations of the two are present in pyrrhotite. Figure 35 shows an example of these features which may be compared with similar structures produced experimentally by Clark and Kelly (1973, p. 342).

Where the primary silicate minerals of Basal zone rocks have been altered and the rock textures changed by the

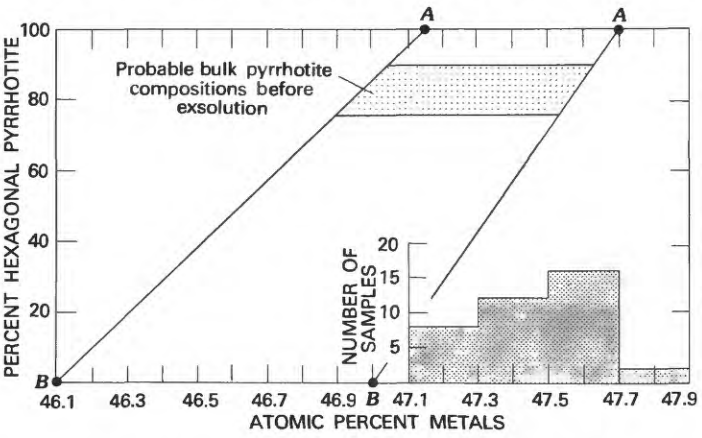

FIGURE 34.—Diagram used to estimate bulk composition of pyrrhotite. Points labeled A are compositions of hexagonal pyrrhotite from table 9. Points labeled B are the range of compositions for monoclinic pyrrhotite after Misra and Fleet (1973). Histogram shows compositions of hexagonal pyrrhotites in Basal zone. Samples also contain 10 to 20 percent monoclinic pyrrhotite.

FIGURE 35.—Photomicrograph of pyrrhotite texture. Crossed nicols. Deformation features. Area in photograph is 2 mm across.

development of amphiboles, talc, serpentine, and other minerals, the sulfide mineral textures are also changed. Pyrrhotite in part retains its original interstitial texture but more frequently occurs in veins, stringers, and irregular masses that are intimately intergrown with the silicate alteration minerals. In some samples the textures grade from the primary interstitial shapes in unaltered parts of the sample into diffuse, irregular masses of pyrrhotite in the altered parts of the sample. The gradation takes place with no apparent sharp contacts between pyrrhotite of different textures and without any apparent changes in sulfide mineralogy. In other samples where veins and stringers are more prevalent pyrrhotite shows replacement textures with magnetite. Locally pyrrhotite and magnetite may form pseudomorphs after each other. The textural changes are evidence that pyrrhotite was either mobilized in the solid state or recrystallized and locally transported under hydrous conditions.

PENTLANDITE

Pentlandite occurs in all three types of sulfide-bearing rocks either as blocky masses between pyrrhotite grains or as flamelike masses in pyrrhotite. Locally, the blocky pentlandite grains form finer grained necklaces around coarser pyrrhotite grains. Grain size of blocky pentlandite ranges from 1 to 10 mm and averages 6 mm; the average width of the flamelike masses is about 10 to 50 μm. Two types of blocky pentlandite have been found: The most common type consists of locally fractured pentlandite with magnetite and pyrrhotite in the fractures; the other consists of vermicular pentlandite intergrowths identical with those described by Page (1971b) in the G and H zone chromitites. The identity of the fine wormy intergrowth material is unknown.

From analyses of pentlandite and the associated assemblages, Graterol and Naldrett (1971), Page (1972) and

Harris and Nickel (1972) concluded that the nickel content of pentlandite was a function of the associated sulfide mineral assemblage. Misra and Fleet (1973) summarized these conclusions, presented new experimental evidence and additional compositional data on pentlandite assemblages, and showed that the nickel content is indeed a function of nickel content of the bulk sulfide mineral assemblage. Page (1972, p. 815) reported microprobe analyses of three pentlandites from the basal zone ranging from 23.8 to 28.0 atomic percent Ni. This range agrees with the range presented by Misra and Fleet (1973, p. 530) for the assemblage pentlandite-hexagonal pyrrhotite-monoclinic pyrrhotite. Other microprobe analyses of pentlandite in the Basal zone have not yet been made, but it is suspected from the homogeneity of mineral assemblages that the results would not differ from those presently accepted.

CHALCOPYRITE FAMILY

Three recently described minerals, mooihoekite, haycockite, and talnakhite (Cabri and Hall, 1972; Cabri, 1967, 1973) have compositional and structural similarities to chalcopyrite as well as very similar appearance in polished section. According to Cabri and Hall (1972), the close similarity of these minerals makes their positive identification extremely difficult and requires detailed electron microprobe analyses in conjunction with careful X-ray diffraction studies. Because both mooihoekite and talnakhite tarnish with prolonged exposure to air and chalcopyrite and haycockite do not, the slight variations in reflectivity and degree of tarnish are evidence that more than one phase may be present.

Sulfide-bearing rocks from the Basal zone contain minerals with the appearance of chalcopyrite that show small variations in reflectivity, degree of tarnish, and anisotrophism. This suggests that more than one phase is present. Early in this study an electron microprobe analysis of a phase that had not tarnished in air was made using the same methods as Page (1972) with the following results in weight percent: Cu, 33.0; Fe, 31.1; Ni, 0.06; S, 34.6; for a total of 98.7. The calculated metal-to-sulfur ration of 0.998 is close to the theoretical ratios of 1.005-1.02 for chalcopyrite. Because haycockite, the other phase that does not tarnish, has a metal-sulfur ratio of 1.125, the analyzed phase is presumed to be chalcopyrite. Because of this early result and relatively recent understanding of these complexities in the copper-iron-sulfur system, other phases with the appearance of chalcopyrite were not analyzed and were assumed to be chalcopyrite. Recent reexamination of the polished sections has revealed differences in tarnishing; further investigation of the nature and distribution of the chalcopyritelike phases must await a later study. In this paper, for convenience, "chalcopyrite" is used to include possible occurrence of all four minerals, although chalcopyrite is believed to be the major phase.

In all three groups of sulfide-bearing rocks chalcopyrite usually forms mutual grain boundaries with pyrrhotite, pentlandite, or both but may form irregular masses apparently not in contact with another sulfide phase. Rare cubanite lamellae occur in some samples of chalcopyrite. Several textural varieties of chalcopyrite are present, perhaps the most common variety consists of blocky, granular to ovoid grains at the margins, grain boundaries, or triple points between pyrrhotite grains. Chalcopyrite frequently occurs in individual interstices of the silicate phases, with one edge or margin against a silicate mineral and its other margins against pyrrhotite, pentlandite, or both. Irregular masses of chalcopyrite exhibit similar features. In some outcrops, hand specimens, polished slabs of massive sulfide rocks, and a few sulfide-bearing cumulate rocks, chalcopyrite occurs as lenses and layers a few millimeters to several centimeters wide approximately concordant with other layering or foliation features. Elsewhere masses of chalcopyrite form veins or stringers that crosscut foliation or layering. On a polished section scale, stringers and veinlets of chalcopyrite locally cut across pyrrhotite and pentlandite masses.

In general, the blocky to ovoid grains and concordant lenses and layers appear to be primary crystallization features, whereas some of the irregular masses and all of the crosscutting features appear to be later features.

MAGNETITE, ILMENITE, AND HEMATITE

There are at least three distinct generations of magnetite, ilmenite, or magnetite-ilmenite-hematite intergrowths in sulfide-bearing rocks of the Basal zone. The earliest generation is characterized by euhedral to subhedral magnetite crystals that contain abundant lamellae of ilmenite and by subhedral to anhedral ilmenite crystals. Locally, composite grains of ilmenite with fine lamellae of hematite are mantled by magnetite with ilmenite lamellae (fig. 36*A*). The shape and textures of the oxide grains and their relation to silicate and sulfide minerals are evidence that this generation crystallized very early in the sequence. The primary oxide phases were either titaniferous magnetite or hematitic ilmenite that later exsolved ilmenite or hematite, respectively, owing to changing physical conditions. Oxide phases of this generation occur in pyroxene cumulates with matrix sulfide and in massive sulfide rocks probably as cumulates. Included in this early generation of oxides in interstices associated with postcumulate silicates are isolated subhedral to anhedral grains of ilmenite and magnetite that may be postcumulus phases. The presence of ilmenite as lamellae and grains in amounts up to 3 volume percent of the rock suggests that the early generation of oxides crystallized from a silicate rather than a sulfide-oxide melt because magnetite that has crystallized from a sulfide-oxide melt generally has a low titanium content (Hawley, 1962; Naldrett and Kullerud, 1967; Naldrett, 1969).

The second generation of oxide minerals consists of magnetite included within sulfide minerals in interstices of

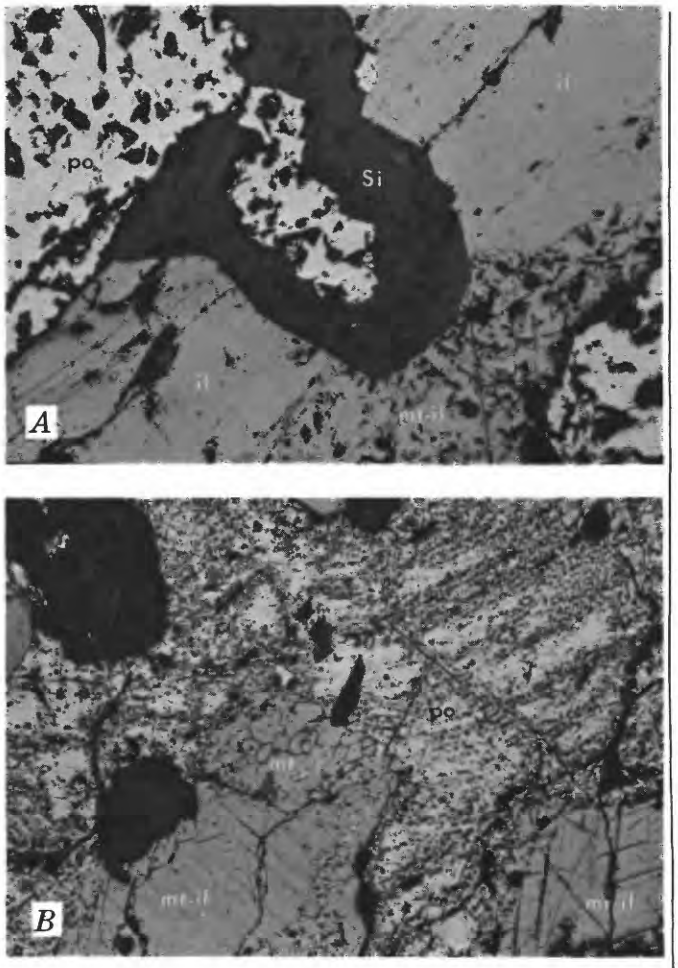

FIGURE 36.—Oxide-sulfide mineral relations. *A*, Ilmenite (il) with hematite lamellae with later magnetite-ilmenite (mt-il) in matrix pyrrhotite(po). Si, silicate NB1/310 polished section. *B*, Magnetite-ilmenite grain with magnetite overgrowths etched with hydrofluoric acid.

matrix sulfide rocks and in massive sulfide rocks. The magnetite occurs as isolated subhedral grains enclosed in the sulfide phase and, because it lacks ilmenite lamellae, apparently has a low titanium content. Grains of magnetite-ilmenite that are included in massive sulfide material occur as bulbous anhedral magnetite intergrown with pyrrhotite rimming the magnetite-ilmenite grains (fig. 36*B*). Both isolated grains and overgrowth magnetite are rare but appear to be more abundant in the massive sulfide rocks. According to Naldrett's (1969) experimental studies of the Fe-S-O system, the isolated grains may have crystallized from a sulfide-oxide melt. The overgrowth magnetite could have originated during sulfide crystallization from a sulfide-oxide melt or by reaction of the earlier magnetite-ilmenite crystals with the sulfide material.

The third generation of magnetite consists of euhedral to anhedral fine-grained magnetite veins and crosscutting masses associated with the alteration minerals serpentine, amphibole, and chlorite. These formed after the sulfide and silicate rocks were crystallized.

OTHER OPAQUE MINERALS

Other primary opaque minerals include chromite, cubanite, and a member of the cobaltite group. Chromite is a cumulus phase and is found locally in trace amounts as fine-grained euhedral crystals. Cubanite is rare and has only been observed as lamellae in three specimens of chalcopyrite. A member of the cobaltite group occurs locally in amounts up to 2 percent by volume as euhedral to subhedral crystals associated with the other primary sulfide minerals. Page and Jackson (1967, p. D125) reported the following range of compositions, in weight percent: 20-22 percent Co, 9-11 percent Ni, 7-8 percent Fe, 16-18 percent S, and 43-49 percent As. These analyses suggest that the mineral is gersdorffite.

Other opaque minerals that are found only in near-surface or surface exposures and in faults include violarite, marcasite, pyrite, mackinawite, cuprite, native copper, and goethite. Violarite replaces pentlandite locally and fine-grained marcasite plus pyrite replaces pyrrhotite near fine fractures filled with goethite. Goethite veins and fracture fillings appear to be one of the latest features in the rocks. Native copper and cuprite were found in surface fractures up to a millimeter wide; cuprite appears to replace the native copper.

PROPORTIONS OF SULFIDE MINERALS

Accurate estimates of the relative amounts of pyrrhotite, chalcopyrite, and pentlandite are difficult to make. Part of the problem revolves around the requirements of size and nature of samples necessary to characterize the three different sulfide-bearing rocks. Disseminated sulfide rocks probably can be characterized by small samples because each relatively small sulfide-bearing area appears to have responded to physical and chemical conditions as an entity. The other two sulfide-bearing rocks generally require large samples to obtain a representative estimate of the amount of the minerals present. Two different ways of estimating sulfide mineral proportions were used; one is based on modes counted on polished sections, the other is examination of published copper and nickel grades for the Basal zone.

Perhaps more reliable estimates of the proportions of chalcopyrite and pentlandite can be based on the copper and nickel grade data given by Roby (1949) and Dayton (1971). An average grade of 0.25 percent nickel and 0.25 percent copper has been reported for ore reserves of the Basal zone (Dayton, 1971). Analyses of core and mine tunnel samples of Basal zone rocks from the Mouat area (more specifically the Verdigris Creek area) listed by Roby (1949) indicate that the nickel content reaches a maximum of 1.35 percent and copper content a maximum of 1.3 percent, if three higher copper values are ignored (fig. 37). More than 75 percent of the analyses for copper and nickel showed concentrations less than 0.5 percent, and more than 40 percent of the analyses showed concentrations less than 0.2 percent.

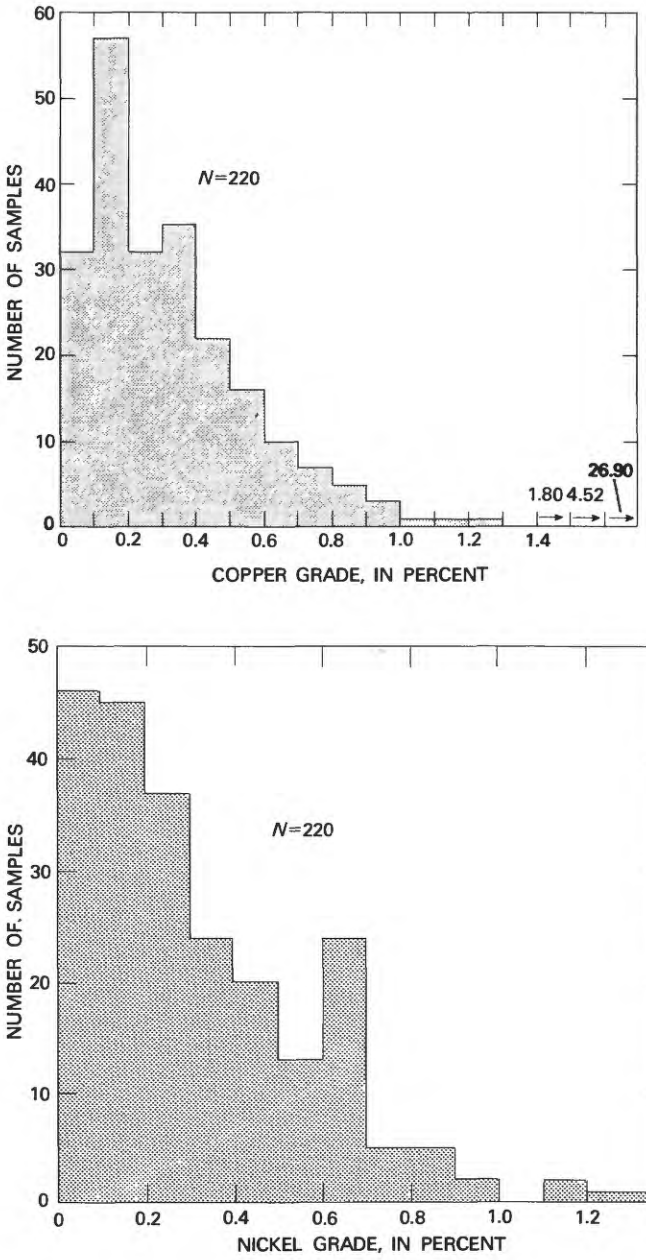

FIGURE 37.—Copper and nickel content of drill core and mine-tunnel samples. *N*, total number of samples. Data from Roby (1949).

Copper-to-nickel ratios for Stillwater samples are given in figure 38 and range from about 1:0.33 to 1:10, comparable with values from the Duluth Complex (Cornwall, 1972), Strathcona mine (Naldrett and Kullerud, 1967), Carr Boyd Complex (Purvis and others, 1972), and the Lunnon Shoot (Ewers and Hudson, 1972).

Relative volumes of sulfide minerals in sulfide-bearing rocks have been estimated by point counting over 1000 points on polished sections that range from 2.5 cm in diameter to 4 by 4 cm in area (fig. 39). The modes represent wide ranges in proportions of pyrrhotite to chalcopyrite and pentlandite, but in general pyrrhotite is the most abundant sulfide mineral. The pattern of these modal data is similar to plots given by Hawley (1962, p. 117) for random samples from the Sudbury ores. His data tend to show higher concentrations of pentlandite in samples rich in chalcopyrite but in general form a broad band parallel to the pyrrhotite-chalcopyrite side of the triangular diagram (fig. 39).

INTERRELATION BETWEEN SULFIDE MINERALIZATION AND SILICATE ROCKS

The relation between sulfide mineralization and the enclosing igneous rocks provides evidence on: (1) Correlation of textures, volumes, compositions, and ratios between both materials; (2) comagmatic or external sources of the sulfide mineralization; (3) the existence of a sulfide-oxide liquid immiscible in the silicate magma; and (4) the timing and processes of concentration of the sulfide mineralization. This evidence imposes limits on models for sulfide mineralization in the Stillwater Complex.

Attempts to quantitatively correlate characteristics of the sulfide mineralization in the Basal zone quantitatively with properties of the silicate rock containing the sulfide minerals have been unsuccessful. No consistent correlations of volumes, compositions, ratios, and textures of the sulfide minerals with lithology, mineralogy, texture, stratigraphic position, relative proportions of minerals, and compositions of minerals of the silicate rocks have been found. Similar comparisons of sulfide and oxide mineral properties were unenlightening. Three qualitative generalizations can be made on the basis of observations presented earlier: (1) Finer grained ophitic and subophitic rocks tend to contain smaller volumes of sulfide minerals than cumulate rocks, which may locally contain large amounts of sulfide, (2) the rocks lower in the Basal zone tend to contain larger volumes of sulfide mineralization than those higher in the sequence, and (3) the sulfide minerals occupy interstitial spaces that in unmineralized rock would be filled by silicates. Only within the framework of these generalizations does the sulfide mineralization appear related to the silicate rock which contains it.

Most if not all sulfide mineralization is thought to be comagmatic with the silicate material, and both are considered to be derived from the same parent magma or magmas. Evidence for this opinion includes (1) the overall distribution and occurrence of sulfide mineralization, (2) the fact that sulfide minerals fill interstices between cumulus phases and occur as small masses or molded about the silicates with no evidence of replacement of the primary silicates, and (3) the occurrence of small, 10-100 μm inclusions and clusters of polymineralic inclusions of sulfide material within the centers of cumulus plagioclase and pyroxene grains. Further evidence stems from incompatibilities between the textures of the sulfide-bearing rocks and those expected from other origins such as external introduction by hydrothermal processes. Hydrothermal deposition of sulfides requires that space be made for the ore

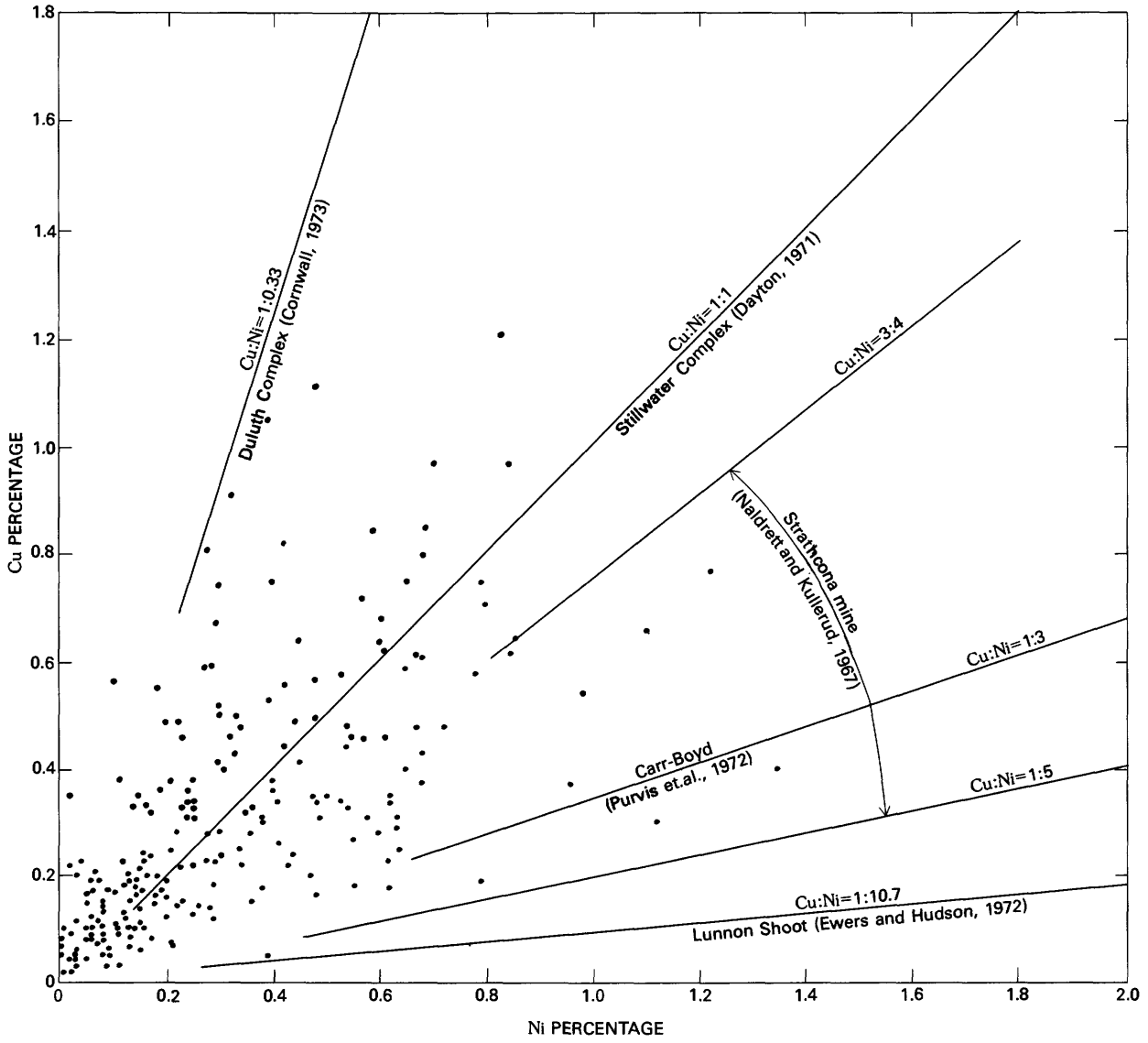

FIGURE 38.--Copper and nickel content data from various sources.

by replacement of existing postcumulus silicates. Because of the distribution of sulfides in interstices of different types of cumulates, such a replacement process must have been extremely selective and seems therefore highly unlikely.

If the comagmatic origin of the sulfide and silicate minerals is accepted, the next question concerns whether the sulfides were part of a sulfide-oxide immiscible liquid or were in solution in the silicate magma. Skinner and Peck (1969) studied basaltic lava in Hawaii and showed that the magma in Alae lava lake was saturated with sulfide at 1065° C with a sulfur content of 0.038 weight percent. Other measurements of sulfur content at saturation in basaltic magmas are scarce, but experimental and theoretical studies suggest that the maximum amount of sulfur soluble in a basaltic magma varies between 0.05 and 0.2 weight percent as the FeO content varies between 5 and 20 weight percent (Haughton and others, 1974) at 1200° C. For comparison several different estimates of the sulfur content of the Stillwater magma were made.

Estimates of the sulfur content of the Basal zone or the original parental magma are difficult to make with any confidence because of sampling problems. This is illustrated by the variable sulfur content, from 0 to 4.66 weight percent, of the ophitic, subophitic, and ragged noncumulate igneous rocks (table 4) that may represent crystallized magmatic liquids. One approach in estimating sulfur content of the Basal zone is to average many rock analyses. Roby (1949, p. 7) gave results of sulfur analyses of six composite diamond-drill core samples that represented sample lengths of 3.0 to 18.9 m in sulfide enriched zones. The sulfur content ranges from 4.99 to 14.41 weight percent. The weighted average (weighting based on length of sample) is 10.4 weight

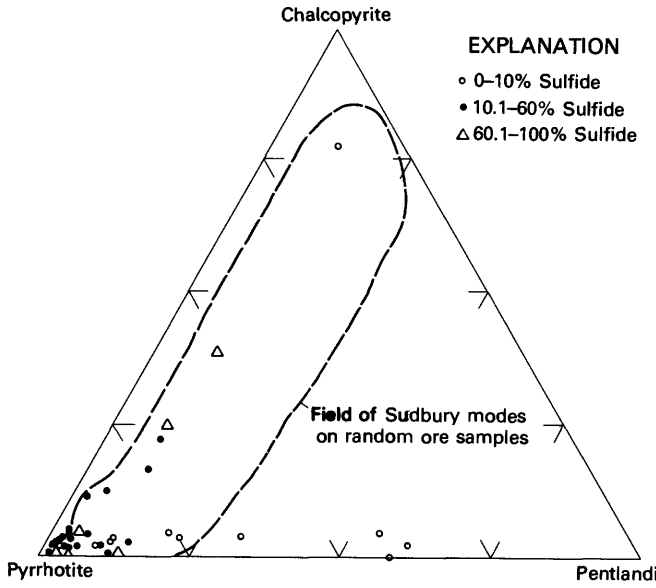

FIGURE 39.—Pyrrhotite, pentlandite, and chalcopyrite modes of sulfide-bearing rocks. Field of modes for Sudbury ore samples from Hawley (1962, p. 117.)

percent sulfur for 58.5 m of core sample. Another approach is to consider the volume of sulfide minerals estimated during core logging. An average volume percent sulfide minerals, based on data in figure 30, over a core length of 160 m, is 18.2 percent. This corresponds to a maximum estimated sulfur content of about 8 or 9 weight percent. Visual impressions and estimates of sulfide content based on field and laboratory studies suggest that these estimates if taken for the whole Basal zone are too large and that more probable average values are on the order of 1 or 2 percent for the Basal zone. Using composite samples Hess (1960) gave average values of 0.04 weight percent sulfur for the Ultramafic, Banded, and Upper zones suggesting that even this estimate may be too high. Comparison of the several estimated sulfur contents of the Basal zone with Skinner and Peck's (1969) value for a sulfur-saturated basaltic magma suggests that the magma of the Basal zone was saturated with sulfur and that an immiscible sulfide-oxide liquid was present in the Basal zone.

It is appropriate to consider whether the sulfur content of the Basal zone may have been derived from the magma reservoir that formed the entire Stillwater Complex. A calculation of the contribution of the sulfur content of the Basal zone distributed throughout the Stillwater magma was made using the following assumptions and approximations: (1) The maximum exposed thickness for the complex of 5.49 km approximates the thickness of the magma chamber; (2) the magma density was 2.67 g/cm^3, the calculated value for Jackson's (1971) analysis of the parent magma (see table 4) using Bottinga and Weill's (1970) method; (3) the Basal zone is 0.163 km thick, its average thickness; and (4) a rectangular prism 1 km square through the chamber is representative of the entire Stillwater Complex. For estimates of 1 and 10 weight percent sulfur in the Basal zone, the contribution to the entire Stillwater magma is about 0.003 and 0.03 weight percent sulfur, respectively. Adding these estimates to the average value, Hess (1960) suggests that the total Stillwater magma could have contained 0.04-0.07 weight percent sulfur. Perhaps a better value for the sulfur content of the Stillwater magma would be the value estimated by Moore and Fabbi (1971) for the juvenile sulfur content of basaltic magma of 0.080±0.015 weight percent based on analyses of outer quenched surfaces of submarine basalts. The lower calculated value borders on possible sulfur saturation, whereas the higher value is definitely saturated, according to Skinner and Peck's (1969) value for Hawaiian basaltic magmas. From these calculations, estimates, and comparisons of sulfur content of the Basal zone, it is concluded that the sulfides were derived from a sulfur-supersaturated magma.

Sulfide-oxide liquids were probably present in the Stillwater magma at a very early stage in the intrusive history of the Basal zone and were continually present throughout deposition of most of the lower part of the complex. Evidence for the early presence of sulfide-oxide liquids includes: (1) Massive sulfide rocks intruded by ophitic to ragged-textured noncumulate rocks and showing the reverse sequence of intrusion; both groups are intrusive into the metasedimentary rocks below the base of the complex; (2) intrusive breccias consisting of metasedimentary rock fragments and a massive sulfide matrix (fig. 33); and (3) fine polymineralic inclusions of sulfide minerals in the centers of some cumulus silicate and oxide phases throughout the Basal zone. The occurrence of fine-grained ophitic and subophitic igneous rocks with low contents of sulfide minerals could be interpreted as evidence contrary to early separation of sulfide-oxide immiscible liquids, but the variable and possibly gradational sulfur content of the noncumulate rocks (table 4) suggests that sulfide-oxide liquids were present at least locally when these noncumulate rocks crystallized. The field and laboratory evidence implies that sulfide-oxide liquids developed as an immiscible fraction of the Stillwater magma before or immediately after emplacement. Concentration or collection processes of the sulfide-oxide melt must have been operative during the early formation of the liquids to account for the field relations of large masses of sulfide within metasedimentary rocks such as those in the Verdigris Creek and part of the Mountain View area.

INTERPRETATION AND MODEL OF SULFIDE CRYSTALLIZATION

Most modern investigators agree that large amounts of basaltic magma are generated by partial melting of an ultramafic mantle under physical and chemical conditions that are presently poorly defined. Assuming this source for the Stillwater basaltic magma, the arguments and deductions of MacLean (1969, p. 878-880) suggest that the magma

would have been saturated with sulfur. Such a sulfur-saturated magma could contain dispersed. fine-grained, immiscible, sulfide-oxide liquid droplets if it contained 0.080±0.015 weight percent juvenile sulfur, as suggested by Moore and Fabbi's (1971) study. The existence of such droplets would depend upon the magma's emplacement history in the crust. Whether the magma contained such droplets before emplacement is unimportant to the interpretation of the sulfide crystallization history.

The postemplacement crystallization history is discussed under four topics: (1) Mechanisms for separation of immiscible sulfide liquid and evaluation of these mechanisms in terms of published experimental data and observations of the Basal zone; (2) collection and formation of the observed sulfide masses; (3) initial crystallization of the sulfic liquids; and (4) later, lower temperature equilibration of the sulfide minerals to the presently observed assemblages.

MECHANISMS FOR SEPARATION OF IMMISCIBLE SULFIDE-OXIDE LIQUIDS FROM BASALTIC MAGMA

Mechanisms that would generate sulfide-oxide liquids from basaltic magma either during ascent or after emplacement in the Stillwater magma chamber require changes in physical or compositional parameters of part or all of the magma system. Such changes must enrich the sulfide-oxide liquid in sulfide either by crystallization of other phases, specifically those rich in FeO, or by expanding the region of liquid immiscibility in the magma system. The activity of FeO in the magma is probably the main factor controlling sulfide solubility and liquid immiscibility (MacLean, 1969, p. 866); the higher the activity of FeO, the higher the sulfide solubility, and the less sulfide-oxide liquid generated. The experimental studies in compositionally limited sulfide-silicate systems by Fincham and Richardson (1954), Naldrett and Richardson (1967), Naldrett (1969), MacLean (1969), and Shamazaki and Clark (1973), suggest that the following changes in conditions will also produce more extensive immiscible sulfide liquid in a basaltic magma: (1) Decreasing the total pressure on the system; (2) decreasing the temperature; (3) increasing sulfur fugacity; (4) increasing oxygen fugacity; and (5) increasing SiO_2 Na_2O, K_2O, MgO, and Al_2O_3 content (activity) in the magma; or (6) decreasing the FeO content.

Reducing the total pressure on the Stillwater magma while keeping other parameters equal would probably result in a slight release of sulfide to an immiscible sulfide-oxide liquid (MacLean, 1969, p. 881-882). There is no direct experimental evidence for this conclusion, but it can be deduced from two sets of experiments. Brett and Bell (1969) showed that the temperature of the eutectic in the Fe-FeS system is nearly the same at 30 kbar as at 1 bar and Naldrett and Richardson (1967) demonstrated that 2 kbar fluid pressure has very little influence on the melting temperatures of pyrrhotite-magnetite liquids. Complete evaluation of this mechanism must await further experimental studies. All mafic magmas generated in the mantle and emplaced in the crust undergo a pressure release, but not all such intrusions show evidence of immiscible sulfide-oxide liquids or are associated with sulfide deposits. By implication, a pressure-release mechanism is not the major factor in controlling sulfide generation in the Stillwater Complex.

A decrease in the temperature of a basaltic magma can result in an increased amount of immiscible sulfide-oxide liquid in two ways: (1) By crystallizing and accumulating silicate and oxide phases rich in FeO, thus increasing the sulfide content of the magma, and (2) by expanding the immiscible sulfide-oxide liquid region at lower temperatures for certain magma compositions. Interpretations of the ophitic and subophitic textures of the fine-grained noncumulate igneous-textured rocks, and the appearance low in the Basal zone of more ferrous orthopyroxenes before magnesian orthopyroxenes, suggest an early decrease in the temperature of the Stillwater magma after or during its emplacement. The conventional interpretation of fine-grained ophitic rocks as rapidly cooled or quenched magmas implies a temperature decrease, but it is not certain that this interpretation can explain these textures in the middle of the Basal zone. The appearance of ferrous orthopyroxenes before magnesian orthopyroxenes can be interpreted as due to supercooling, with higher rocks in the section reflecting adjustment of temperatures toward equilibrium conditions. Decreasing temperature probably contributed to the amount of immiscible sulfide-oxide liquids but, as with the pressure-release argument, the consideration that most basaltic rocks do not contain sulfide deposits suggests that it was not the major mechanism.

An increase in the sulfur fugacity either directly by the addition of more sulfur to the magma through contamination or indirectly by a change in other parameters will result in increased amounts of immiscible sulfide liquid (Richardson and Fincham, 1954; MacLean, 1969). Sulfurization, the process of incorporation of preexisting sulfur into magma, has been suggested as a process for forming sulfide accumulations similar to those in the Basal zone (Kullerud, 1963). No positive evidence that such a process occurred in the Stillwater Complex has been observed, and while it is conceivable that the iron formation below the complex in the Initial to Benbow area had a sulfide facies that was incorporated into the basaltic magma, none of the iron formation elsewhere below the complex is rich in sulfides. The other metasedimentary rocks below the complex appear to be low in sulfur, and although they have contaminated the magma locally, they probably are not a source of major additions of sulfur. Thus, the direct addition of sulfur to increase the amount of sulfide-oxide immiscible liquid in the Stillwater magma appears to be a minor mechanism, and increases in sulfur fugacity must have been caused by changes in other parameters of the magma or conditions of the chamber.

As shown by MacLean (1969) a magma generated in the mantle would have an oxygen fugacity close to that fixed by the quartz-fayalite-magnetite buffer, and an increase in the oxygen fugacity, especially a rapid rise, would cause a large proportion of the sulfur originally soluble in the magma to separate as a sulfide-oxide immiscible liquid. Rapid oxidation could take place before emplacement in the magma chamber and depending upon the magma's rate of upward movement, could result in either a large volume of dispersed sulfide-oxide immiscible liquid droplets in the magma or in larger masses of sulfide liquid (Naldrett and Kullerud, 1967). Rapid oxidation could also occur in the magma chamber where accumulation of sulfide-oxide liquid would account for the sulfide distribution. One obvious cause of rapid oxidation might be the incorporation of H_2O from the country rocks with concomitant loss of H_2 to the surface. Incorporation of H_2O into the magma chamber need not be a diffusion-controlled process but might be controlled by other mechanisms such as zone refining (D. M. Shaw, 1972; Harris, 1957), which would involve circulating magma past wet country rocks and scavenging H_2O from them. If such a mechanism is applicable to the Stillwater magma, the oxide and silicate assemblages should show some evidence for high-oxygen fugacities unless assemblages that may have crystallized under high-oxygen fugacities were resorbed and reequilibrated when the magma system was closed to the influx of water and adjusted to lower oxygen fugacity. Evidence for high initial oxygen fugacities is sparse in the Basal zone, as is evidence for the presence of large volumes of water, but it is present. The presence of ilmenite-hematite intergrowths mantled by magnetite with ilmenite lamellae, found as subhedral inclusions in matrix sulfides and massive sulfide rocks, requires that oxygen fugacities were initially high, perhaps near those of the magnetite-hematite buffer, and later decreased to conditions near the quartz-magnetite-fayalite buffer. The close association of the ilmenite-hematite intergrowths with the sulfide minerals and the absence of the intergrowths in nearby cumulates in which the oxide phases are magnetite and ilmenite strongly supports the hypothesis of early oxidation. The presence of brown hornblende and red-brown biotite (table 3) in most rocks from the Basal zone and in the early cumulates of the Ultramafic zone (Page, Shimek, and Huffman, 1972) requires the presence of some water in the initial stages of magmatic accumulation. An oxidation mechanism to generate the amount of sulfide-oxide liquid necessary for the sulfide mineralization on the Basal zone is strongly supported.

An increase in the SiO_2, Na_2O, K_2O, MgO, and Al_2O_3 content (activity) in the magma has the same effect as a decrease in the FeO content and results in increased amounts of immiscible sulfide-oxide liquid. Two processes by which the composition of the magma can be changed are contamination from the country rocks and differentiation by fractional crystallization. Previous discussion of the problems of contamination and the mixed rocks demonstrated that the MgO, SiO_2, Al_2O_3, or CaO content of all the magma in the Stillwater magma chamber could not be changed appreciably through contamination with metasedimentary rocks. Moreover, contamination can only change the magma composition locally and is not a likely mechanism for the formation of most of the immiscible sulfide-oxide liquid. Because the mass of magma from which the relatively thin Basal zone probably was derived is large, differentiation and fractional crystallization cannot have greatly changed the initial composition of the basaltic magma in the chamber. In addition such a process of differentiation and fractional crystallization does not appear capable of producing large amounts of sulfide-oxide immiscible liquid rapidly enough to account for the concentration of sulfide mineralization near and below the base of the complex. Fractional crystallization could increase sulfide-oxide liquid by removing phases rich in iron in smaller batches of magma or in local environments. Throughout the Basal zone, the sulfide content shows repetitive cycles of increase and decrease (fig. 29). These cycles appear to be roughly correlated with the cycles of changing orthopyroxene compositions and stratigraphy. Higher sulfide contents in the Basal zone tend to occur near the zones of more ferrous orthopyroxenes and sulfide content tends to decrease with increasing magnesium enrichment. Thus, fractional crystallization may be the cause of the cycling, repetitive nature of the sulfide mineralization on a local scale.

In summary, a basaltic magma that may have been saturated with sulfide was generated in the mantle and emplaced in the crust. Either during emplacement or in the magma chamber of the Stillwater Complex it was rapidly oxidized by an influx of water. Oxidation caused a rapid increase in immiscible sulfide-oxide liquid, which accumulated to varying degrees to form a spectrum of sulfide mineralization textures. Soon thereafter, the chamber was sealed from the external source of oxygen and reverted to more reducing crystallization trends. During deposition and accumulation of the silicates and oxides in the Basal zone, local fractional crystallization of orthopyroxene appears to have depleted the magma of FeO, thus acting as a secondary control on the deposition of sulfide-oxide liquid.

COLLECTION AND CONCENTRATION MODELS

Having established that immiscible sulfide-oxide liquids were probably generated in the Stillwater magma by one or more processes, possible models for the collection and concentration of these liquids at the base of the complex need to be examined. At least two different situations can be visualized: (1) The magma chamber may have filled rapidly and remained as a stagnant, nonconvecting mass similar to Jackson's (1961a) model for the deposition of the Ultramafic zone; or (2) after filling, the magma chamber may have convected in either a single cell or many cells, allowing

current-controlled processes to become equal in importance to or more important than gravity-controlled processes. The stagnant magma situation is the simpler one for which to develop models and is used here as a basis for discussion; the effects of current are considered to be modifications of the stagnant process. Models for either situation depend in part upon relations between settling velocities, viscosity, and size and on diffusion of sulfur in a basaltic magma.

Several assumptions must be made to estimate settling velocities of sulfide-oxide immiscible liquids in the Stillwater magma. First, the sulfide-oxide liquids are assumed to have had spherical or spheroidal shapes, like similar melts produced experimentally by MacLean (1969, figs. 3 and 4). Second, the spheres are assumed to have behaved as rigid spheres in order to apply Stoke's law. Third, a composition for the sulfide-oxide liquid must be assumed from which their density may be estimated. Finally, assumptions used in deriving the viscosity, temperature, and density relations of the silicate magma in the previous sections are included in these calculations.

A density for the solid sulfide-oxide phases from the bulk sulfide composition can be calculated and this value may be modified by what is known about the density of molten sulfide minerals to yield an estimate of the density of the sulfide-oxide liquid. Very few bulk sulfide analyses are available for the Stillwater sulfides, but Roby (1949) reported the analysis of one large composite sample taken for metallurgical testing which is used to calculate the sulfide compositions and volume percentages. Comparison of the volume percentage of chalcopyrite, pentlandite, and pyrrhotite calculated in table 10 with the modal data in figure 39 shows that Roby's (1949) sample appears to be representative of the modal data. The bulk density calculated for the solid massive sulfide is 4.805 g/cm^3, assuming that the densities of the mineral components are additive proportional to their mole fraction.

Gubanov (1957) reported that the densities of Cu_2S, Ag_2S, Sb_2S_3, FeS, and CuS decrease by only a few percent upon melting. Also, the limited data on thermal expansion of sulfides (see Skinner, 1966), suggest only small changes in the densities of sulfide minerals upon melting. Calculations show that a 5 percent range (5.045 to 4.565 g/cm^3) about the estimated solid density, to account for differences between solid and melt, causes little difference in calculated settling velocities. Figure 40 shows settling velocities in basaltic magma at 1,200°C and 1,300°C for various size spheres of sulfide (density, 4.805 g/cm^3) in comparison with settling velocities of orthopyroxene. The size ranges of sulfide inclusions in cumulus phases and as independent interstitial material are indicated (detailed size data given in Page, 1972). Size ranges of disseminated sulfides that show continuous conductivity are also shown in figure 40 and the size ranges of disseminated sulfides that have continuous electrical conductivity for individual samples are given in figure 41. The largest disseminated clot of sulfide observed was 4 cm in diameter, but most of the clots are less than 1 cm in diameter. Figure 40 shows that sulfide spheres with radii greater than about 0.5 mm fall at settling velocities greater than 8 m/yr.

TABLE 10.—*Calculations of sulfide compositions based on Roby's (1945) large composite sample of sulfide material*

Element or mineral	Weight percent	Normalized mole percent	Calculated		
			Weight percent	Mole fraction	Volume percent
Ni	0.74	0.99			
Cu	1.28	1.558			
Fe	35.00	48.480			
S	20.30	48.975			
As	.08				
Insoluble	33.40				
Chalcopyrite[1]			6.59	0.0339	5.64
Pentlandite[2]			3.92	.0048	4.02
Pyrrhotite[3]			89.49	.9613	90.35

[1]$CuFeS_2$, density =4.088 g/cm^3.
[2]$Ni_{4.5}Fe_{4.5}S_8$, density=4.911 g/cm^3.
[3]FeS, density=4.830 g/cm^3.

Spheroidal droplets of immiscible sulfide-oxide liquid could form under stagnant conditions in at least two ways: (1) All of the immiscible sulfide spheres may have nucleated at about the same time, had the same size, and been equally distributed in the magma if the same physical and chemical conditions prevailed throughout the magma chamber; or (2) sulfide spheres may have nucleated continuously through a period of time producing spheres of different sizes in different locations and at different levels in the chamber.

In the first case, assuming a constant growth rate of sulfide spheres dependent upon the diffusion of sulfide material from an adjacent volume of magma, all the immiscible sulfide-oxide spheres would have the same settling velocity and would not collide and coalesce during settling to form larger spheres. The sulfide-oxide liquid spheres must grow large enough to allow them to settle at rates equal to or higher than the cumulus phases in order to collect as dispersed sulfide throughout the magma chamber near the base of the complex. Under stagnant conditions sulfide-oxide spheres must have a radius of at least 0.04 mm to fall as fast as the slowest settling cumulus phases and a radius of at least 0.5 mm to fall 8 meters per year (fig. 41). Unless nucleated and growing sulfide-oxide spheres are able to coalesce, there is no process for concentration and simultaneous nucleation in a stagnant magma does not appear to be a likely mechanism. However, the presence of currents with velocities sufficient to cause individual sulfide-oxide spheres to collide and coalesce might make the mechanism work. Currents or convection of this kind require initial differences in chemical and physical properties throughout the magma chamber, which in turn would probably not allow simultaneous nucleation throughout the chamber. Therefore, the first possibliity appears inapplicable to the collection of sulfides in the Basal zone of the Stillwater Complex.

Continuous nucleation of sulfide-oxide spheres over a period of time, producing spheres of different sizes at

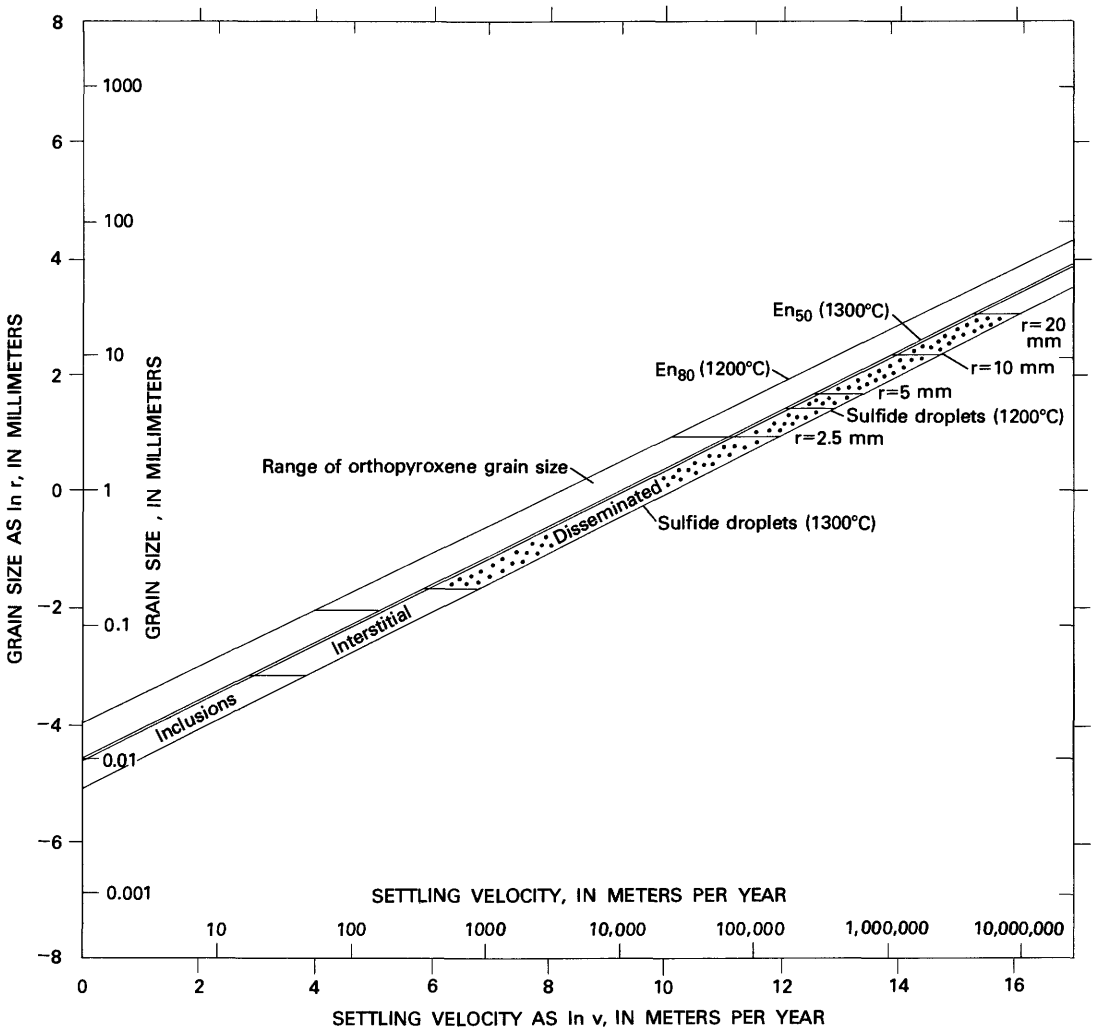

FIGURE 40.—Settling velocities of sulfide liquid spheres. Basaltic magma density at 1,200°C=2.726 g/cm³, viscosity=149.9 poises; at 1,300°C, density=2.712 g/cm³, viscosity=59.1 poises. Sulfide density =4.805 g/cm³.

different levels in the magma chamber, requires that either chemical or physical parameters or both vary within the chamber. Given the range in composition of ophitic and subophitic rocks of the Basal norite, compositional variation within the magma chamber appears to be likely. This compositional variation would in turn produce variations in liquidus temperatures, viscosity, density, settling velocity, and other properties that control the initial distribution of sulfide-oxide liquid spheres. The thickness of the magma chamber, approximately 8 km, would yield a lithostatic pressure differential between top and bottom of over 2,000 bars, a possible liquidus temperature differential of about 24°C assuming a gradient of 3°C/km (see Irvine, 1970b), and an adiabatic temperature differential of 2.4°C. Such variation might affect the nucleation and growth properties of immiscible liquids and in part control their distribution. Assuming that local inhomogeneities in physical and chemical properties can produce a variable size distribution of immiscible sulfide-oxide spheres at different levels of a stagnant magma chamber, there are at least two possible processes that would enlarge the spheres to a critical size for rapid settling. One is simply growth through diffusion as more sulfide is exsolved from the basaltic magma; the other is collision and coalescence of spheres during their descent. The distribution of sulfide grain sizes offers some clues as to how enlargement may have taken place.

In the Stillwater Complex, sulfide minerals occur either as inclusions within cumulus phases, as matrix material, or as interstitial material to cumulus phases. Page (1971b) examined size distribution of sulfide material in the G and H zone chromitites and observed that all of the sulfide grains had diameters less than 0.75 mm. Figure 42*B*, constructed from Page's (1971b) size data, shows the distribution of sulfide grain diameters in terms of the fraction of grains with a specific diameter. A large percentage of the sulfide grains are less than 0.10 mm in diameter. Figure 40 shows that these sulfide grains would have settling velocities in the range of meters to tens of meters per year. Similar-sized sulfide in-

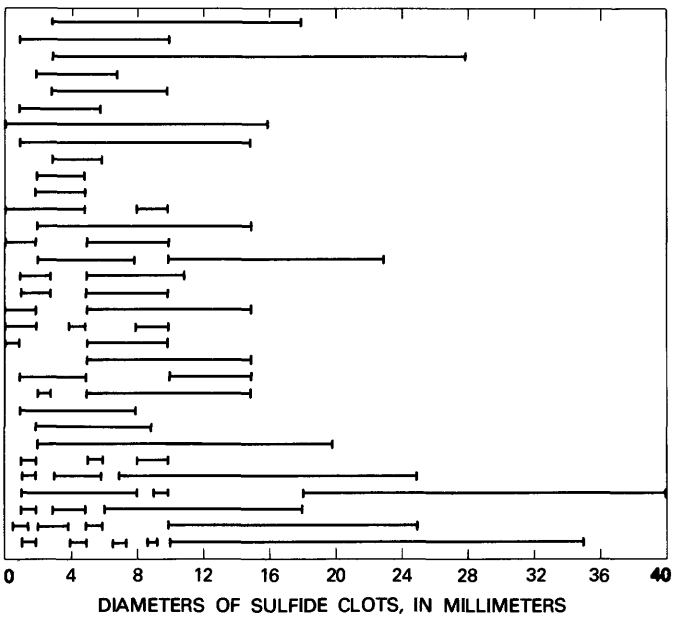

FIGURE 41.—Ranges of diameters of disseminated sulfide clots for individual samples. Each bar represents one sample.

clusions are present in the Basal zone within cumulus phases. They represent sulfide materials with relatively slow settling velocities and are probably typical of immiscible sulfide-oxide liquids that did not settle far from where they nucleated before being enclosed in a cumulus phase. They may also be indicative of the size of sulfide spheres that grew only by diffusion and not by coalescence with other spheres. Stated in another way, the size distribution of sulfide inclusions in cumulus phases probably represents the part of sulfide trapped or possibly left over from any collection process if the process preceded the cumulate process.

The size distribution of disseminated sulfide clots in the Basal zone is illustrated in figure 42*A*. The distribution was calculated from data used in figure 41. Most of this material would have settling velocities greater than 1,000 m/yr (fig. 40). The clots represent the part of sulfide that coalesced and was capable of settling at least as rapidly as the other cumulus phases.

The idealized hypothetical curves in figure 43 provide a frame of reference against which the size distribution curves in figure 42 and the process of collision and coalescence may be evaluated. Each curve represents the distribution of the fraction of sulfide-oxide spheres with a specific diameter at different times during the accumulation of the Basal zone. The two curves labeled t_f represent the final distribution as inclusions and disseminated sulfides generalized from the distributions in figure 42. The curve t_0 represents an assumed distribution of the spheres within the magma column soon after nucleation and initial growth. If the process of collision and coalescence of spheres is active, then the curve t_i would represent a distribution of sizes at some intermediate time.

The process of collision and coalscence envisioned for the collection of sulfide-oxide liquids appears to be analogous to the process of raindrop growth. Langmuir (1948), Houghton (1950), Matveev (1967), Soo (1967), and Mason (1957) developed and reviewed the experimental and theoretical studies concerning raindrop growth. The size ranges of raindrops and their nuclei are similar to those envisioned for sulfide spheres; other physical parameters are quite different, but such a model appears applicable. The following model for the collision and coalescence of sulfide-oxide liquids in the Stillwater magma is based on these studies and outlines only one approach to the problem that would give averaged or smoothed rates of droplet growth. Telford (1955), Twomey (1964, 1966), and Berry (1967) have pointed out that coalescence of raindrops is a stepwise process and therefore developed stochastic equations for their growth. Such extension of the model to sulfide spheres is unnecessary here.

First, consider the growth of a single sulfide-oxide liquid sphere of radius R caused by collisions with smaller spheres of radius r. In a short interval of time dt, a sphere of radius R falls under the influence of gravity relative to the smaller spheres a distance $(v_R - v_r)\,dt$, where v_R and v_r are the settling velocities of spheres of radii R and r. The change in volume of the large sphere dV_R, is a function of (1) the volume of the small spheres, $V_r = 4/3\pi r^3$; (2) the cross-sectional area of the cylinder inside which spheres of radius r will collide with the sphere of radius R, $A = \pi(R+r)^2$; (3) the size distribution of the spheres $f(r)$; (4) the number of spheres per unit volume n; and (5) the effective collision area or the collision efficiency of the sphere with radius R, ξ. The collision efficiency ξ is a function of both R and r and other physical parameters. By coalescence of spheres with radii from r to $r+dr$, the volume added to the sphere with radius R in time dt is

$$dV_R = \xi A(v_R - v_r)4/3\pi r^3 n f(r)\,dr\,dt.$$

The total volume increment dV_R is

$$\int dV_R = 4/3\pi^2 n \int_0^R \xi\,(R+r)^2 r^3 f(r)\,(v_R - v_r)\,dr.$$

Since the volume of a large sphere is $V_R = 4/3\pi R^3$, the volume increment is $dV_R = 4\pi R^2 dR$. Therefore the change of sphere radius with time by collision is

$$\frac{dR}{dt} = \frac{\pi n}{3R^2}\int_0^R \xi (R+r)^2\, r^3 f(r)(v_R - v_r)\,dr.$$

Let us examine parts of the above equation in more detail. The settling velocities v_R and v_r probably obey Stoke's law up to sphere with radii between 4 and 9 mm in the magma under consideration, which has densities of 2.726 and 2.712 g/cm^3 and viscosities of 149.9 and 59.1 poises. This conclusion is based on the equation

$$r_{max} = \left[\frac{9\eta^2 \mathbf{R}}{4g\rho_l(\rho_s - \rho_l)}\right]^{1/3}$$

where $\mathbf{R}$ is the Reynolds number; η, the viscosity; g, the acceleration of gravity; ρ_l, the density of the magma; and ρ_s,

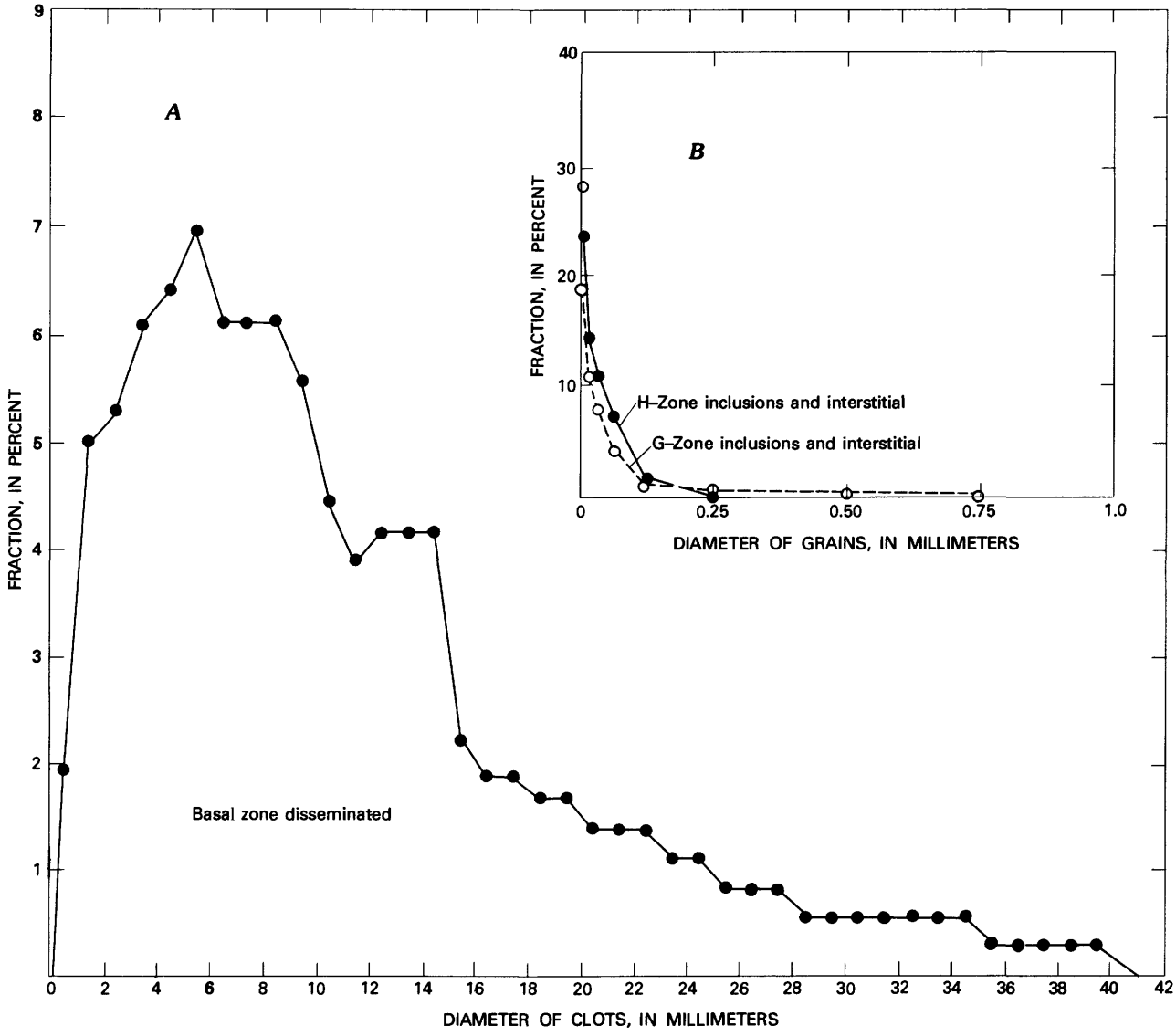

FIGURE 42.—Clot size (*A*) and grain size (*B*) distributions of disseminated sulfides and inclusions.

the density of the spheres (Shaw, 1965). The maximum sphere radius r_{max} for Stoke's law settling is therefore dependent upon **R**, values of which are taken in the range 0.05 to 0.1 that are the limits for Stoke's settling (Christiansen, 1935; McNown and Malaika, 1950). Settling of the large spheres (fig. 41) must be described by other functions (Rubey, 1933).

Studies of size distributions of cumulus minerals in the Stillwater Complex (Jackson, 1961a, p. 28) suggest that most size distributions are lognormal. Within sediments some size distributions are lognormal but many are not, and various equations to describe other size distributions have been given (Pettijohn, 1957). For raindrops lognormal size distributions have been used, but other distribution laws have been suggested (Matveev, 1967). The size distribution of the sulfide-oxide spheres during the growth of a sphere during coalescence $f(r)$, if assumed to be lognormal, may be expressed as

$$f(r) = \frac{1}{\sigma\sqrt{2\pi r}} \exp\left[\frac{-(\ln r - \ln r_0)^2}{2\sigma^2}\right]$$

where $\ln r_0$ is the arithmetic mean of logarithms of sphere radii and $\sigma = \sqrt{(\ln r - \ln r_0)^2}$. The size distribution $f(r)$ changes with time during collisions as does $\ln r_0$ and σ.

Evaluation of the collision efficiency ξ for a sphere of radius R involves consideration of the trajectories taken by the smaller spheres of radius r as they approach the large sphere. Some of the smaller spheres within the cylinder swept out by the larger spheres can flow around the large spheres by the motion of the magma streamlining around the spheres. Besides streamlining, attractive and repulsive forces between sulfide-oxide spheres could modify collision ef-

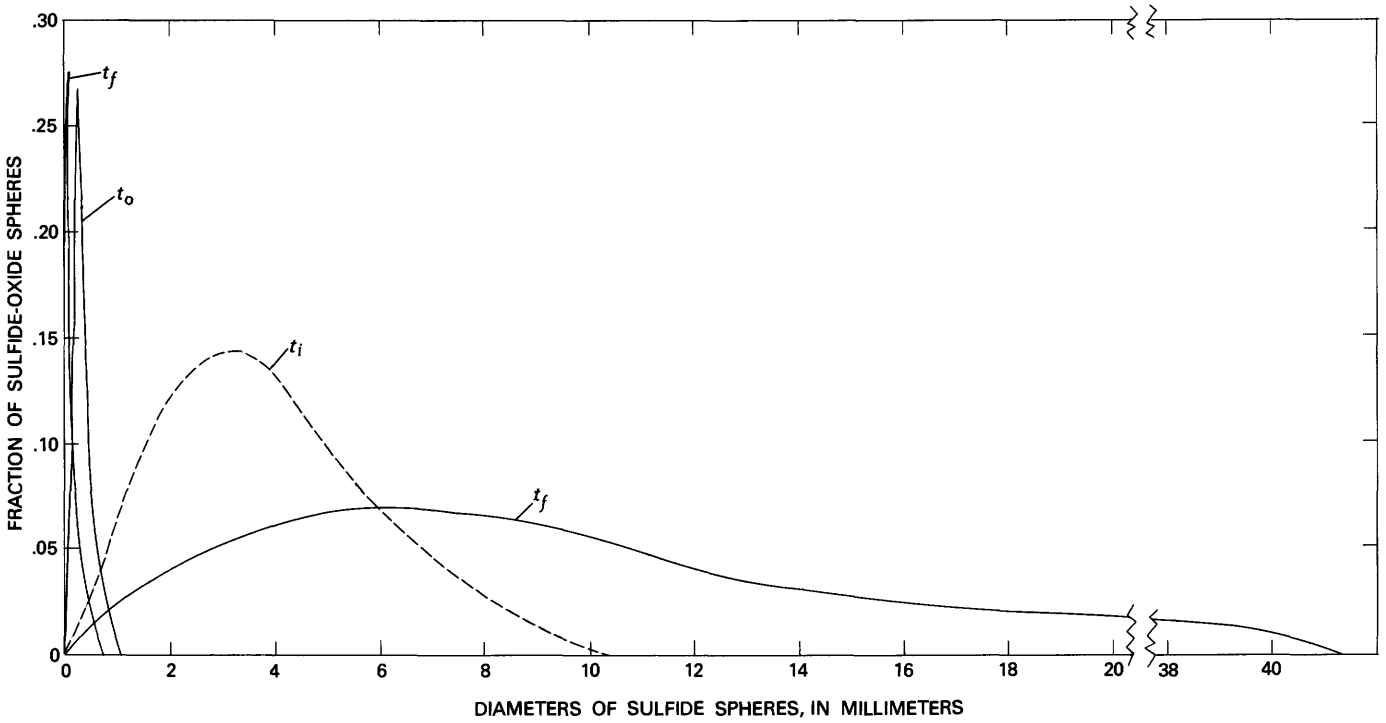

FIGURE 43.—Hypothetical size distributions of sulfide spheres in the Stillwater magma.

ficiency. Empirical and theoretical expressions for the collision efficiency of raindrops (Langmuir, 1948; Matveev, 1967) have been developed and the parameter ξ has been shown to be a function of the Reynolds number, Froude number, and drag coefficient, as well as the size of the collector and the size of the particles collected. The extension of collision efficiencies of raindrops in air to sulfide-oxide spheres in basaltic magma does not appear to be possible, and solution of the problem must await experimental data.

In order to complete a model of collision and coalescence of sulfide-oxide spheres, values of collision efficiency and size distributions of the spheres are needed. Both probably could be derived from appropriate experiments. However, from the raindrop analogy and analysis presented above, it appears that collision and coalscence are adequate to concentrate sulfide-oxide liquids from the basaltic magma. The present distribution of sulfide material—as disseminated clots, matrix sulfide, and massive sulfide—is a result of supply of sulfide-oxide liquids and their coalescence into masses that could settle rapidly enough to collect.

CRYSTALLIZATION OF THE COLLECTED SULFIDE-OXIDE LIQUID

Experimental studies of the phase relations in the Fe-Ni-S system, recently summarized and extended to lower temperatures by Misra and Fleet (1973), imply that the ore mineral assemblages of the Basal zone provide only indirect evidence on the conditions existing when the sulfides collected. Pyrrhotite-pentlandite-chalcopyrite assemblages probably result from chemical adjustments to changing physical conditions down to 230°C and lower temperatures. Diffusion of metallic ions within sulfide phases is an important process that will alter original high-temperature histories (Ewers and Hudson, 1972). Later thermal events such as the intrusion of the quartz monzonite sequence or low-grade metamorphism and deformation can alter any primary high-temperature artifacts. Nevertheless, it is worthwhile to try to unravel the crystallization history of the sulfide material within this unfavorable framework.

That the sulfide material collected as sulfide-oxide liquids is shown by the fact that postcumulus plagioclase locally forms euhedral laths where it projects into disseminated, matrix, and massive sulfide just as euhedral cumulus minerals project into the postcumulus minerals. The sulfide fraction must have been liquid and must have completed crystallization after the postcumulus phases. Other features present before the crystallization of the sulfide liquid include the magnetite-ilmenite intergrowths that occur as subhedral to euhedral crystals predominantly in the matrix and massive sulfide, but locally in disseminated sulfide. These oxide intergrowths are interpreted as cumulus crystals that were trapped in the sulfide liquid as were the cumulus silicate minerals.

The composition of the sulfide-oxide liquid would have been controlled by the host basaltic magma. From arguments based on his experimental study of the Fe-S-O system, Naldrett (1969) suggests that small sulfide-oxide droplets interact with the basaltic magma and thus

equilibrate with it, equalizing the oxygen and sulfur fugacities between the magma and the sulfide-oxide liquids. Such an interaction depends upon rapid exchange or diffusion of oxygen and sulfur, or possibly ferrous and ferric iron, between the two liquids. If the collision and coalescence model developed in the previous section applies to the accumulation of the sulfides, then it is important to ask at what size of droplet will the processes of diffusion be able to maintain equilibrium.

The variable magnetite content of sulfide inclusions and interstitial sulfide material suggests that equilibrium was not always reached. Naldrett's (1969) analysis predicted that there would not be any magnetite crystallized from the sulfide-oxide liquid if it were in equilibrium, and therefore sulfide inclusions, interstitial sulfide material, and disseminated sulfide material should not contain magnetite. One might conclude that sulfide containing no magnetite crystallized from sulfide-oxide liquid in equilibrium with the adjoining basaltic magma, whereas that containing magnetite did not.

Sulfide-oxide liquid that accumulated as disseminated sulfides probably was in the form of larger droplets that fell onto the accumulating crystal pile and replaced the existing interstitial basaltic magma because of the density contrast. Matrix sulfide may have been droplets that were supplied rapidly to the pile and that coalesced on and in the crystal pile as they displaced silicate magma. Conversely, the same texture might develop if the cumulus silicates were growing slowly. Massive sulfide represents droplets that accumulated more rapidly than the silicates and that displaced basaltic magma as well as floated cumulus silicates. After collecting in their various forms, the sulfides began to crystallize.

Two early crystallization patterns are defined, one based on texture, the other on experimental evidence. The gersdorffite group of minerals, although sparsely distributed, tends to occur as euhedral to subhedral crystals molded by pyrrhotite, pentlandite, and chalcopyrite, and probably crystallized early from the sulfide-oxide liquid. Similar observations have been made about gersdorffite in the sulfide deposits associated with the Sudbury intrusives (Hawley, 1962). Experimental studies by Naldrett, Craig, and Kullerud (1967), Yund and Kullerud (1966), Craig and Kullerud (1969), and Naldrett (1969), in which copper and nickel were added to the Fe-S-O system, show that sulfide-oxide liquid in the Basal zone with less than 15 weight percent nickel and 4 weight percent copper would begin to crystallize a nickel-copper pyrrhotite solid solution between 1150° and 1050°C. A fluid pressure of 2 kb would not alter this temperature interval by much (Naldrett, 1969) nor would nickel and copper contents below the stated values. Over this temperature range nickel-copper pyrrhotite solid solution and sulfide liquid would be present. Solidification of the sulfide-oxide liquids would continue, and if the sulfide mass were isolated from the basaltic magma, crystallization of nickel-copper pyrrhotite solid solution would be accompanied by crystallization of magnetite. If the sulfide mass were able to exchange with the basaltic magma, the crystalline sulfide product would contain no magnetite. In the Basal zone sulfide materials, both situations prevailed and sulfide-oxide liquids crystallized to nickel-copper pyrrhotite solid solutions with variable amounts of magnetite.

Coexistence of a solid and liquid phase opens the possibility that within larger sulfide masses, the sulfide-oxide liquid could differentiate by gravity separation of the nickel-copper pyrrhotite from the liquid, or that the liquid could separate from the crystals filter-pressing. Either mechanism could produce variable compositions of sulfide-oxide liquid that might have different crystallization histories. For some compositions, chalcopyrite solid solutions could crystallize at about 970°C and coexist with nickel-copper pyrrhotite and copper-enriched sulfide liquids (Craig and Kullerud, 1969, p. 356). This would allow separation and local concentration of copper-enriched sulfide liquid. Whether these processes operated in the Basal zone is not yet documented.

Experimental work (Craig and Kullerud, 1969; Naldrett and others, 1967; Misra and Fleet, 1973) shows that the temperature of exsolution of pentlandite and chalcopyrite from the nickel-copper pyrrhotite solid solution depends primarily on the nickel, copper, and sulfur contents. Below about 600° C pentlandite could exsolve from the solid solution, and below 575° C both pentlandite and chalcopyrite could exsolve from the pyrrhotite solid solution (Craig and Kullerud, 1969). Comparison of pyrrhotite-pentlandite-chalcopyrite textures in the sulfide masses with other similar types of deposits suggests that the sulfide minerals present are products of this type of exsolution. Both blocky pentlandite necklaces and flame textures could have been formed in this way. According to Misra and Fleet (1973), the compositions of the phases would continue to adjust as temperature decreases. The low nickel content of pyrrhotite (Page, 1972) suggests that reequilibration continued below 230°C (see Misra and Fleet, 1973, p. 531), at which temperature both hexagonal and monoclinic pyrrhotite are considered stable phases. The combination of experimental evidence and textures suggest that the present mineral assemblages and compositions reflect only very low temperature attempts at equilibration.

Superimposed on these characteristics of the sulfide material are the effects of the quartz monzonite intrusive bodies in the eastern part of the complex and deformation features near fault zones. In the eastern part of the complex, some massive sulfide rocks contain veins enriched in chalcopyrite that may have been remobilized. These veins appear to be in fractures, possibly related to quartz monzonite emplacement. Pyrrhotite deformation features have been observed throughout the Basal zone sulfide and generally can be related to late faulting.

LIMITATIONS AND SPECULATIONS ON ORIGIN OF BASAL ZONE

Models for the origin, emplacement, and crystallization history of the Basal zone of the Stillwater Complex that include consideration of its shape, stratigraphy, rock type, textures, and their relations are limited by the following observations and deductions:

1. The contact between the metasedimentary rocks of Precambrian age and the Basal zone does not follow a single stratigraphic horizon but cuts across stratigraphic and lithologic units in the country rocks.

2. The overall shape of the Basal zone approximates a tabular prism with an extremely large breadth to thickness ratio (about 256 to 1, based on the exposed complex) but in detail consists of a series of basinlike shapes linked by thinner interbasin areas.

3. A variety of rocks are present: Cumulates, dominated in abundance by orthopyroxene cumulates but with minor amounts of one- and two-phase cumulates consisting of olivine, clinopyroxene, inverted pigeonite, plagioclase, and chromite; noncumulate igneous rocks with ophitic, subophitic, and ragged textures; contaminated and mixed rocks; rocks derived by partial melting of metasedimentary rocks; sulfide-bearing and sulfide rocks; and complex breccias of these rocks.

4. The rocks and their constituents form fluctuating and repeating patterns of chemical and physical properties which include: (a) The ascending lithologic sequence ophitic, subophitic, ragged, and cumulus-textured rocks; (b) cumulate sequences of orthopyroxene, orthopyroxene + plagioclase; olivine + orthopyroxene, orthopyroxene; and plagioclase, plagioclase +orthopyroxene; (c) fine- to medium- to coarse-grained cumulate sequences; (d) variation in volume of cumulus phases present; (e) variation in orthopyroxene and plagioclase compositions; and (f) variation in the distribution of sulfide minerals.

5. A lower member, the Basal norite, is extremely variable both laterally and vertically in mineralogy, texture, grain size, crystallization sequences, and fabric and is overlain by an upper member, the Basal bronzite cumulate, which exhibits relatively regular properties laterally.

6. Evidence exists for variability in processes and products in the Basal zone in contrast to the evidence for extreme uniformity in processes and products in the overlying Ultramafic zone.

7. Other facets, not covered by this report, such as heat transfer and balance during solidification, source(s) of the magma(s), original extent and size of the complex, and many detailed observations not mentioned specifically in the first six limitations have a bearing on the origin of the complex.

Suggestions and interpretations, offered as part of a model for the origin of the Basal zone, contain many elements included in the above observations but, if applied stringently on local scales, have their limitations. The following interpretation is offered as compatible with the essential facts as presently known.

During or immediately after initial emplacement of magma, several characteristics of the basal contact zone developed. Quantities of silicate magma and sulfide-oxide liquid were injected into the metasedimentary rocks, forming the tongues, dikes, and lenses that account for the complicated intrusive relations in areas such as Verdigris Creek in the Mountain View area. Some of the early silicate magma was emplaced in rocks that were cool enough to cause it to crystallize as ophitic, subophitic, and ragged-textured noncumulate rocks; subsequent injections of magma cooled more slowly and developed textures approaching those of cumulate rocks; and the massive sulfide lenses crystallized last. Within the main magma chamber near the contact and attached to metasedimentary rocks, noncumulate igneous rocks crystallized by relatively rapid cooling or possibly quenching. Large blocks and inclusions of metasedimentary rocks, locally with rinds of noncumulate igneous-textured rocks, were rafted upward in the magma chamber. Locally crystallization and accumulation of cumulates began, were interrupted either by a new influx of magma or by convection, and then began anew. This process of approaching a mechanical equilibrium, interrupting it, and approaching another was probably the major mechanism operating during the development of the Basal norite. As the magma underwent mechanical perturbation, it tried to reach thermal and chemical equilibrium. Most likely the repetitions and inhomogeneities exhibited by the Basal norite are a result of approaches to both chemical and mechanical equilibrium, interrupted by influxes of magma. Perhaps, by the time the upper part of the Basal norite was crystallizing or at least by the time the Basal bronzite cumulate was accumulating, there were no new influxes of magma and the crystallization pattern was established without further interruption.

REFERENCES CITED

Arnold, R. G., 1962, Equilibrium relations between pyrrhotite and pyrite from 325° C to 743° C: Econ. Geology, v. 57, p. 72-90.

———1967, Range in composition of 82 natural terrestrial pyrrhotites: Canadian Mineralogist, v. 9, p. 31-50.

Arnold, R. G., and Reichen, L. E., 1962, Measurement of the metal content of naturally occurring, metal-deficient, hexagonal pyrrhotite by an X-ray spacing method: Am. Mineralogist, v. 47. p. 105-111.

Berry, E. X., 1967, Cloud droplet growth by collection: Jour. Atmos. Sci., v. 24, p. 688-701.

Bottinga, Yan, and Weill, D. F., 1970, Densities of liquid silicate systems calculated from partial molar volumes of oxide components: Am. Jour. Sci., v. 269, p. 169-182.

———1972, The viscosity of magmatic silicate liquids—A model for calculation: Am. Jour. Sci., v. 272, p. 438-475.

Bouma, A. H., 1962, Sedimentology of some flysch deposits: New York, Elsevier Publishing Co., 168 p.

Bowes, D. R., Skinner, W. R., and Skinner, D. L., 1973, Petrochemistry of the Stillwater Igneous Complex, Montana: South Africa Geol. Soc. Trans. and Proc., v. 76, pt. 2, p. 153-163.

Brett, Robin, and Bell, P. M., 1969, Melting relations in the Fe-rich portion of the system Fe-FeS at 30 kb pressure: Earth and Planetary Sci. Letters, v. 6, no. 6, p. 479-482.

Brown, G. M., 1957, Pyroxenes from the early and middle stages of fractionation of the Skaergaard Intrusion, East Greenland: Mineralog. Mag., v. 31, p. 511-543.

Cabri, L. J., 1967. A new copper-iron sulfide: Econ. Geology, v. 62, p. 910-925.

———1973, New data on phase relations in the Cu-Fe-S system: Econ. Geology, v. 68. p. 443-454.

Cabri, L. J., and Hall, S. R., 1972, Mooihoekite and haycockite, two new copper-iron sulfides, and their relationship to chalcopyrite and talnakhite: Am. Mineralogist, v. 57, p. 689-708.

Carmichael, I. S. E., 1964. The petrology of Thingmuli, a Tertiary volcano in eastern Iceland: Jour. Petrology, v. 5, p. 435-460.

Casella, C. J., 1969, A review of the Precambrian geology of the eastern Beartooth Mountains, Montana and Wyoming, *in* Igneous and metamorphic geology: Geol. Soc. America Mem. 115, p. 53-71.

Chinner, G. A., and Schairer, J. F., 1962, The join $Ca_2Al_2Si_3O_{12}$-$Mg_3Al_2Si_3O_{12}$ and its bearing on the system CaO-MgO-Al_2O_3-SiO_2 at atmospheric pressure: Am. Jour. Sci., v. 260, p. 611-634.

Christiansen, J. E., 1935, Distribution of silt in open channels: Am. Geophys. Union Trans., v. 16, p. 478-485.

Clark, B. R., and Kelly, W. C., 1973, Sulfide deformation studies—I. Experimental deformation of pyrrhotite and sphalerite to 2,000 bars and 500°C: Econ. Geology, v. 68, p. 332-352.

Cornwall, H. R., 1972, Nickel, *in* Brobst, D. A., and Pratt, W. P., eds., United States mineral resources: U.S. Geol. Survey Prof. Paper 820, p. 425-436.

Cowan, J. C., 1968, Geology of the Strathcona ore deposit: Canadian Mining and Metall. Bull., v. 1, no. 669, p. 38-54.

Craig, J. R., and Kullerud, G., 1969, Phase relations in the Cu-Fe-Ni-S system and their application to magmatic ore deposits, *in* H. D. B. Wilson, ed., Magmatic ore deposits: Econ. Geology Mon. 4, p. 344-358.

Dayton, Stan, 1971, Hot air over Stillwater, profile of a hearing on mineral entry: Eng. and Mining Jour., v. 172, no. 10, p. 75-84.

Desborough, G. A., and Carpenter, R. H., 1965, Phase relations of pyrrhotite: Econ. Geology, v. 60, p. 1430-1450.

Engel, A. E. J., Engel, C. G., and Havens, R. G., 1965, Chemical characteristics of oceanic basalts and the upper mantle: Geol. Soc. America Bull., v. 76, p. 719-734.

Ewers, W. E., and Hudson, D. R., 1972, An interpretive study of a nickel-iron sulfide ore intersection, Lunnon Shoot, Kambalda, Western Australia: Econ. Geology, v. 67, p. 1075-1092.

Fincham, C. J. B., and Richardson, F. D., 1954, The behavior of sulphur in silicate and aluminate melts: Royal Soc. [London] Philos. Trans., v. 223, p. 40-62.

Foose, R. M., Wise, D. V., and Garbarini, G. S., 1961, Structural geology of the Beartooth Mountains, Montana and Wyoming: Geol. Soc. America Bull., v. 72, p. 1143-1172.

Fraser, H. J., 1935, Experimental study of the porosity and permeability of clastic sediments: Jour. Geology, v. 43, no. 8, p. 910-1010.

Graterol, Magaly, and Naldrett, A. J., 1971, Mineralogy of the Marbridge No. 3 and No. 4 nickel-iron sulfide deposit: Econ. Geology. v. 66. p. 886-900.

Graton, L. C., and Fraser, H. J., 1935, Systematic packing of spheres—with particular relation to porosity and permeability: Jour. Geology, v. 43, no. 8, p. 785-909.

Gribble, C. D., 1966, The thermal aureole of the Haddo House norite in Aberdeenshire: Scottish Jour. Geology, v. 2, no. 3, p. 306-313.

———1967, The basic intrusive rocks of Caledonian age of the Haddo House and Arnage districts, Aberdeenshire: Scottish Jour. Geology, v. 3, no. 1, p. 125-136.

———1968, The cordierite-bearing rocks of the Haddo House and Arnage districts, Aberdeenshire: Contr. Mineralogy and Petrology, v. 17, p. 315-330.

———1970, The role of partial fusion in the genesis of certain cordierite-bearing rocks: Scottish Jour. Geology, v. 6, pt. 1, p. 75-82.

Gribble, C. D., and O'Hara, M. J., 1967, Interaction of basic magma and pelitic materials: Nature, v. 214, p. 1198-1201.

Gruenewaldt, G. von, 1970, On the phase-change orthopyroxene-pigeonite and the resulting textures in the Main and Upper zones of the Bushveld Complex in the Eastern Transvaal, *in* D. J. L. Visser and G. von Gruenewaldt, eds., Symposium on the Bushveld igneous complex and other layered intrusions: Geol. Soc. South Africa Spec. Pub., no. 1, p. 67-73.

Gubanov, A. I., 1957, Change of properties of semiconductors during melting: Soviet Physics-Tech. Physics, v. 2, p. 2335-2340.

Hambleton, W. W., 1947, A petrofabric study of layering in the Stillwater Complex, Montana: Northwestern Univ., Evanston, Ill., M.S. thesis, 62 p.

Harris, D. C., and Nickel, E. H., 1972, Pentlandite compositions and associations in some mineral deposits: Canadian Mineralogist, v. 11, p. 861-878.

Harris, P. G., 1957, Zone refining and the origin of potassic basalts: Geochim. et Cosmochim. Acta, v. 12, p. 195-208.

Haughton, D. R., Roeder, P. L., and Skinner, B. J., 1974, Solubility of sulfur in mafic magmas: Econ. Geology, v. 69, p. 451-467.

Hawley, J. E., 1962, The Sudbury ores—Their mineralogy and origin: Canadian Mineralogist, v. 7, pt. 1, p. 1-207.

Haynes, S. J., and Hill, P. A., 1970, Pyrrhotite phases and pyrrhotite-pyrite relationships—Renison Bell, Tasmania: Econ. Geology, v. 65, p. 838-848.

Hess, G. B., 1972, Heat and mass transport during crystallization of the Stillwater Igneous Complex: Geol. Soc. America Mem. 132, p. 503-520.

Hess, H. H., 1938a, A primary peridotite magma: Am. Jour. Sci., 5th ser., v. 35, no. 209, p. 231-344.

———1938b, Primary banding in norite and gabbro: Am. Geophys. Union Trans., 19th Ann. Mtg., pt. 1, p. 264-268.

———1939, Extreme fractional crystallization of a basaltic magma—The Stillwater igneous complex [abs.]: Am. Geophys. Union Trans., 20th Ann. Mtg., pt. 3, p. 430-432.

———1940, An essay review—The petrology of the Skaergaard intrusion Kangerdlugsuag, East Greenland: Am. Jour. Sci., v. 238, p. 372-378.

———1941, Pyroxenes of common mafic magmas: Am. Mineralogist, v. 26, pt. 1, no. 9, p. 515-535; pt. 2, no. 10, p. 573-594.

———1949, Chemical composition and optical properties of common clinopyroxenes, pt. 1: Am. Mineralogist, v. 34, p. 621-666.

———1960, Stillwater igneous complex, Montana—A quantitative mineralogical study: Geol. Soc. America Mem. 80, 230 p.

Hess, H. H., and Phillips, A. H., 1938, Orthopyroxenes of the Bushveld type: Am. Mineralogist, v. 23, p. 450-456.

———1940, Optical properties and chemical composition of magnesian orthopyroxenes: Am. Mineralogist, v. 25, p. 271-285.

Himmelberg, G. R., and Jackson, E. D., 1967, X-ray determinative curve for some orthopyroxenes of composition Mg_{48-85} from the Stillwater Complex, Montana, *in* Geological Survey research 1967: U.S. Geol. Survey Prof. Paper 575-B, p. B101-B102.

Hotz, P. E., and Jackson, E. D., 1963, X-ray determinative curve for olivines of composition Fo_{80-95} from stratiform and alpine-type peridotites, *in* Geological Survey research 1962; U.S. Geol. Survey Prof. Paper 450-E, p. E101-E102.

Houghton, H. G., 1950, A preliminary quantitative analysis of precipitation mechanisms: Jour. Atmos. Sci., v. 7, no. 6, p. 363-369.

Howland, A. L., 1933, Sulphides and metamorphic rocks at the base of the Stillwater Complex, Montana: Princeton Univ., Princeton, N.J., Ph.

D. thesis, 76 p.

———1955, Chromite deposits in the central part of the Stillwater complex, Montana: U.S. Geol. Survey Bull. 1015-D, p. 99-121.

Howland, A. L., Garrels, E. M., and Jones, W. R., 1949, Chromite deposits of Boulder River area, Sweetgrass County, Montana: U.S. Geol. Survey Bull. 948-C, p. 63-82.

Howland, A. L., Peoples, J. W., and Sampson, Edward, 1936, The Stillwater igneous complex and associated occurrences of nickel and platinum metals: Montana Bur. Mines and Geology Misc. Contr., v. 7, 15 p.

Hytönen, Kai, and Schairer, J. F., 1960, The system enstatite-anorthite-diopside: Carnegie Inst. Washington Year Book 1959, p. 71-72.

Irvine, T. N., 1970a, Crystallization sequences in the Muskox intrusion and other layered intrusions—I. Olivine-pyroxene-plagioclase relations: Geol. Soc. South Africa Spec. Pub. 1, p. 441-476.

———1970b, Heat transfer during solidification of layered intrusions—I. Sheets and sills: Canadian Jour. Earth Sci., v. 7, p. 1031-1061.

Jackson, E. D., 1960, X-ray determinative curve for natural olivine of composition Fo_{80-90}, *in* Geological Survey research 1960: U.S. Geol. Survey Prof. Paper 400-B, p. B432-B434.

———1961a, Primary textures and mineral associations in the ultramafic zone of the Stillwater Complex, Montana: U.S. Geol Survey Prof. Paper 358, p. 1-106.

———1961b, X-ray determinative curve for some natural plagioclases of composition An_{60-85}, *in* Geological Survey research 1961: U.S. Geol. Survey Prof. Paper 424-C, p. C286-C288.

———1963, Stratigraphic and lateral variation of chromite composition in the Stillwater Complex: Mineral. Soc. America Spec. Paper 1, p. 46-54.

———1967, Ultramafic cumulates in the Stillwater, Greak Dyke, and Bushveld intrusions, *in* P. J., Wyllie, ed., Ultramafic and related rocks: New York, John Wiley and Sons, p. 20-38.

———1968a, The chromite deposits of the Stillwater Complex, Montana, *in* Ore deposits of the United States, 1933-1967 (Graton-Sales Volume), v. 2: New York, Am. Inst. Mining, Metall., and Petroleum Engineers, p. 1495-1510.

———1968b, The character of the lower crust and upper mantle beneath the Hawaiian Islands: Internat. Geol. Cong., 23d, Prague 1968, Proc., sec. 1, p. 135-150.

———1969, Chemical variation in coexisting chromite and olivine in chromite zones of the Stillwater Complex, *in* Magmatic ore deposits, a symposium: Econ. Geology Mon. 4, p. 41-71.

———1970, The cyclic unit in layered intrusions—A comparison of repetitive stratigraphy in the ultramafic parts of the Stillwater, Muskox, Great Dyke, and Bushveld Complexes: Geol. Soc. South Africa Spec. Pub. 1, p. 391-424.

———1971, The origin of ultramafic rocks by cumulus processes: Fortschr. Mineralogie, v. 48, p. 128-174.

Jackson, E. D., Howland, A. L., Peoples, J. W., and Jones, W. R., 1954, Geologic maps and sections of the eastern part of the Stillwater Complex in Stillwater County, Montana: U.S. Geol. Survey open-file report.

Jaeger, J. C., 1959, The temperature in the neighborhood of a cooling intrusive sheet: Am. Jour. Sci., v. 255, p. 306-318.

Jones, W. R., Peoples, J. W., and Howland, A. L., 1960, Igneous and tectonic structures of the Stillwater Complex, Montana: U.S. Geol. Survey Bull. 1071-H, p. 281-340.

Kanehira, Keiichiro, 1966, A note of the texture of pyrrhotite in some rocks of the Muskox intrusion: Canadian Mineralogist, v. 8, pt. 4, p. 531-536.

Kullerud, G., 1963, The Fe-Ni-S System: Carnegie Inst. Washington Year Book 1962, p. 175-189.

Langmuir, Irving, 1948, The production of rain by a chain reaction in cumulus clouds at temperatures above freezing: Jour. Atmospheric Sci., v. 5, no. 5, p. 175-192.

Loney, R. A., Himmelberg, G. R., and Coleman R. G., 1971, Structure and petrology of the alpine-type peridotite at Burro Mountain, California, U.S.A.: Jour. Petrology, v. 12, no. 2, p. 245-309.

Macdonald, G. S., and Katsura, T., 1964, Chemical composition of Hawaiian lavas: Jour. Petrology, v. 5, p. 82-133.

MacLean, W. H., 1969, Liquidus phase relations in the FeS-FeO-Fe_3O_4-SiO_2 system and their application in geology: Econ. Geology, v. 64, p. 865-884.

McNown, J. S., and Malaika, J., 1950, Effects of particle shape on settling velocity at low Reynolds numbers: Am. Geophys. Union Trans., v. 31, p. 74-83.

Mason, B. J., 1957, The physics of clouds: Oxford, Clarendon Press, 671 p.

Matveev, L. T., 1967, Fundamentals of general meteorology—Physics of the atmosphere: Jerusalem, Israel Program for Sci. Translations, 699 p.

Misra, K. C., and Fleet, M. E., 1973, The chemical compositions of synthetic and natural pentlandite assemblages: Econ. Geology, v. 68, p. 518-539.

Moore, J. G., and Fabbi, B. P., 1971, An estimate of juvenile sulfur content of basalt: Contr. Mineralogy and Petrology, v. 33, p. 118-127.

Murase, Tsutomu, and McBirney, A. R., 1973, Properties of some common igneous rocks and their melts at high temperatures: Geol. Soc. American Bull., v. 84, p. 3563-3592.

Naldrett, A. J., 1969, A portion of the system Fe-S-O between 900 and 1080°C and its application to sulfide ore magmas: Jour. Petrology, v. 10, p. 171-201.

Naldrett, A. J., Craig, J. R., and Kullerud, G., 1967, The central portion of the Fe-Ni-S system and its bearing on pentlandite exsolution in iron-nickel sulfide ores: Econ. Geology, v. 62, p. 826-847.

Naldrett, A. J., and Kullerud, Gunnar, 1967, A study of the Strathcona mine and its bearing on the origin of nickel-copper ores of the Sudbury district, Ontario: Jour. Petrology, v. 8, p. 453-531.

Naldrett, A. J., and Richardson, S. W., 1967, Effect of water on the melting of pyrrhotite-magnetite assemblages: Carnegie Inst. Washington Year Book 1966, p. 429-431.

Nunes, P. D., and Tilton, G. R., 1971, Uranium-lead ages of minerals from the Stillwater Igneous Complex and associated rocks, Montana: Geol. Soc. America Bull., v. 82, p. 2231-2250.

Osborn, E. F., DeVries, R. C., Gee, K. H., and Kraner, H. M., 1954, Optimum composition of blast furnace slag as deduced from liquidus data for the quaternary system CaO-MgO-Al_2O_3-SiO_2: Jour. Metals, v. 6, no. 1, sec. 1, p. 33-45.

Page, N. J, 1971a, Comments on the role of oxygen fugacity in the formation of immiscible sulfide liquids in the H chromitite zone of the Stillwater Complex, Montana: Econ. Geology, v. 66, p. 607-610.

———1971b, Sulfide minerals in the G and H chromitite zones of the Stillwater Complex, Montana: U.S. Geol. Survey Prof. Paper 694, 20 p.

———1972, Pentlandite and pyrrhotite from the Stillwater Complex, Montana—Iron-nickel ratios as a function of associated minerals: Econ. Geology, v. 67, p. 814-820.

———1977, Stillwater Complex, Montana—Rock succession, metamorphism, structure of the complex and adjacent rocks: U.S. Geol. Survey Prof. Paper 999, 79 p.

Page, N. J, and Dohrenwend, J. C., 1973, Mineral resources potential of the Stillwater Complex and adjacent rocks in the northern part of the Mt. Wood and Mt. Douglas quadrangles, southwestern Montana: U.S. Geol Survey Circ. 684, 9 p.

Page, N. J, and Jackson, E. D., 1967, Preliminary report on sulfide and platinum-group minerals in the chromitites of the Stillwater Complex, Montana, *in* Geological Survey research 1967: U.S. Geol. Survey Prof. Paper 575-D, p. D123-D126.

Page, N. J, and Koski, R. A., 1973, Precambrian diamictite below the base of the Stillwater Complex, southwestern Montana: U.S. Geol. Survey Jour. Research, v. 1, no. 4, p. 403-414.

Page, N. J, and Nokleberg, W. J., 1970a, A suite of granitic intrusive rocks below the base of the Stillwater Complex, Mt. Wood quadrangle, Montana [abs.]: Geol. Soc. America, Abstracts with Programs, v. 2, no. 5, p. 342.

———1970b, Preliminary geologic map of the Stillwater Complex, Montana: U.S. Geol. Survey open-file report.

———1972, Genesis of mesozonal granitic rocks below the base of the Stillwater Complex, in the Beartooth Mountains, Montana, *in* Geological Survey research 1972: U.S. Geol. Survey Prof. Paper 800-D, p. D127-D141.

———1974, Geologic map of the Stillwater Complex, Montana: U.S. Geol. Survey Misc. Geol. Inv. Map I-797, 5 sheets, scale 1:12,000.

Page, N. J, Riley, L. B., and Haffty, Joseph, 1969, Platinum, palladium, and rhodium analyses of ultramafic and mafic rocks from the Stillwater Complex, Montana: U.S. Geol. Survey Circ. 624, 12 p.

———1971, Lateral and vertical variation of platinum, palladium, and rhodium in the Stillwater Complex, Montana: Geol. Soc. America, Abs. with Programs, v. 3, no. 6, p. 401.

———1972, Vertical and lateral variation of platinum, palladium, and rhodium in the Stillwater Complex, Montana: Econ. Geology, v. 67, p. 915-924.

Page, N. J, Shimek, Richard, and Huffman, Claude, Jr., 1972, Grain-size variations within anolivine cumulate, Stillwater Complex, Montana, *in* Geological Survey research 1972: U.S. Geol. Survey Prof. Paper 800-C, p. C29-C37.

Page, N. J, Simons, F. S., and Dohrenwend, J. C., 1973a, Reconnaissance geologic map of the Mt. Douglas quadrangle, Montana: U.S. Geol. Survey Misc. Field Studies Map MF-488.

———1973b, Reconnaissance geologic map of the Mt. Wood quadrangle, Montana: U.S. Geol. Survey Misc. Field Studies Map MF-491.

Peoples, J. W., 1932, The geology of the Stillwater igneous complex: Princeton Univ., Princeton, N. J., Ph. D. thesis, 180 p.

———1933, The Stillwater igneous complex, Montana: Am. Mineralogist, v. 18, p. 117.

———1936, Gravity stratification as a criterion in the interpretation of the structure of the Stillwater complex, Montana: Internat. Geol. Cong., Washington, 16th, 1933, Rept., v. 1, p. 353-360.

Peoples, J. W., and Howland, A. L., 1940, Chromite deposits of the eastern part of the Stillwater complex, Stillwater County, Montana: U.S. Geol Survey Bull. 922-N, p. 371-416.

Peoples, J. W., Howland, A. L., Jones, W. R., and Flint, Delos, 1954, Geologic map, sections, and map of underground workings of the Mountain View Lake area, Stillwater County, Montana: U.S. Geol. Survey open-file report.

Pettijohn, F. J., 1957, Sedimentary rocks, 2d ed: New York, Harper and Bros., 718 p.

Poldervaart, Arie, and Hess, H. H., 1951, Pyroxenes in the crystallization of basaltic magma: Jour. Geology, v. 59, p. 472-489.

Presnall, D. C., 1969, The geometrical analysis of partial fusion: Am. Jour. Sci., v. 267, p. 1178-1194.

Prince, A. T., 1954, Liquidus relationships on 10% MgO plane of the system lime-magnesia-alumina-silica: Am. Ceramic Soc. Jour., v. 37, no. 9, p. 402-408.

Purvis, A. C., Nesbitt, R. W., and Hallberg, J. A., 1972, The geology of part of the Carr Boyd Rocks Complex and its associated nickel mineralization, western Australia: Econ. Geology, v. 67, p. 1093-1113.

Raleigh, C. B., 1965a, Glide mechanisms in experimentally deformed minerals: Science, v. 150, p. 739-741.

———1965b, Structure and petrology of an alpine peridotite on Cypress Island, Washington, U.S.A.: Beitr. Mineralogie u. Petrologie, v. 11, p. 719-741.

Richards, P. W., 1952, Structural geology of the Crazy Mountain Syncline-Beartooth Mountains border east of Livingston, Montana: Cornell Univ., New York, Ph. D. thesis.

———1958, Geology of the area east and southeast of Livingston, Park County, Montana: U.S. Geol. Survey Bull. 1021-L, p. 385-438.

Richardson, F. D., and Fincham, C. J. B., 1954, Sulfur in silicate and aluminate slags: Iron and Steel Inst. [London] Jour., v. 178, p. 4-15.

Roby, R. N., 1949, Investigations of copper-nickel deposits of the Stillwater Complex, Stillwater and Sweetgrass Counties, Montana: U.S. Bur. Mines Rept. Inv. RI-4431, 10 p.

Rubey, W. W., 1933, Settling velocities of gravel, sand, and silt particles: Am. Jour. Sci., v. 25, p. 325-338.

Schairer, J. F., 1954, The system K_2O-MgO-Al_2O_3-SiO_2—I. Results of quenching experiments on four joins in the tetrahedron cordierite-forsterite-leucite-silica and on the join cordierite-mullite-potash-feldspar: Am. Ceramic Soc. Jour., v. 37, no. 11, p. 501-533.

Schairer, J. F., and Yoder, H. S., Jr., 1970, Critical planes and flow sheet for a portion of the system CaO-MgO-Al_2O_3-SiO_2 having petrological applications: Carnegie Inst. Washington Year Book 1968, p. 202-214.

Shamazaki, Hidehiko, and Clark, L. A., 1973, Liquidus relations in the FeS-FeO-SiO_2-Na_2O system and its geologic implications: Econ. Geology, v. 68, no. 1, p. 79-96.

Shaw, D. M., 1972, Development of the early continental crust—Part I, Use of trace element distribution coefficient models for the Protoarchean crust: Canadian Jour. Earth Sci., v. 9, p. 1577-1595.

Shaw, H. R., 1965, Comments on viscosity, crystal settling, and convection in granitic magmas: Am. Jour. Sci., v. 263, p. 120-152.

———1969, Rheology of basalt in the melting range: Jour. Petrology, v. 10, p. 510-535.

———1972, Viscosities of magmatic silicate liquids—An empirical method of prediction: Am. Jour. Sci., v. 272, p. 870-893.

Shaw, H. R., Wright, T. L., Peck, D. L., and Okamura, R., 1968, The viscosity of basaltic magma—An analysis of field measurements in Makaopuhi Lava Lake, Hawaii: Am. Jour. Sci., v. 266, p. 225-264.

Skinner, B. J., 1966, Thermal expansion, *in* S. P. Clark, Jr., ed., Handbook of physical constants: Geol. Soc. America Mem. 97, p. 78-96.

Skinner, B. J., and Peck, D. L., 1969, An immiscible sulfide melt from Hawaii, *in* H.D.B. Wilson, ed., Magmatic ore deposits: Econ. Geology Mon. 4, p. 310-322.

Soo, S. L., 1967, Fluid dynamics of multiphase systems: Waltham, Mass., Blaisdell Publishing Co., 524 p.

Subramaniam, A. P., 1956, Mineralogy and petrology of the Sittampundi Complex, Salem district, Madras State, India: Geol. Soc. America Bull., v. 67, p. 317-390.

Telford, J. W., 1955, A new aspect of coalescence theory: Jour. Atmos. Sci., v. 12, no. 5, p. 436-444.

Toulmin, Priestley, III, and Barton, P. B., Jr., 1964, A thermodynamic study of pyrite and pyrrhotite: Geochim, et Cosmochim Acta, v. 28, p. 641-672.

Twomey, S., 1964, Statistical effects in the evolution of a distribution of cloud droplets by coalescence: Jour. Atmos. Sci., v. 21, p. 553-557.

———1966, Computations of rain formation by coalescence: Jour. Atmos. Sci., v. 23, p. 405-411.

U.S. Geological Survey, 1971, Aeromagnetic map of the Stillwater Complex and vicinity, south-central Montana: U.S. Geol. Survey open-file report.

Vail, P. R., 1955, The igneous and metamorphic complex of East Boulder River area, Montana: Northwestern Univ., Evanston, Ill., Ph. D. thesis.

Vaughan, D. J., Schwarz, E. J., and Owens, D. R., 1971, Pyrrhotites from the Strathcona mine, Sudbury, Canada—A thermomagnetic and mineralogical study: Econ. Geology, v. 66, p. 1131-1144.

Vhay, J. S., 1934, Geology of part of the Beartooth Mountain front near Nye, Montana: Princeton Univ., Princeton, N. J., Ph. D. thesis.

Wager, L. R., and Brown, G. M., 1967, Layered igneous rocks: San Francisco, Calif., W. H. Freeman and Co., 588 p.

Wager, L. R., Brown, G. M., and Wadsworth, W. J., 1960, Type of igneous cumulates: Jour. Petrology, v. 1, p. 73-85.

Wager, L. R., and Deer, W. A., 1939, Geological investigation in East Greenland—Part III. The petrology of the Skaergaard intrusion, Kangerdlugssuag, East Greenland: Medd. Grönland, v. 105, no. 4, 352 p.

Westgate, L. G., 1921, Deposits of chromite in Stillwater and Sweet Grass Counties, Montana: U.S. Geol. Survey Bull. 725, p. 67-84.

White, R. W., 1966, Ultramafic inclusions in basaltic rocks from Hawaii: Contr. Mineralogy and Petrology, v. 12, p. 245-314.

Willemse, J., and Viljoen, E. A., 1970, The fate of argillaceous material in the gabbroic magma of the Bushveld Complex, *in* D. J. L. Visser, and G. von Gruenewaldt, eds., Symposium on the Bushveld igneous complex and other layered intrusions: Geol. Soc. South Africa Spec. Pub. 1, p. 336-366.

Wilson, J. F., 1968, The geology of the country around Mushaba: Rhodesia Geol. Survey Bull. 62, 239 p.

Wimmler, N. L., 1948, Investigation of chromite deposits of the Stillwater Complex, Stillwater and Sweet Grass Counties, Montana: U.S. Bur. Mines Rept. Inv. 4368, 41 p.

Wyllie, P. J., 1959, Microscopic cordierite in fused Torridonian arkose: Am. Mineralogist, v. 44, p. 1039-1046.

Yund, R. A., and Kullerud, Gunnar, 1966, Thermal stability of assemblages in the Cu-Fe-S system: Jour. Petrology, v. 7, no. 3, p. 454-488.

INDEX

[Page numbers of major references are in italic]

★ U.S. GOVERNMENT PRINTING OFFICE : 1979—O—677-026/41